Volume 44 No. 1 2015
ISSN 0146-6453
ISBN 9781473944398

Annals of the ICRP

ICRP Publication 129

Radiological Protection in Cone Beam Computed Tomography (CBCT)

Annals of the ICRP

Published on behalf of the International Commission on Radiological Protection

Aims and Scope

The International Commission on Radiological Protection (ICRP) is the primary body in protection against ionising radiation. ICRP is a registered charity and is thus an independent non-governmental organization created at the 1928 International Congress of Radiology to advance for the public benefit the science of radiological protection. ICRP provides recommendations and guidance on protection against the risks associated with ionising radiation from artificial sources such as those widely used in medicine, general industry, and nuclear enterprises, and from naturally occurring sources. These reports and recommendations are published approximately four times each year on behalf of ICRP as the journal *Annals of the ICRP*. Each issue provides in-depth coverage of a specific subject area.

Subscribers to the journal receive each new report as soon as it appears so that they are kept up to date on the latest developments in this important field. While many subscribers prefer to acquire a complete set of ICRP reports and recommendations, single issues of the journal are also available separately for those individuals and organizations needing a single report covering their own field of interest. Please order through your bookseller, subscription agent, or direct from the publisher.

ICRP is composed of a Main Commission, a Scientific Secretariat, and five standing Committees on: radiation effects, doses from radiation exposure, protection in medicine, the application of ICRP recommendations, and protection of the environment. The Main Commission consists of a Chair and twelve other members. Committees typically comprise 10–15 members each.

ICRP uses Task Groups to prepare its reports. A Task Group is usually chaired by an ICRP Committee member and usually contains a number of specialists from outside ICRP. Thus, ICRP is an independent international network of specialists in various fields of radiological protection, and, at any one time, about two hundred eminent scientists and policy makers are actively involved in the work of ICRP. The Task Groups are assigned the responsibility for drafting documents on various subjects, which are reviewed and finally approved by the Main Commission. These documents are then published as the *Annals of the ICRP*.

Annals of the ICRP

ICRP PUBLICATION 129

Radiological Protection in Cone Beam Computed Tomography (CBCT)

Editor-in-Chief
C.H. CLEMENT

Associate Editor
N. HAMADA

Authors on behalf of ICRP
M.M. Rehani, R. Gupta, S. Bartling, G.C. Sharp, R. Pauwels, T. Berris, J.M. Boone

PUBLISHED FOR

The International Commission on Radiological Protection

by

SAGE

Please cite this issue as 'ICRP, 2015. Radiological Protection in Cone Beam Computed Tomography (CBCT). ICRP Publication 129. Ann. ICRP 44(1).'

CONTENTS

SAGE

ICRP Publication 129

ICRP
Annals of the ICRP

Guest Editorial

CBCT: WIDE RANGE OF CLINICAL APPLICATIONS AND WIDE RANGE OF DOSES

This publication on radiological protection in cone beam computed tomography (CBCT) is both timely and practical. Previous ICRP publications have addressed managing the dose in patients undergoing computed tomography (*Publication 87*), and managing patient dose in multi-detector computed tomography (MDCT) (*Publication 102*) (ICRP, 2000a, 2007a). While some of the same principles apply to CBCT, new challenges exist. CBCT is a technology that is becoming more prevalent in clinical practice. These scanners extend the use of computed tomography (CT) into new clinical environments and by new practitioners, not all of whom have had the radiation safety training that radiological technologists, medical physicists, radiologists, and radiation oncologists have traditionally received. In addition, this technology is in evolution, and opportunities exist for device manufacturers to standardise dose displays. Thus, there is a need for education, guidelines, and standardisation in the industry.

Over the past decades, conventional CT has been 'game-changing' technology in patient care. Abdominal CT scans have replaced more invasive surgical procedures. Head CT scans and CT angiography have replaced many catheter-based angiograms. In a survey of 235 internists, CT and magnetic resonance imaging ranked highest on the list of innovations whose loss would have the greatest adverse effect on patients (Fuchs and Sox, 2001). CT ranked ahead of several mainstream medical technologies such as gastrointestinal endoscopy, balloon angioplasty, and coronary artery bypass grafts. However, use of CT imaging comes with responsibility. Knowledge and tools are needed to balance the benefits and the harms. Now, as CBCT is used in other clinical areas by other providers, the need for education, standardisation, and guidelines presents an opportunity that must be met.

The use of CBCT spans a wide range of clinical specialties and procedures: radiotherapy; orthopaedics; urology; dental/maxillofacial; neurointerventions; and vascular and non-vascular interventions. Patient dose also demonstrates a large range, from <1 mGy for organ absorbed dose to >400 mGy for skin dose. This range could be even wider depending on the number of CBCT scans performed and the complexity of intervention. This publication provides practical guidance for dose management in general and in specific clinical settings.

Dose reduction comes with trade-offs. This will require standard measurements of both dose and image quality across all manufacturers. For equipment used for

fluoroscopy and CBCT, the aggregate dose to the patient for the entire procedure should be available. These data should be displayed on the operator console, and should be available for incorporation into the electronic health record. There are many ways to reduce dose. These include the design of CBCT equipment and how the equipment is used in specific clinical settings. This publication appropriately reinforces fundamental concepts such as 'as low as reasonably achievable'. However, this publication also addresses another critical source of dose reduction. One of the best ways to reduce dose is to ensure that the imaging is appropriate or clinically indicated. Conventional CT examinations may be performed that do not represent the most appropriate imaging test for the clinical question being asked. Multiple strategies have been developed to address unnecessary use of imaging overall (Bernardy et al., 2009). Guidelines on appropriate use of CBCT need to be widely adopted.

In an era of population health, further development and use of CBCT should be driven by appropriate clinical need, balanced with risk to patients and workers. This publication provides a helpful direction for policy makers, imaging professionals, medical physicists, and manufacturers to optimise protection of both patients and workers, while preserving the expectation of high diagnostic yields from imaging and excellent clinical outcomes.

JAMES V. RAWSON

REFERENCES

ICRP, 2000. Managing Patient Dose in Computed Tomography. ICRP Publication 87. Ann. ICRP 30(4).

ICRP, 2007a. Managing patient dose in multi-detector computed tomography (MDCT). ICRP Publication 102. Ann. ICRP 37 (1).

Fuchs, V.R., Sox, H.C. Jr., 2001. Physician s views of the relative importance of thirty medical innovations. Health Aff. 20, 30–42.

Bernardy, M., Ullrich, C.G., Rawson, J.V., et al., 2009. Strategies for managing imaging utilization. J. Am. Coll. Radiol. 6, 844–850.

SAGE

ICRP Publication 129

ICRP
Annals of the ICRP

Radiological Protection in Cone Beam Computed Tomography (CBCT)

ICRP PUBLICATION 129

Approved by the Commission in January 2015

Abstract–The objective of this publication is to provide guidance on radiological protection in the new technology of cone beam computed tomography (CBCT). *Publications 87* and *102* dealt with patient dose management in computed tomography (CT) and multi-detector CT. The new applications of CBCT and the associated radiological protection issues are substantially different from those of conventional CT. The perception that CBCT involves lower doses was only true in initial applications. CBCT is now used widely by specialists who have little or no training in radiological protection. This publication provides recommendations on radiation dose management directed at different stakeholders, and covers principles of radiological protection, training, and quality assurance aspects. Advice on appropriate use of CBCT needs to be made widely available. Advice on optimisation of protection when using CBCT equipment needs to be strengthened, particularly with respect to the use of newer features of the equipment. Manufacturers should standardise radiation dose displays on CBCT equipment to assist users in optimisation of protection and comparisons of performance. Additional challenges to radiological protection are introduced when CBCT-capable equipment is used for both fluoroscopy and tomography during the same procedure. Standardised methods need to be established for tracking and reporting of patient radiation doses from these procedures. The recommendations provided in this publication may evolve in the future as CBCT equipment and applications evolve. As with previous ICRP publications, the Commission hopes that imaging professionals, medical physicists, and manufacturers will use the guidelines and recommendations provided in this publication for implementation of the Commission's principle of optimisation of protection of patients and medical workers, with the objective of keeping exposures as low as reasonably achievable, taking into account economic and societal factors, and consistent with achieving the necessary medical outcomes.

Keywords: Cone beam CT; C-arm CBCT; ICRP recommendations; Dose management CBCT; Interventional CBCT; CT fluoroscopy

AUTHORS ON BEHALF OF ICRP
M.M. REHANI, R. GUPTA, S. BARTLING, G.C. SHARP,
R. PAUWELS, T. BERRIS, J.M. BOONE

PREFACE

The International Commission on Radiological Protection (ICRP) provides recommendations and guidance on application of its principles of radiological protection. This has been done through specific publications on the use of ionising radiation in medicine in various imaging and therapeutic modalities. This is in addition to the reports published by ICRP providing general advice on radiological protection and safety in medicine through *Publication 105* (ICRP, 2007c). Analysis of current technology from the point of view of radiological protection has resulted in recommendations directed at manufacturers that have potential for technological developments for safer technology. In this manner, ICRP has acted as an important resource presaging safety issues based on current and future use of technology, and identifying needs where technology can contribute. Of course, there are vast areas of optimisation where users can play a large role in minimising radiation doses to patients without compromising diagnostic or clinical purpose. In recent years, there have been evaluations of practices which have indicated that a large number of imaging procedures have not met the appropriateness guidelines. While ICRP has provided three levels of justification, there is increasing need to scrutinise justification at Level 3, and provide guidance on justification of an examination. The current climate of interest in radiological protection has enhanced the audience of ICRP publications to cover policy makers, health authorities, public health organisations, patient groups, organisations developing criteria on the appropriateness of different techniques and their use, and a variety of medical specialists who have now started using imaging technology that was not available to them a decade or so ago. This publication addresses the challenges faced with the new technology of cone beam computed tomography (CBCT) that is being used increasingly in day-to-day practice in hospitals by increasing numbers of medical specialists. The advice from ICRP is timely. Issues of patient and worker protection are also addressed in this publication.

The Commission launched a Task Group on Radiological Protection in CBCT in 2013.

The membership of the Task Group was as follows:

M.M. Rehani (Chairman) S. Bartling R. Gupta

The corresponding members were:

T. Berris (to October 2013) J.M. Boone
G.C. Sharp R. Pauwels (from December 2013)

Committee 3 critical reviewers were:

C. Martin R. Loose

Main Commission critical reviewers were:

C. Cousins H-G. Menzel

The membership of Committee 3 during the period of preparation of this report was:

(*2009–2013*)

E. Vañó (Chair)
M.R. Baeza
J.W. Hopewell
D.L. Miller
H. Ringertz
B. Yue
J-M. Cosset (Vice-Chair)
L.T. Dauer
P-L. Khong
P. Ortiz López
M. Rosenstein
M.M. Rehani (Secretary)
I. Gusev
S. Mattson
K.Å. Riklund
Y. Yonekura

(*2013–2017*)

E. Vañó (Chair)
K. Applegate
S. Demeter
R. Loose
K.Å. Riklund
B. Yue
D.L. Miller (Vice-Chair)
M. Bourguignon
K. Kang
C. Martin
P. Scalliet
M.M. Rehani (Secretary)
L.T. Dauer
P-L. Khong
P. Ortiz López
Y. Yonekura

MAIN POINTS

- **The guidelines and recommendations on radiological protection in cone beam computed tomography (CBCT) are important because CBCT extends the use of computed tomography (CT) to areas that were not typically associated with CT imaging in the past, e.g. surgery, dental and otolaryngology [ear/nose/throat (ENT)] clinics, angiography suites, radiotherapy treatment vaults, and orthopaedic polyclinics.**
- **The manufacturers of CBCT scanners have invested considerable effort into meeting the electrical and mechanical safety requirements of the users. Similar diligence is needed for issues related to radiation dose and radiological protection.**
- **This publication provides a basis to develop informed decisions and to direct the use of CBCT for optimising the trade-off between clinical benefit and radiation risk.**
- **The International Commission on Radiological Protection (ICRP) emphasises that protection should be optimised not only for whole-body exposures, but also for exposures to specific tissues, especially those of the lens of the eye, the heart, and the cerebrovascular system.**
- **Equipment used for both fluoroscopy and CBCT should provide aggregate dose indices for individual patients throughout the procedure through electronic display on the operator console and a radiation dose structured report.**
- **Optimisation of both patient and worker doses, particularly when workers have to be near the machine, is important when monitoring of doses becomes an essential tool. Recording, reporting, and tracking of radiation dose for a single patient should be made possible in a consistent manner across vendors.**
- **Low-dose protocols may be sufficient to answer diagnostic questions focused on high-contrast structures, such as lung, bones, dental and maxillofacial scans, ENT scans (paranasal sinuses, skull, temporal bone), interventional material, and contrast-enhanced vessels (angiographic interventions).**
- **Higher-dose protocols should only be selected if visualisation of soft tissue structures, such as intracranial haemorrhage, soft tissue tumours, or abscesses, is the primary focus.**
- **Most interventional and intraprocedural C-arm CBCT systems can scan an angular range spanning 180–240^{o} plus the cone angle of the x-ray beam. Localised critical organs, such as the thyroid, eyes, female breasts, and gonads, should be on the 'detector side' of the arc whenever possible.**
- **Clinical need permitting, every effort should be made by users to ensure that the volume of interest is fully incorporated in the field of view (FOV) provided by the CBCT scanners, while radiosensitive organs should be placed outside the FOV.**
- **The aim of CBCT should be to answer a specific diagnostic or intra-operative question vis-à-vis other imaging modalities, and not to obtain image quality that rivals multi-detector CT (MDCT). The decision by the referring practitioner to use CBCT should be made in consultation with an imaging professional.**
- **There is a need to provide checks and balances, such as dose check alerts implemented in CT in recent years, to avoid high patient doses compared with locally defined reference values.**

- **Methods that provide reliable estimates of dose to the eye under practical situations should be established and used.**
- **The user of CBCT in interventions can influence the radiation dose imparted to the patient significantly by judicious use of a 'low-image-quality or low-dose' scan instead of a 'high-image-quality or high-dose' scan.**
- **In radiotherapy, justified use of CBCT has potential at different stages of therapy such as: pretreatment verification of patient position and target volume localisation; evaluation of non-rigid misalignments, such as flexion of the spine or anatomical changes in soft tissue; and during or after treatment to verify that the patient position has remained stable throughout the procedure. Low-dose CBCT protocols should be used for pretreatment alignment of bony structures.**
- **Many machines were only capable of fluoroscopy initially, but can now also perform CBCT. Due to the improved clinical information in CBCT and its ability to remove overlying structures, the user may be tempted to over-use the CBCT mode. The CBCT mode should be used judiciously.**
- **In orthopaedics, justified use of CBCT can help in assessing the position of fractures and implants with respect to the bony anatomy, especially in situations where fluoroscopy alone is insufficient, and thus can help in patient dose management.**
- **In urology, low-dose CBCT protocols should be used when imaging high-contrast structures, such as calcified kidney stones.**
- **Dental and maxillofacial CBCT scans should be justified, considering alternative imaging modalities. Once justified, they should be optimised to obtain images with minimal radiation dose without compromising the diagnostic information.**
- **The level of training in radiological protection should be commensurate with the level of expected radiation exposure.**
- **All workers intending to use CBCT for diagnostic purposes should be trained in the same manner as for diagnostic CT, and those intending to perform interventional CBCT should be trained in the same manner as for interventional CT.**

GLOSSARY

Absorbed dose, D

The absorbed dose, D, is the quotient of $d\bar{\varepsilon}$ by dm, where $d\bar{\varepsilon}$ is the mean energy imparted by ionising radiation to matter of mass dm, thus:

$$D = \frac{d\bar{\varepsilon}}{dm}$$

The unit of absorbed dose is J kg^{-1}. The special name for the unit of absorbed dose is gray (Gy); $1\,Gy = 1\,J\ kg^{-1}$.

Automatic exposure control (AEC)

A device that automatically determines and provides the exposure needed to produce a preselected image quality by sampling the x-ray intensity at the image receptor.

Collimation

Geometrical limitation of the extent of the radiation beam.

Cone-beam computed tomography (CBCT)

In this publication, the term 'CBCT' is used to designate a subset of computed tomography (CT) scanners that share certain key design features, image quality characteristics, and application domains that distinguish this set of scanners from multi-detector CT (MDCT) scanners. The most characteristic design feature that distinguishes CBCT scanners from MDCT scanners is the use of a two-dimensional digital flat-panel detector to yield a three-dimensional volumetric image in one rotation. Flat-panel detectors in CBCT allow wide cone angle, large z-coverage, and high spatial resolution at the expense of low-contrast resolution.

Dental and maxillofacial imaging

In this publication, dental and maxillofacial imaging refers to imaging of high-contrast structures related to the teeth and jaw bones. Visualisation of other structures (e.g. maxillary sinus, temporomandibular joint, facial skeleton) can be considered as dental and maxillofacial imaging if the primary indication for imaging relates to dentistry. Ear/nose/throat imaging is considered as a separate application in this publication, although it often involves similar radiographic equipment.

Detector quantum efficiency (DQE)

A widely used metric that describes the quality of an x-ray detector. It measures the efficiency (i.e. signal-to-noise performance) of the detector to produce an image from a given incident fluence. Intuitively, it captures how well a detector translates the fluence incident on it into an image, relative to an ideal detector.

Deterministic effect

Injury in populations of cells, characterised by a threshold dose and an increase in the severity of the reaction as the dose is increased further. Also termed 'tissue reaction'. In some cases, deterministic effects are modifiable by post-irradiation procedures including biological response modifiers.

Diagnostic reference level (DRL)

Dose levels in medical radiodiagnostic practices or, in the case of radiopharmaceuticals, levels of activity for typical examinations for groups of standard-sized patients or standard phantoms for broadly defined types of equipment. These levels are not expected to be exceeded for standard procedures when good and normal practice regarding diagnostic and technical performance is applied.

Dose limit

The value of the effective dose or the equivalent dose to an organ received by an individual within a specified period from planned exposure situations that shall not be exceeded. Dose limitation is one of three fundamental principles of radiological protection originally defined by ICRP.

Effective dose, E

The tissue-weighted sum of the equivalent doses in all specified tissues and organs of the body, given by the expression:

$$E = \sum_T w_T H_T$$

where H_T is the equivalent dose in a tissue or organ, T, and w_T is the tissue-weighting factor. The SI unit for effective dose is sievert (Sv), equal to $J\,kg^{-1}$.

Equivalent dose, H_T

The dose in a tissue or organ T given by:

$$H_T = \sum_R w_R D_{T,R}$$

where $D_{T,R}$ is the mean absorbed dose from radiation R in a tissue or organ T, and w_R is the radiation weighting factor. The unit for equivalent dose is the same as for effective dose (sievert, Sv), equal to J kg^{-1}.

Hounsfield unit (HU)

Number used to represent the mean x-ray attenuation associated with each elemental area of the CT image. Measured values of attenuation are transformed into HU (also known as CT numbers) using the Hounsfield scale:

$$HU = \frac{\mu_{material} - \mu_{water}}{\mu_{water}} \cdot 1000$$

where μ is the effective linear attenuation coefficient of the measured material relative to water for the x-ray beam used. The scale is defined so that water has a value of 0 HU and air has a value of −1000 HU.

Justification

One of three fundamental principles of radiological protection originally defined by ICRP. The justification principle requires that the net benefit of radiation exposure should be positive.

Multi-detector computed tomography (MDCT)

According to *Publication 102* (ICRP, 2007a), 'MDCT systems are CT scanners with a detector array consisting of more than a single row of detectors. The 'multi-detector-row' configuration of MDCT scanners refers to the use of multiple detector arrays (rows) in the longitudinal direction (i.e. along the length of the patient). MDCT scanners use third-generation CT geometry in which the arc of detectors and the x-ray tube rotate together. All MDCT scanners use a slip-ring gantry, allowing helical acquisition.' An arc of detector rows used in MDCT should be distinguished from a digital flat-panel detector typically employed by CBCT scanners, as these two different detector technologies

have a very distinct acquisition time, latency, dynamic range, and spatial resolution.

Noise

A fundamental statistical phenomenon that is present in all images. Noise tends to reduce the visibility of structures and objects, especially those that have relatively low contrast. In medical imaging, the objective is not to eliminate the noise, but to reduce it to a clinically acceptable level. Noise is the point-to-point variation in image brightness that does not contain useful information. The magnitude of noise is indicated by the standard deviation of the grey values within a region of interest in the image.

Occupational exposure

All exposure incurred by workers in the course of their work, with the exception of: (1) excluded exposures and exposures from exempt activities involving radiation or exempt sources; (2) any medical exposure; and (3) the normal local natural background radiation.

Optimisation of protection

The likelihood of incurring exposure, the number of people exposed, and the magnitude of their individual doses should all be kept as low as reasonably achievable, taking into account economic and societal factors. In medical imaging, optimisation of protection implies lowest dose for the clinical purpose.

Phantom

A device that absorbs or scatters radiation in an equivalent manner to a patient, used to estimate radiation doses and test imaging systems without actually exposing a patient. A phantom may be an anthropomorphic or a physical test object.

Population dose

An expression for the aggregate radiation dose incurred by a population, defined as the product of the number of individuals exposed to a source and their average radiation dose. The collective dose is expressed in man-sieverts (man-Sv), and is intended solely as an instrument in the optimisation of radiological protection.

Scatter

Deviation of x rays from their original trajectory due to interaction with matter.

Shielding

The placement of a high-absorption material (e.g. lead) between the source and its environment for the purpose of reducing radiation dose to workers, patients, or the public.

Slice

A tomographic section (defined by the position and thickness) of a test phantom or patient under investigation during a single CT or CBCT exposure.

Stochastic effects

Malignant disease and heritable effects for which the probability of an effect occurring, but not its severity, is regarded as a function of dose without threshold.

Worker

Any person who is employed, whether full-time, part-time, or temporarily, by an employer, and who has recognised rights and duties in relation to occupational radiological protection.

1. INTRODUCTION

- **The guidelines and recommendations on radiological protection in cone beam computed tomography (CBCT) are important because CBCT extends the use of computed tomography (CT) to areas that were not typically associated with CT imaging in the past, e.g. surgery, dental and otolaryngology [ear/nose/throat (ENT)] clinics, angiography suites, radiotherapy treatment vaults, and orthopaedic polyclinics.**
- **The manufacturers of CBCT scanners have invested considerable effort into meeting the electrical and mechanical safety requirements of the users. Similar diligence is needed for issues related to radiation dose and radiological protection.**
- **This publication provides a basis to develop informed decisions and to direct the use of CBCT for optimising the trade-off between clinical benefit and radiation risk.**

(1) The guidelines and recommendations on radiological protection in CBCT are important because CBCT extends the use of CT to areas that were not typically associated with CT imaging in the past, e.g. surgery, dental and otolaryngology (ENT) clinics, angiography suites, radiotherapy treatment vaults, and orthopaedic polyclinics.

(2) The International Commission on Radiological Protection's (ICRP) radiological protection principles and recommendations provided in earlier publications, particularly *Publications 87* and *102* (ICRP, 2000a, 2007a), apply to these newer applications and should be adhered to.

(3) The cone beam nature of the radiation field presents new challenges in dose management to ensure patient safety. The manufacturers of CBCT scanners have invested considerable effort into meeting the electrical and mechanical safety requirements of the users. Similar diligence is needed for issues related to radiation dose and radiological protection.

(4) This publication provides a basis to develop informed decisions and direct the use of CBCT for optimising the trade-off between clinical benefit and radiation risk.

(5) Appropriate use of CBCT, including radiological protection, is a joint responsibility of the referring practitioner and the imaging professionals. Imaging professionals also have responsibility towards optimisation of protection. When referring a patient for a diagnostic CBCT examination, the referring practitioner should be aware of the strengths and weaknesses for CBCT vis-à-vis multi-detector CT (MDCT), magnetic resonance imaging, and other competing imaging modalities. The decision to use CBCT should be made in consultation with an imaging professional.

(6) In this publication, the term 'CBCT' is used to designate a subset of CT scanners that share certain key design features, image quality characteristics, and application domains that distinguish this set of scanners from MDCT scanners. The most characteristic design feature that distinguishes CBCT scanners from MDCT scanners is the use of a two-dimensional (2D) digital flat-panel detector (FPD) to yield a three-dimensional (3D) volumetric image in one rotation. FPDs in CBCT allow a wide cone angle, large z-coverage, and high spatial resolution at the expense of low-contrast resolution. Some cone beam scanners still use an image-intensifier

tube. These scanners have a lot in common with flat-panel-based CT scanners and should be considered as CBCT devices. All CBCT scanners have a wide cone angle and large *z*-coverage. The use of a flat panel or image intensifier as a detector means that CBCT scanners have a lower dynamic range and lower soft tissue contrast than MDCT scanners, making them suitable for high-contrast structures such as bones and contrast-enhanced vasculature. Generally, CBCT scanners require longer scan times.

(7) It should be noted that a wide cone angle or large *z*-coverage is not, in itself, sufficient to define a CBCT scanner for the purposes of this publication. Many traditional MDCT scanners, built using individual rows of detectors made of scintillating ceramics, have a wide cone angle and large *z*-axis coverage. For example, the Aquilion One™ (Toshiba Medical Systems) is a 320-row scanner with 16 cm of *z*-coverage. This scanner, and others in its class, should be designated as wide-area MDCT scanners rather than CBCT scanners.

(8) CBCT represents an emerging technology that enables high-resolution volumetric scanning of the anatomy under investigation. Just as in MDCT, use of CBCT is increasing steadily in clinical practice. Although it is a relatively new modality, CBCT is already being used for a variety of clinical applications, such as dental imaging, head and neck imaging (including sinus CT), paediatric imaging, high-resolution bone imaging, and intra-operative and interventional imaging.

(9) CBCT imaging is also used in radiotherapy for pretreatment verification of patient position and target volume localisation. In this case, the CBCT system is usually mounted on the gantry of a linear accelerator at 90° to the therapeutic beam. For radiotherapy, CBCT imaging is often used for daily repositioning. Under classical fractionation schedules, high cumulative imaging dose to tissues outside the exposure field can accrue.

(10) Although the concept of CBCT has existed for over 25 years, it has only recently become possible to develop clinical CBCT systems that are both sufficiently inexpensive and sufficiently small to be used in operating rooms, outpatient clinics, emergency rooms, and intensive care units. Technological and application-specific factors that have converged to make clinical CBCT possible are:

1. compact, high-quality FPD arrays;
2. computer power sufficient for timely cone beam image reconstruction; and
3. x-ray tubes designed for cone beam scanning.

(11) Most modern CBCT systems use a digital FPD instead of an image intensifier for image capture. By virtue of these specialised detectors, which are different from the detectors used in conventional MDCT, CBCT is capable of ultra-high spatial resolution and large-volume coverage in a single (or partial) rotation of the C-arm. Digital FPDs used in CBCT scanners also enable fluoroscopy, radiography, volumetric CT, and dynamic imaging using a single or partial rotation. These capabilities are extremely useful for intra-operative and vascular applications.

(12) The manufacturers of CBCT scanners have invested considerable effort into meeting the electrical and mechanical safety requirements of the users, which are mandated by national regulatory bodies. Similar diligence is needed for issues related to radiation dose. In this respect, the cone beam nature of the radiation field presents new challenges in dose management to ensure patient safety; guidelines are needed for various stakeholders in this new modality. This publication briefly describes the current state-of-the-art CBCT technology, reviews current dose measurement and management approaches, provides recommendations for safe use of CBCT scanners, and identifies gaps that relate to radiological protection where further research is needed.

(13) CBCT systems differ from MDCT systems in several ways that affect image quality and radiological protection. Some key differences are listed below.

(14) Due to the cone beam nature of the irradiated field and the associated non-uniformities in the primary and scatter radiation imparted to the scan volume, the standard dose metrics popularised by MDCT cannot be applied to CBCT, or even to wide-area MDCT scanners.

(15) CBCT systems usually have superior spatial resolution for high-contrast objects (e.g. bone, lung), but inferior contrast resolution for low-contrast objects (e.g. soft tissue). A trained and skilled user of CBCT can influence the radiation dose imparted to the patient significantly by judicious use of 'high-dose' and 'low-dose' scans. A high-dose scan is generally required if soft tissue structures are the main diagnostic focus, while a low-dose scan may be sufficient for angiographic scans with arterial or venous contrast media, or for defining the position of interventional catheters.

(16) Due to the higher spatial resolution of an FPD, CBCT slices are intrinsically thinner and have lower signal-to-noise ratios (SNRs) for the same dose than MDCT slices. Any attempt to match the SNR in a thin CBCT slice with a thick MDCT slice will result in a proportionate increase in dose. Instead, increasing the slice thickness, or other similar image processing methods, should be applied to improve the SNR in CBCT.

(17) In many CBCT scanners, the angular span over which the projection data are acquired can be customised. This feature may also be available in some MDCT scanners (e.g. some systems allow tube current to be reduced when the beam is covering radiation-sensitive organs such as the breast, thyroid, or lens of the eye). It should be used in both types of scanner systems to minimise the dose to selected organs.

(18) The purpose of this publication is to identify radiological protection issues for patients and workers and, in line with other ICRP publications, recommendations are set out for all stakeholders ranging from day-to-day clinical users, auxiliary support workers, buyers, manufacturers, and policy directing committees.

(19) The primary target audience of this publication, as for most other publications produced by the Commission related to protection in medicine, is health professionals working with CBCT, other workers tasked with radiological protection

and image quality optimisation in CBCT, manufacturers of imaging equipment, regulators, and policy makers in charge of radiological protection.

1.1. History of development

(20) The first CBCT scanner was built for angiography at the Mayo Clinic, Rochester, NY, USA in 1982 (Robb, 1982). Multiple teams in the early 1990s pursued the idea of multi-angle projections from a wide-area detector for medical imaging. For example, Saint-Félix et al. (1994) tested a system called the 'Morphometer' consisting of two imaging chains, each with an x-ray tube and an image intensifier. This CBCT system was designed for 3D angiography using the gantry of a conventional CT scanner. It reconstructed vascular images from a set of digitally subtracted angiography images. This gantry platform, which was never released clinically, was abandoned in favour of a C-arm supporting a single imaging chain.

(21) Fahrig et al. (1997, 1998) also developed a CBCT system based on an image intensifier and C-arm for use in angiography. Wiesent et al. (2000) developed a similar system comprising a C-arm plus an image intensifier for interventional angiography. Ning et al. (2000a,b) and Wang (1997) developed a CBCT angiography imager based on a GE 8800 CT scanner with an image intensifier–charge-coupled device chain and later with an FPD. Schueler et al. (1997) and Kawata et al. (1996) developed a CBCT angiography scanner based on a biplanar C-arm system.

(22) Siewerdsen and Jaffray developed a CBCT system for radiotherapy guidance based on an amorphous silicon FPD (Siewerdsen and Jaffray, 1999, 2001; Jaffray and Siewerdsen, 2000). Efforts are also underway to build a dedicated CBCT-based imaging system for mammography (O'Connell et al., 2010; Kalender et al., 2012; Packard et al., 2012).

(23) CBCT devices were introduced in dental and maxillofacial radiology in the late 1990s (Mozzo et al., 1998; Arai et al., 1999).

1.2. Current standards in radiological protection in CBCT

(24) The guidelines and recommendations on radiological protection in CBCT are particularly important as CBCT extends the use of CT to areas that were not typically associated with CT imaging in the past, e.g. surgery, dental and otolaryngology (ENT) clinics, angiography suites, and orthopaedic polyclinics. Fundamentally, CBCT is a form of CT; as such, most facility design and quality assurance (QA) requirements that apply to MDCT should also be applied to CBCT. This, however, can lead to an erroneous impression that CBCT is identical to MDCT, making it difficult to manage CBCT from operational and radiation safety points of view. Further complications arise when a user is tempted to regard CBCT as a 'light' or 'low-dose' CT; a view that is maintained because CBCT functionality is often an adjunct to existing capabilities, such as fluoroscopy and angiography in a C-arm or other clinic-based system. Embedded in these user biases is the risk for potential

overuse of CBCT resulting in unnecessary radiation dose to the patients and/or workers.

(25) Traditionally, the use of CBCT in dentistry has entailed a relatively low radiation dose. However, this is not always the case, and many recent applications of CBCT, especially in ENT and interventional procedures, can impart much higher radiation doses that equal or exceed those from MDCT (Kyriakou et al., 2008a; Dijkstra et al., 2011; Schulz et al., 2012). There are also situations in which multiple CBCT procedures have to be performed on one patient (such as CBCT-guided interventions), enhancing the need to keep the inflicted radiation dose to a minimum. Therefore, dose implications of CBCT pose a risk from the perspective of an individual patient, as well as for the risk from radiation exposure of the population as a whole.

(26) Imaging professionals and medical physicists are well aware of the radiation dose issues in CT. This knowledge, however, does not directly translate to CBCT, for which the trade-off between image quality and radiation dose can be quite complex. At the same time, clinical users, as well as those undertaking QA and members of radiation safety committees, need clear guidelines on operating and regulating these systems. This publication, which is thought to be the first on radiological protection in CBCT from an international source, provides a basis for developing informed clinical decisions on the use of CBCT and guidance for optimising the trade-off between clinical benefit and radiation risk.

1.3. Responsibilities of different stakeholders

(27) Approximately 80 million CT scans are performed every year in the USA, and this number is increasing on a yearly basis (Sierzenski et al., 2014). Multiple recent papers have drawn attention to the population dose from these scans (Brenner, 2010). There is also increasing realisation that a large fraction of this radiation dose to the population is avoidable as it comes from unjustified or inappropriate examinations. Currently, data on inappropriate use are mostly available for CT rather than CBCT. Appropriate use of CT scanning is a joint responsibility of the referring practitioner and the imaging professional, and most national regulations assign this responsibility either jointly or to the imaging professional. As a referring practitioner best understands the clinical need for the examination, he/she must interact with an imaging professional to decide upon the radiological examination or procedure that is in the best interests of the patient. Electronic referrals with decision support have the potential to simplify and streamline this interaction while making this process more evidence based (Sistrom et al., 2009). Such systems can go a long way towards facilitating the desired radiological examination performed with the lowest radiation dose, while maintaining the image quality needed for the clinical purpose. Practitioners, technologists, and medical physicists must understand their roles and responsibilities in this endeavour. To this end, there is a need to further develop methods that facilitate the interaction between referring

practitioner and imaging professional to translate their joint responsibility for radiological safety into practice.

(28) Over the years, manufacturers have played a vital role in technological developments to reduce patient doses from particular CT examinations. The Commission, while acknowledging this role, hopes that manufacturers will remain at the forefront of developing new technologies for radiological protection of patients and workers.

1.4. Why is it important to know CBCT doses?

(29) It is easy for a practitioner, not versed in the details of dose management, to dismiss CBCT as upgraded fluoroscopy coupled with 3D reconstruction. For the most part, the dose from CBCT is indeed lower than that from MDCT, which may reinforce this belief. However, uncritical application of CBCT under the assumption that it is a modality with minimal dose consequences could result in significant doses in some circumstances, and is not appropriate for protection of the patient.

(30) CBCT is a relatively new development in clinical practice. Data on radiation doses and possible effects of CBCT are still being gathered and analysed. Even at this early stage, however, studies indicate that there is room for optimisation to keep the radiation dose as low as reasonably achievable. This publication systematically summarises the available dose data related to use of CBCT, and discusses radiological protection issues for patients and workers. Given the potential of CBCT to become a significant source of radiation dose to patients in the future, it is appropriate to be mindful of the radiation exposure while using the full diagnostic potential of this exciting modality. In 1999–2000, while preparing *Publication 87* (ICRP, 2000a; Rehani and Berry, 2000), the Commission had similarly presaged the need to watch for increasing radiation doses from MDCT. Although this concern was not well appreciated at that time, it has become a major issue in subsequent years with multiple high-profile reports in the media. This publication provides a similar review of the current CBCT literature, and presents the data regarding radiation doses to patients and workers associated with the use of CBCT.

1.5. Safety in perspective

(31) Safety is achieved most readily when it is built into the system, rather than a matter of choice for users. A good example is a collision avoidance system; an innovation that started in the automobile industry but has been implemented in multiple types of imaging gantries to avoid accidents. With such a system in place, if the gantry of the imaging device comes into contact with a person or object, it simply stops moving. In the absence of such a system, when collision avoidance has to be accomplished primarily via user education, training, and instructions, the risk of injury from collisions will be higher. There are instances when both detection of an anomalous condition and its automatic avoidance cannot be implemented simultaneously. In such cases, detection and warning may accomplish a similar end result.

For example, radars for detection of speed limits have been shown to decrease the incidence of speeding violations.

(32) For radiation safety in MDCT, a display of radiation exposure information on the operator console has been present for a number of years. After a series of accidental exposures was reported in the USA in 2007–2008, MDCT systems can now automatically detect settings to prevent accidental exposure (NEMA, 2010). Such systems provide an additional layer of non-intrusive checks and balances in the conduct of a scan. Display of such information on CBCT consoles needs to be standardised. The Commission recommends development and implementation of safety systems that require the least amount of interaction from the operator and workers while providing:

- regular and continuous monitoring of radiation output throughout the examination;
- automatic comparison with reference or desired dose levels that need to be established;
- timely feedback to the system operator;
- wide availability of automatic adjustment of the dose to a prescribed level in a manner that is somewhat similar to automatic exposure control (AEC); and
- alerts when dose is higher than specified. Currently, dose checks do not apply to CBCT systems (NEMA, 2010).

(33) Other technologies that many CBCT vendors need to implement uniformly include automatic collimation control so that the x-ray beam always falls on the detector, guidance for instruments during image-guided interventions, and minimisation of scatter dose resulting from mechanical components.

1.6. Scope of this publication

(34) As a substantial amount of information is currently available on dental and maxillofacial CBCT, including a publication issued by the European Commission (EC) project SEDENTEXCT (Safety and Efficacy of a New and Emerging Dental X-ray Modality) (http://www.sedentexct.eu/) (EC, 2012a), the decision was made to cover dental and maxillofacial CBCT briefly in this publication

(35) It should be emphasised that the main focus of this report is on doses to patients and workers from CBCT acquisitions. CBCT acquisition can be part of fluoroscopically guided procedures. In such cases, it is necessary to account for the dose from fluoroscopy and relevant implications. *Publication 117* included information pertinent to radiological protection of patients and workers in fluoroscopic procedures performed outside the imaging departments (ICRP, 2010), and *Publication 120* covered radiological protection of patients and workers during interventional fluoroscopy (ICRP, 2013). The term ‘patient dose’ has been used in this publication in a qualitative and relative sense, and wherever quantitative figures are provided, the appropriate dose quantity [i.e. skin dose, organ dose, kerma-area product (KAP), effective dose, etc.] has been mentioned.

2. CBCT TECHNOLOGY

2.1. Introduction

(36) In the past decade, development of digital FPDs for conventional x-ray radiography, fluoroscopy, and mammography has propelled the use of CBCT into the mainstream of medical imaging. Most CBCT systems in current use leverage the power of dynamic FPDs (i.e. able to acquire several frames s^{-1} compared with static FPDs) to provide volumetric 3D datasets.

(37) A C-arm gantry consisting of a digital FPD and a large cone-angle x-ray tube is the most commonly used platform for CBCT. There are a number of other implementations of CBCT that differ in the mechanical gantry used for scanning, the detector subsystem, the type of x-ray tube and filtration, the cone angle employed for imaging, and the algorithm used for reconstructions. The following section describes and introduces different types of CBCT scanners.

2.2. Technological issues

(38) As far as tomographic capabilities of a CBCT scanner are concerned, in simple terms, one can think of them as a conventional MDCT in which the rows of detector elements (typically 16–64 rows) have been replaced by an area detector (Ross et al., 2004; Grasruck et al., 2005; Popescu et al., 2005). In general, a CBCT scanner consists of an x-ray source, a detector, and a gantry to move this imaging chain around the patient. The most commonly used subsystems are described briefly below.

2.2.1. X-ray source

(39) The x-ray source used in a CBCT scanner must provide a broad, cone-shaped beam of radiation. Consequently, CBCT scanners use a much larger anode angle than a tube used in an MDCT scanner. Typical operating conditions are an x-ray tube voltage of 50–140 kVp, a tube current of 10–800 mA, and a total power of 10–80 kW. In order to take advantage of the small detector pixel size, the focal spot size ranges from 0.2 mm to 0.8 mm. The typical field of view (FOV) covered in one rotation, using a single FPD, can be as much as 25 cm in the angular direction, and 20 cm in the z-direction. Larger sizes are possible when multiple panels or dual scans are used, such that the principal axis of the x-ray illumination is offset from the centre of the panel to allow beam correction.

2.2.2. Detector

(40) While some older systems still use an image intensifier, most modern CBCT scanners use a digital FPD. FPDs provide higher dose efficiency and dynamic range

than other detector technologies they replaced (x-ray film, film/screen combinations, and image intensifiers); however, their dynamic range is lower than that of standard MDCT detectors (Miracle and Mukherji, 2009a). FPDs also generally provide higher spatial resolution than image intensifiers and conventional detector arrays used in MDCT. Direct digital readout up to 30 frames s^{-1} ensures that the data are available in a directly usable form for both projection and 3D reconstruction.

(41) The native resolution of a flat panel is typically at or below 200 μm, although higher resolution detector panels are available. After accounting for magnification and x-ray focal spot size, this yields an isotropic voxel resolution of approximately 150 μm. Generally, in 3D acquisition mode, FPDs are operated in a 2×2 binning mode (summing signals from two rows and two columns to increase the SNR and the readout speed, and reduce the matrix size), and the isotropic resolution is of the order of 200 μm. Therefore, compared with conventional MDCT scanners, a flat-panel-based CBCT system improves the spatial resolution by a factor of almost 12 on a voxel-by-voxel basis. Its high spatial resolution is capable of visualising complex human anatomy, including fine structures of the maxillofacial region and skull base.

(42) Typically, FPDs used in CBCT are composed of a matrix of detector elements that can span anywhere from $5 \times 5\,cm^2$ to $40 \times 40\,cm^2$. Such scanners, therefore, are capable of producing a large number of slices spanning anywhere from 5 to 20 cm in one rotation. The *z*-coverage afforded by these scanners can be large enough to image an entire organ such as the brain, heart, liver, or kidneys in one axial scan.

2.2.3. Gantry

(43) Depending on the mechanical system of the gantry, CBCT scanners can allow conventional fluoroscopy, angiography, and radiography in the same setup as well as providing high spatial resolution and large-volume coverage. These facilities make such machines especially attractive for intra-operative and vascular applications. The various gantry platforms in common use are described below.

C-arm-based CBCT

(44) All major imaging equipment vendors now provide C-arm scanners that employ digital FPDs integrated with a C-arm gantry (Fig. 2.1). The C-arm platform offers open architecture and ready patient access. There are two major C-arm-based setups that need to be distinguished: C-arm-based interventional CBCT systems and dedicated C-arm-based CBCT systems.

(45) *C-arm-based interventional CBCT systems*. One can use the C-arm for fluoroscopy and projective angiography (including digitally subtracted angiography). However, by putting the C-arm in a fast-spin mode while acquiring images, one can obtain projection data that can be converted into relatively high-quality, high-contrast CT images. Interventional procedures are usually performed using

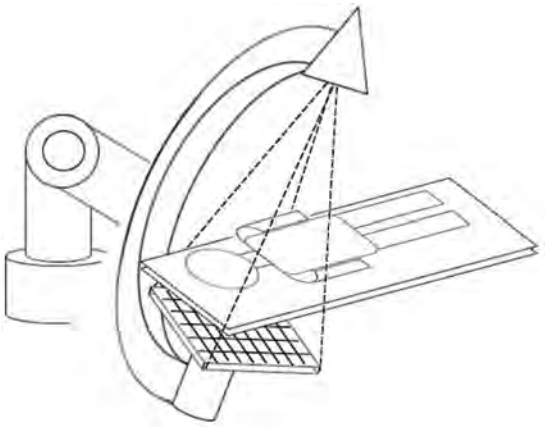

Fig. 2.1. C-arm-based cone beam computed tomography. A C-arm is used to mount the imaging chain, and this provides the necessary amount of freedom required to revolve around the patient. C-arm systems are used in surgical, orthopaedic, urologic, or interventional environments (image provided by Rolf Kueres).

fluoroscopy. The operator can use the CBCT mode intermittently for clarification and 3D localisation (Orth et al., 2008; Schafer et al., 2011). These machines, therefore, enable a seamless integration of these previously separate modalities. They are used in angiographic, surgical, orthopaedic, urologic, and other interventional settings.

(46) *Dedicated C-arm-based CBCT systems*. A number of systems dedicated for dental, ENT, head and neck, extremity imaging, and mammography are available. One popular variation of C-arm-based CBCT systems is the so-called 'seat scanner', in which a small C-arm, with a horizontal imaging chain consisting of an FPD and an x-ray tube, revolves around the head of the patient while they sit on a chair (Fig. 2.2). Alternatively, for certain models, the patient is in a supine or standing position. These scanners are dedicated to dental, maxillofacial, and temporal bone applications because of their relatively small scan FOV. Besides weight and mechanical considerations, there is no fundamental reason why their FOV cannot be increased. They are currently limited to these niche applications.

CT-gantry-based CBCT

(47) A flat-panel volume CT scanner combines a continuously rotating CT gantry with digital FPD technology (Fig. 2.3). It is, in fact, a CT machine in which the detector rows have been replaced by an FPD. From an operational point of view, the main difference between a CT-gantry-based and a C-arm-based cone beam system lies in basic engineering: the gantry-based systems are more stable and have fewer

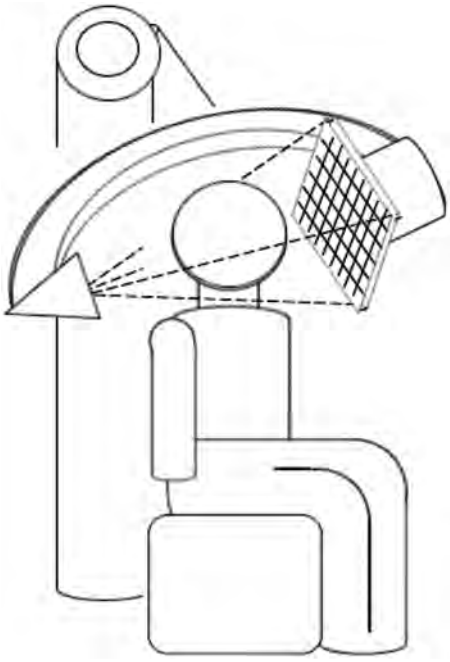

Fig. 2.2. Clinic-based cone beam computed tomography. The imaging chain is mounted on a horizontal rotating C-arm. These systems are usually used in head and neck applications (image provided by Rolf Kueres).

geometric inaccuracies compared with the C-arm-based systems. In addition, the isocentre of any CT gantry, by virtue of its mechanical design, is defined much more precisely than the best C-arm gantries. As a result, gantry-based designs may, in most cases, offer better spatial resolution.

(48) In a C-arm system, the detector and the x-ray tube are connected to the control hardware by an umbilical cord of cables that prevents them from spinning continuously around the patient. This is not the case for a CT-gantry-based system, in which a slip ring is used to take data from a rotating component. Elaborate collision avoidance schemes have been implemented to ensure operator safety. No such concerns exist for CT-gantry-based systems.

(49) By virtue of an FPD, CT-gantry-based CBCT systems are capable of ultra-high spatial resolution, direct volumetric imaging, and continuous rotation around a patient. Continuous rotation enables dynamic CT scanning; the ability to observe a process evolving with time [e.g. perfusion of an entire organ such as the brain, liver, or kidney (e.g. after transplant or an ischaemic event)].

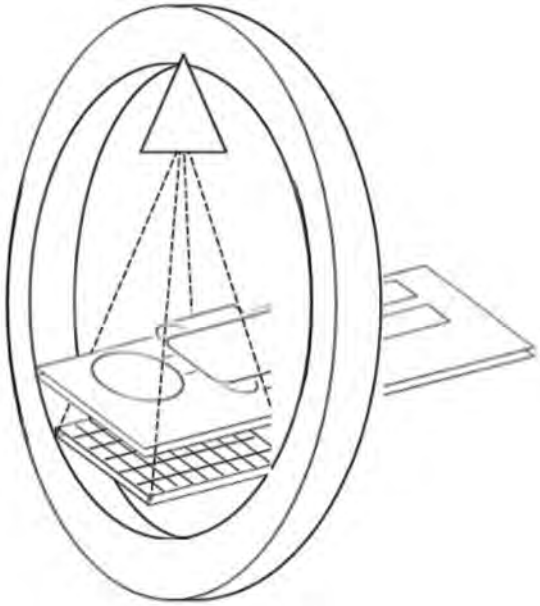

Fig. 2.3. Gantry-based cone beam computed tomography. The patient lies on a patient bed, and the imaging chain revolves around the patient as in multi-detector computed tomography (image provided by Rolf Kueres).

CBCT in radiotherapy

(50) In radiotherapy, CBCT is used for precise alignment of the target volume with a therapeutic, hard x-ray beam from a linear accelerator. Two separate arrangements (kV CBCT and MV CBCT) are popular. In kV CBCT, a separate imaging chain consisting of an x-ray tube operated in the kV range is used as the x-ray source, and an FPD is used for imaging. The entire imaging chain is mounted on the linac gantry, in an orientation that is orthogonal to the therapeutic beam. Similar to C-arm systems, a linac gantry only rotates up to 360°, after which the gantry must be rotated back. Some systems enable a larger FOV to be imaged by scanning target volumes asymmetrically using two 180° rotations, and shifting the FPD laterally for the second. Such systems use separate half-bowtie filters for the two parts of the scan. A routine CBCT scan is conducted prior to therapy for precise alignment.

(51) MV CBCT uses the high-energy x rays from the linac itself for imaging. An FPD that can operate at very high x-ray photon energies is used to acquire the projection data, and a separate imaging chain is not required. Given the high photon energy and associated decrease in photoelectric absorption, the soft tissue contrast of MV CBCT is markedly worse than that of kV CBCT. However, it is

sufficient to visualise bony anatomy, which may be acceptable for alignment purposes.

Co-integrated systems

(52) Co-integrated systems exist mainly in nuclear medicine (e.g. single photon emission tomography) (Sowards-Emmerd et al., 2009). Here, a flat-panel CBCT system is mounted on the same gantry as the nuclear imaging chain. The CBCT data are used for attenuation correction and anatomical localisation.

2.3. Clinical scenarios where CBCT is used

(53) In current clinical practice, CBCT scanners are used for a variety of imaging applications ranging from preclinical to clinical imaging (Table 2.1). Their use is primarily motivated by taking advantage of the following characteristics: (1) combining dynamic fluoroscopy/angiography and tomographic imaging; (2) large z-coverage; and (3) high-resolution imaging of high-contrast structures.

Table 2.1. Cone beam computed tomography (CBCT) in a variety of medical applications ranging from research to clinical imaging.

Application	Setup	Synonyms	Main reason why CBCT is used*	Use cases	Common use examples of CBCT
Non-vascular interventional procedures	C-arm system	3D C-arm, CBCT	1, 2	Liver intervention, abscess drainage, skeletal interventions	Spatial position of intervention instruments and material
Vascular head/body interventions	C-arm system	Angiographic CT, rotational angiography CT	1	Tumour embolisation, bleeding, revascularisation in peripheral occlusive disease	Spatial position of intervention instruments, rule out bleeding, embolisation therapy control
Vascular cardiac interventions	C-arm system	Rotational angiography CT	1	Electrophysiological catheter ablation	Spatial position of intervention instruments
Orthopaedic interventions	Mobile C-arm/O-arm systems		1, 2	Osteosynthesis	Spatial position of implants, complex fractures
Radiation therapy planning/guidance	Gantry or C-arm (with treatment system)		2	Tumour therapy	Patient registration, physiological motion control
Dental and maxillofacial, ENT	Over-the-head C-arm 'seat-scanner'/ gantry based	DVT	3	Dental workup, paranasal sinus, temporal bone	Diagnostic imaging, datasets for navigation (e.g. implant placement)
Breast†	Horizontal gantry based		2, 3	Rule out carcinoma, biopsy	

(continued on next page)

Table 2.1. *(continued)*

Application	Setup	Synonyms	Main reason why CBCT is used*	Use cases	Common use examples of CBCT
Urology	C-arm		2, 3	Lithotripsy, diagnostic workup	Diagnostic imaging, stone detection
Nuclear medicine hybrid imaging (SPECT/CT)	Transmission and emission systems mounted on rotating gantry		2	Attenuation correction, anatomical localisation (fused physiological and anatomical data sets)	Myocardial perfusion imaging, skeletal imaging, oncology imaging
Peripheral bone imaging	C-arm/gantry based		3	Osteoporosis	Bone microstructures, bone density
Animal imaging/specimen imaging	Bench-top, gantry based		2, 3	Research and veterinary	Experimental imaging

3D, three dimensional; CT, computed tomography; ENT, ear/nose/throat; DVT, digital volume tomography; SPECT, single photon emission computed tomography.

*1, combining dynamic fluoroscopy/angiography and tomographic imaging; 2, large *z*-coverage; and 3, high-resolution imaging of high-contrast structures.

†Digital breast tomosynthesis may also be regarded as a form of limited-angle CBCT with a specialised reconstruction algorithm.

3. BIOLOGICAL EFFECTS OF RADIATION

- **ICRP emphasises that protection should be optimised not only for whole-body exposures, but also for exposures to specific tissues, especially those of the lens of the eye, the heart, and the cerebrovascular system.**

3.1. Introduction

(54) The health effects of ionising radiation are classified into two main categories: tissue reactions (deterministic effects) and stochastic effects. Tissue reactions include skin erythema, hair loss, cataracts, infertility, vascular disease, and haematopoietic and gastroenterological effects. Stochastic effects, on the other hand, are cancer and heritable (genetic) effects.

(55) Tissue reactions appear when the radiation dose exceeds a specific threshold. The severity of the reaction depends on the total radiation dose received by the organ or part of the organ. Stochastic effects are governed more by the inherent randomness in microscopic interactions between radiation and biological matter. In most cancer models, the probability of cancer induction due to exposure to radiation is considered to be proportional to the radiation dose. Moreover, for the purpose of radiological protection, no matter how low the radiation dose, theoretically there is always a small probability that it will induce cancer or heritable effects.

3.2. Tissue reactions

(56) For tissue reactions, the damage to cells is related directly to radiation dose, and a dose threshold exists. *Publication 103* (ICRP, 2007b) states that, 'The reason for the presence of this threshold dose is that radiation damage (serious malfunction or death) of a critical population of cells in a given tissue needs to be sustained before injury is expressed in a clinically relevant form. Above the threshold dose, the severity of the injury, including impairment of the capacity for tissue recovery, increases with dose.' Tissue reactions have thresholds that are typically of the order of a few hundred mGy. Skin effects may occur at absorbed doses of 3 Gy; threshold doses for other organs are provided in Table 3.1.

(57) As a classical example, erythematous effects commonly occurred on workers' hands during the early days of radiology, about a century ago. Such symptoms have occurred rarely in workers using medical x rays in the last 50 years. However, skin injuries have been observed among patients due to fluoroscopic procedures in interventional radiology and cardiology (ICRP, 2000b, 2013; Balter et al., 2010; Rehani and Srimahachota, 2011). Also, in interventional procedures, problems including hair loss and chronic occupational dermatitis have been reported for radiologists and cardiologists on body parts unprotected by the lead apron or lead table shield (Wiper et al., 2005; Rehani and Ortiz López, 2006). To the best of the authors' knowledge, there have been no reports, to date, of skin injuries in patients undergoing CBCT. Regarding MDCT, skin injuries have been observed in the past few years

Table 3.1. Estimates of threshold organ doses for tissue effects in adult human testes, ovaries, lens of the eye, and bone marrow.

Tissue and effect	Threshold for total dose in a single exposure (Gy)	Threshold for annual dose in the case of fractionated exposure (Gy year^{-1})
Testes		
Temporary sterility	0.15	0.4
Permanent sterility	6.0	2.0
Sterility	3.0	>0.2
Lens of the eye		
Cataract (visual impairment)	0.5	
Bone marrow		
Depression of haematopoiesis	0.5	>0.4
Heart or brain		
Circulatory disease	0.5	

Reproduced from ICRP (2007b; Table A.3.1) with updated information regarding the lens of the eye and heart from ICRP (2012b).

in patients undergoing MDCT scans, mainly as a result of inappropriate use of scanners (ICRP, 2007a). Hair loss has been reported among patients undergoing brain perfusion CT (Bogdanich, 2009, 2010; Wintermark and Lev, 2010). Although skin injuries related to CBCT have not been reported among patients or workers, the technique is relatively new; as use of CBCT increases, there may be potential for such injuries, particularly in cases of poor radiological protection practice.

(58) Besides skin injuries, there have been recent reports of radiation effects on the lens of the eye, which is one of the most radiosensitive tissues in the body (Rehani et al., 2011; ICRP, 2012). Radiation-induced cataracts have been demonstrated among workers involved in interventional procedures using x rays (Vañó et al., 1998; ICRP, 2000b), but not with CT or CBCT. However, an earlier study by Klein et al. (1993) and a more recent study by Yuan et al. (2013) indicated that there may be elevated risk for damage to the lens of the eye in patients undergoing CT scans. Similar risks can be anticipated in patients undergoing CBCT (e.g. in neuroradiological interventions when the eye is exposed to the primary beam). Currently, there is a paucity of data and it is difficult to judge the risk for patients. Caution is recommended where the primary beam irradiates the eye, and thus careful attention to optimisation is necessary.

(59) In addition to patients, there are populations exposed to low doses. For some such groups, lens opacities have been documented, including workers in interventional suites (Ciraj-Bjelac et al., 2010, 2012; Vañó et al., 2010, 2013; Rehani et al., 2011), astronauts (Cucinotta et al., 2001; Rastegar et al., 2002), radiological technologists/radiographers (Chodick et al., 2008), atomic bomb survivors (Nakashima

et al., 2006; Neriishi et al., 2007), and people affected by the Chernobyl accident (Day et al., 1995).

(60) Recent epidemiological data suggest that tissue reactions can occur at threshold doses that are lower than considered previously (ICRP, 2010, 2012). These reactions usually take a long time to manifest. For lens opacities, the threshold for damage is now considered to be as low as an absorbed dose of 0.5 Gy, whereas it was previously set at 2 Gy (depending upon exposure scenario). The absorbed dose threshold for circulatory disease has been chosen as 0.5 Gy to the heart or brain, as a precautionary value. ICRP policy has been not to set any dose limits for patients. However, the current recommendation of ICRP for occupational exposure in planned exposure situations is an equivalent dose limit for the lens of the eye of 20 mSv $year^{-1}$, averaged over a defined 5-year period, with no single year exceeding 50 mSv (ICRP, 2012). Occupational doses to the lens of the eye of a few μGy in CBCT have been reported in the literature. Doses to the lens of the eye for patients are a few mGy for dental and head and neck CBCT with direct exposure, but doses are much higher for interventional CBCT. Details regarding doses to the lens of the eye in CBCT for patients and workers are available in Sections 6 and 7.

3.3. Stochastic effects

(61) Cancer and heritable effects come into the category of stochastic effects. The probability of carcinogenic effects is much higher than that of heritable effects. This follows from *Publication 103* (ICRP, 2007b) which states that the detriment-adjusted nominal risk coefficient or stochastic effects for the whole population after exposure to low doses of radiation is 5.5% Sv^{-1} for cancer and 0.2% Sv^{-1} for heritable effects. The latter is a theoretical risk for humans, as all documented cases of radiation-induced heritable effects come from observations in non-human species. Cases in humans have not been observed, even for atomic bomb survivors. Therefore, after careful review of many decades of literature, ICRP has reduced the tissue-weighting factor for the gonads relating to the risk of heritable effects to less than half the previous value, from 0.2 to 0.08 (ICRP, 2007b).

4. PRINCIPLES OF RADIOLOGICAL PROTECTION FOR PATIENTS AND WORKERS

(62) The system of protection recommended by ICRP consists of three fundamental principles of radiological protection: justification, optimisation of protection, and application of dose limits (ICRP, 2007b). Dose limits are only applicable for radiological protection of workers and the public; diagnostic reference levels (DRLs) are used for the protection of patients (ICRP, 2007c).

4.1. Justification

(63) The justification principle requires that any decision that alters the exposure situation should do more good than harm. According to ICRP, there are three levels of justification for the use of radiation in medicine.

- At Level 1, the use of radiation in medicine is acceptable when it results in more good than harm to the patient. It is now taken for granted that the use of x rays in medicine is justified.
- At Level 2, a specified procedure with a specified objective is defined and justified (e.g. a CBCT examination for patients showing relevant symptoms, or a group of individuals at risk of a condition that can be detected and treated).
- At Level 3, the use of radiation in an individual patient should be justified (e.g. the particular CBCT application should be judged to do more good than harm to the individual patient).

(64) According to *Publication 87* (ICRP, 2000a), requests for a CT examination should only be generated by properly qualified medical or dental practitioners as defined by national educational and qualification systems. Justifying individual exposures should include verification that the information required is not already available from previous studies, and that the proposed study is really going to answer the questions posed (ICRP, 2007b). The referring practitioners and imaging professionals should be skilled in the selection of, and indications for, CT, CBCT, and angiography, and possess adequate knowledge concerning alternative techniques. This training should also apply to non-imaging professionals who plan to use CBCT. Further aspects of training are provided in Section 8. The availability of resources and cost should also be considered in the justification process.

(65) Justification of CBCT is a shared responsibility between the referring practitioner and the imaging professional. In the case of self-referral (e.g. practitioners in outpatient dental and ENT clinics), wherein the referring practitioner and the imaging professional are the same person, their responsibilities are combined within one person. Referring practitioners know their patients and their medical histories, but typically have little or no knowledge about radiation doses, or the risks and limitations of diagnostic radiological examinations. On the other hand, imaging professionals have expertise regarding radiological examinations, including knowledge of alternate imaging examinations that can provide similar information with less

radiation exposure of the patient; they, however, lack in-depth knowledge about the individual patient's condition. Consultation between imaging professionals and referring practitioners is essential to make the most of their combined knowledge. While such consultation has been emphasised before, practical constraints have made its implementation difficult to realise in practice, and there is a need for exploration of tools to make this possible.

(66) ICRP has noted that there are many reports documenting lack of justification, particularly for CT examinations although not yet for CBCT (Rehani and Frush, 2010; Fraser and Reed, 2013). ICRP recommends the use of modern technologies such as clinical decision support systems with electronic referral to improve justification.

4.2. Optimisation

(67) Once an examination is justified, protection of medical workers and patients must be optimised.

(68) The primary role for optimisation of CBCT lies with the CBCT facility, and it should ensure that the examination is performed with the lowest radiation dose to the patient while obtaining the image quality required for the clinical purpose.

(69) DRLs have been used to promote optimisation and have shown good results in many countries, particularly for CT applications. They were developed to identify examinations with doses above the 75th percentile in the dose distribution so that corrective actions could be taken. However, as expressed in ICRP's concept of as low as reasonably achievable, they do not obviate the need for optimisation below the 75th percentile dose (Rehani, 2013). With modern technical equipment and optimised protocols, dose levels between the 25th and 50th percentile are achievable (NCRP, 2012), so users should aim to optimise within DRLs (Rehani, 2013). The optimisation of patient protection in CBCT requires the application of examination-specific scan protocols tailored to patient age or size, region of imaging, and clinical indication. Protocols provided by the vendors of CT scanners should be evaluated for optimisation. DRLs are just one of the practical tools to promote the assessment of existing protocols. The ability to compare dose levels between CBCT facilities would facilitate the development of appropriate, new, and improved protocols at each CBCT centre.

(70) DRLs for CBCT procedures need to be established. To achieve this, doctors performing CBCT examinations should work closely with medical physicists.

4.3. Requirements for imaging facilities

(71) Practice varies worldwide but should comply with requirements laid down by national authorities. Typically, each CBCT scanner should be registered with the appropriate database under the overall oversight of a national or designated authority. Frequently, during the process of registration and authorisation, an authority will examine the specifications of the machine, and the size and shielding of the room

where it is going to be used, ensuring that workers and members of the public are sufficiently protected. The International Electrotechnical Commission (IEC, 2012) and the International Organization for Standardization provide international level safety requirements for x-ray machines. In many countries, national standards for x-ray machines are also available. These requirements are intended to protect workers and members of the public who may be exposed to radiation. The registration and authorisation process will also assess the availability of qualified staff. There are requirements for periodic quality control tests for constancy and performance evaluation. Acceptance tests and periodic quality control testing of CBCT equipment can provide confidence in equipment safety and its ability to provide images of optimal image quality. Such periodic testing is essential because a malfunctioning machine may expose patients unnecessarily to radiation without any other overt signs. Nevertheless, whatever national requirements are in place, it is essential that they are followed in order to ensure that facility design and operation are safe for patients, workers, and the public.

5. ASSESSING PATIENT DOSES IN CBCT

- **Equipment used for both fluoroscopy and CBCT should provide aggregate dose indices for individual patients throughout the procedure through electronic display on the operator console and a radiation dose structured report.**

5.1. Dosimetry in CBCT

(72) CBCT uses a wide x-ray beam for 3D imaging of a relatively large volume. Since the mid-1990s, the trend in MDCT has been towards an ever-increasing number of slices with a concomitant increase in x-ray beam width; the *z*-axis coverage of the high-end, wide-area MDCT scanners available today rivals that of CBCT. These developments have created a drive to update CT dosimetry methods so that they are more apropos wide-area detectors. As a result, some of the work from MDCT dosimetry, for which established measurement methods and phantoms exist already, can be translated to CBCT dosimetry. This section and Annex A present the shortcomings of the standard narrow-beam MDCT formalism when it is applied directly to CBCT. Methods to overcome these problems are described in Annex A in order to construct a comprehensive framework for CBCT dosimetry.

(73) CT dosimetry has evolved around the concept of the CT dose index (CTDI). In order to connect CTDI-like measurements with dose, volume CTDI ($CTDI_{vol}$) and dose length product (DLP) have been used extensively in clinical practice as relative patient dose indicators. One of the strengths of CTDI is its relevance as a QA metric, and its measurement in a phantom under conditions mimicking those for a scan of a patient (e.g. attenuation by the table).

(74) The limitation of CTDI for wider beams has led to new approaches in CT dosimetry, details of which are provided in Annex A. The CTDI paradigm is problematic when there is no helical scan or patient motion (as is the case with many CBCT scanners). In such cases, reported $CTDI_{vol}$ values will overestimate the dose significantly (Dixon and Boone, 2010a).

5.2. Point-of-care scanning and clinic-based CBCT systems

(75) Clinic-based systems include head and neck CBCT, breast CT (bCT), and dental and maxillofacial CBCT. A particular property of dental and maxillofacial CBCT scanners is that, depending on the system, varying FOV sizes are offered. This allows for the scanning of localised regions (i.e. a single tooth and its immediate surroundings) as well as maxillofacial scanning. The use of horizontal collimation, as well as other factors, results in complicated dose distributions in the axial plane, providing an additional challenge for dosimetry (Pauwels, 2012a). In addition, most dental and maxillofacial CBCT scanners are seated or standing, resulting in practical complications regarding phantom and dosimeter placement.

(76) Various possible dose indices have been proposed for dental and maxillofacial CBCT (EC, 2012a; Pauwels, 2012a; DIN, 2013). Further validation of possible

indices is required, together with a way to translate dose index readings into patient doses.

(77) Technically, these methods could also be applied to other clinic-based systems including systems for head and neck imaging and possibly bCT. However, there is currently no standardisation for the measurement of such units. This highlights the fact that the issue of standardisation in CBCT dosimetry remains largely unresolved.

5.3. C-arm CBCT systems

(78) C-arm CBCT systems are incapable of performing a full rotation around the patient couch. Some systems, however, can only rotate 180° plus the beam angle (Fahrig et al., 2006), which results in a non-uniform axial dose deposition to the patient/phantom. Certain dental and maxillofacial CBCT scanners also scan along a 180–220° trajectory. In a phantom, the maximum dose occurs at the central plane intersecting the z-axis at $z = 0$, on the side of the phantom closest to the x-ray tube. In the ideal case in which the heel effect is absent, the maximum dose would occur on the bisector of the rotation angle. When the heel effect is present, the maximum dose occurs near the bisector.

(79) For C-arm CBCT systems, Fahrig et al. (2006) proposed a metric representing the average dose to the phantom central plane, following similar averaging to that applied in calculation of the weighted CTDI ($CTDI_w$).

5.4. A unified approach to CT dosimetry

(80) In its Report 87, the International Commission on Radiation Units and Measurements (ICRU, 2012) reviewed a considerable body of work in order to propose a method for CT dosimetry that compensates for the shortcomings of current CTDI-based CT dosimetry methods. In addition, earlier work by Dixon and Boone (2010b) provided a unified formalism for dose measurements on machines capable of helical scanning (e.g. MDCT scanners), as well as on machines that only acquire axial images (which is the case with most CBCT scanners). A set of metrics and the use of a new 600-mm-long polyethylene phantom are proposed. The mathematical foundation for the method is beyond the scope of this publication, but the method is described briefly here; more details can be found in Annex A. The method is based on a measurement of the cumulative absorbed dose at the centre of the 600-mm phantom from a complete scan. As the width of the beam for a CBCT scan is increased, the cumulative dose at the centre will rise. However, as the width of a CBCT beam is increased, the distance of the outer edge of the beam from the centre of the phantom becomes greater, and contributions from scattered photons at the outer edge to the cumulative absorbed dose at the centre become smaller. Beyond a certain beam width, further increases in dose become negligible, and an equilibrium dose is attained. The quantity $H(L)$ is defined as the ratio of the cumulative absorbed dose for a beam width or scan length L and the equilibrium dose.

(81) The physical interpretation of the rise to equilibrium curve presented in Annex A is that the scan and the phantom need to be long enough so that the asymptote tails of the profiles are reached. The longer the scan, the closer $H(L)$ is to unity. This representation shows that the dose to the central CT slice in a scan increases with scan length, demonstrating the relatively low efficiency of short scans for collecting the actual dose; this efficiency increases with longer scans.

5.5. Tracking and reporting of radiation dose

(82) Systems used for both fluoroscopy and tomography (CBCT) face new challenges. Currently, there is no standardised way to assess the aggregate radiation dose to a patient during a single procedure. This situation needs to be addressed, and these imaging systems should provide a means of not only comparing but also consolidating doses from both the fluoroscopy (2D) and CT (3D) components of a procedure. Furthermore, tracking and reporting of the radiation dose for a single patient should be facilitated. Errors for displayed dose estimates should not exceed 20% (IAEA, 2011b; IEC, 2011; EC, 2012b). A radiation dose structured report (RDSR) can be used to report the modality output following the existing RDSR in CT and angiography. KAP values for the different orientation of the beam can be reported inside the RDSR when step-and-shoot acquisition techniques are used. In addition, KAP can be considered for CBCT in fluoroscopy and other applications to facilitate direct comparison (e.g. between 2D and 3D fluoroscopy). Effective dose is not a suitable dosimetric quantity for reporting.

5.6. Epilogue

(83) The unified CT dosimetry method proposed by ICRU (2012) has the potential to standardise CBCT dosimetry. Nevertheless, the value of CTDI-based measurements should not be underestimated. Although CTDI has limitations, it has been evaluated on many systems over the years, and provides important comparisons in output for CT scanners from different manufacturers and ages. Moreover, coefficients for patient dose estimations based on $CTDI_{vol}$ are already available.

6. OPTIMISATION OF PROTECTION OF PATIENTS AND WORKERS IN CBCT

- **Optimisation of both patient and worker doses, particularly when workers have to be near the machine, is important when monitoring of doses becomes an essential tool. Recording, reporting, and tracking of radiation dose for a single patient should be made possible in a consistent manner across vendors.**
- **Low-dose protocols may be sufficient to answer diagnostic questions focused on high-contrast structures, such as lung, bones, dental and maxillofacial scans, ENT scans (paranasal sinuses, skull, temporal bone), interventional material, and contrast-enhanced vessels (angiographic interventions).**
- **Higher-dose protocols should only be selected if visualisation of soft tissue structures, such as intracranial haemorrhage, soft tissue tumours, or abscesses, is the primary focus.**
- **Most interventional and intraprocedural C-arm CBCT systems can scan an angular range spanning 180–240° plus the cone angle of the x-ray beam. Localised critical organs, such as the thyroid, eyes, female breasts, and gonads, should be on the 'detector side' of the arc whenever possible.**
- **Clinical need permitting, every effort should be made by users to ensure that the volume of interest is fully incorporated in the FOV provided by the CBCT scanners, while radiosensitive organs should be placed outside the FOV.**
- **The aim of CBCT should be to answer a specific diagnostic or intra-operative question vis-à-vis other imaging modalities, and not to obtain image quality that rivals MDCT. The decision by the referring practitioner to use CBCT should be made in consultation with an imaging professional.**
- **There is a need to provide checks and balances, such as dose check alerts implemented in CT in recent years, to avoid high patient doses compared with locally defined reference values.**
- **Methods that provide reliable estimates of dose to the eye under practical situations should be established and used.**

6.1. Introduction

(84) CBCT scanners are highly engineered machines, and dose optimisation is a multi-factorial problem. The imparted radiation dose may vary by several orders of magnitude between different scan models and different ways of using the machine. Clinical use of CBCT requires insight into the various trade-offs in order to maximise patient benefit and minimise risk. It is essential to understand various technological factors and scan parameters that influence dose. Knowledge of MDCT alone is not sufficient in this endeavour as CBCT scanner systems differ significantly from MDCT scanners in their mode of operation. For example, while spiral scanning is the norm with MDCT, nearly all CBCT imaging is done using a single axial scan. In addition, several special conditions exist that do not apply to MDCT scanners (e.g. restriction of the FOV of a typical CBCT

scanner). It is therefore essential to involve a medical physicist or another suitably qualified expert (AAPM, 2011a; EC, 2014) early on in optimisation, as well as the audit of patient and occupational dose levels, particularly for high-dose procedures.

6.2. Factors influencing dose to the patient

6.2.1. Equipment-dependent factors

Knowing your equipment

(85) It is important that users understand how their equipment functions, because each CBCT scanner has some unique features, such as the application domain, gantry design, and detector configurations. The complexity of modern equipment necessitates a thorough understanding of the various scan modes, parameter settings, and dose optimisation strategies. This section deals with equipment features that affect radiation dose, and the next section is devoted to operator actions required to achieve optimal radiological protection in clinical scans.

Collimation

(86) In MDCT, the region of interest is usually prescribed on one and sometimes two orthogonal scan projection radiographs [also known as antero-posterior (AP) and lateral (LAT) scout views or topograms]; the scanner covers this scan FOV helically or axially and reconstructs tomographic slices. Similar AP and LAT projection views may also be acquired in CBCT scanning; however, the entire FOV usually fits within a single circular trajectory of the scanner, and helical scanning is not used in most applications. Although the x-ray beam will not generally extend beyond detector dimensions in situations where the detector is movable, a portion of the beam may fall outside the detector margins. Care should be taken to collimate the x-ray beam so that it falls entirely within the detector margins; automatic means for delimiting the collimation window to the detector size may or may not exist, depending on the particular scanner manufacturer and model. Any radiation outside the detector constitutes unnecessary radiation to the patient. The beam should be further collimated to limit its z-extent to the FOV. The source-to-detector distance determines the maximum lateral extent of the FOV that can be scanned, and should be adjusted appropriately depending on the anatomy under consideration. It should be noted that the scatter noise in the projection data increases approximately linearly with the area of the irradiated field. In general, the x-ray beam should be collimated tightly as it not only lowers the x-ray dose but also decreases scatter, thereby improving image quality.

(87) A poorly collimated primary beam, if it is outside the patient, may increase the occupational dose, as well as the patient dose, significantly. It is also desirable to exclude any adjacent sensitive organs that do not need to be

imaged from the scan FOV to address the clinical question at hand. The x-ray beam should be collimated tightly to the scan FOV. As a CBCT scan cannot be extended in the same way as an MDCT scan, caution must be exercised to ensure that the volume of interest is fully incorporated in the FOV provided by the CBCT scanner.

Collimation along the z-axis

(88) Many CBCT scanners provide a means for the user to collimate the beam. Collimation along the *z*-axis to achieve as narrow a beam as possible to fulfil the clinical purpose will reduce the patient dose and improve the image quality. Use of the thinnest possible collimation (2.3 cm) instead of the full field (19 cm) improves the contrast-to-noise ratio.

(89) Free-in-air geometric efficiency is a means of quantifying over-beaming (i.e. the proportion of radiation falling outside the detector margins) (Berris et al., 2013). In CBCT scanners, the x-ray beam is usually fully intercepted by the receptor, so the free-in-air geometric efficiency should be 100%, and over-beaming should not occur. Furthermore, over-scanning (also known as over-ranging), which is required at either end of helical scans to provide additional data for image reconstruction, is not needed for axial CBCT scans (Tzedakis et al., 2005).

(90) An effect that always occurs in CBCT is that parts of the irradiated volume are hit by radiation, but are not fully contained in 180° of projections. Images of these regions, shown in Fig. 6.1, cannot be reconstructed or can only be partially reconstructed. The region that cannot be reconstructed broadens as the cone angle increases (Grimmer et al., 2009).

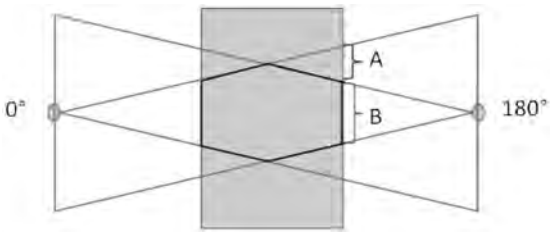

Fig. 6.1. In cone beam computed tomography, data are only available from 180° projections within the region in the hexagon that is marked with parenthesis B. A part of the irradiated volume (parenthesis A) cannot be reconstructed (or only with reduced image quality), because data from all 180° projections are not available. The size of this area depends on the geometry of the scanner (qualitative depiction).

Dose distribution within the scan field of view along the z-axis

(91) Ideal CT scanner systems should irradiate the examined volume along the *z*-axis with a homogenous dose that should decrease rapidly outside the examined volume. In some CBCT systems, the dose distribution is different, and the central slices receive larger amounts of radiation (Gupta et al., 2006). Wherever possible, radiosensitive organs should be placed outside the irradiated volume, which is normally wider than the FOV, provided the clinical requirements of the procedure permit.

Dose distribution in cases of volume-of-interest scanning

(92) In certain situations, only a small volume may be of clinical interest. Some CBCT scanners provide a very narrow beam collimation with a relatively small detector. A large part of the irradiated volume will be out of the primary x-ray beam at most angular projection positions. In general, a scan volume that is delimited in the x–y direction to a small portion of a larger body part results in truncation artefacts. However, small-volume CBCT of high-contrast structures such as bones and teeth, when used in conjunction with an artefact reduction algorithm, may well give clinically acceptable images. For example, a truncation artefact arising from a limited FOV may not affect assessment of a transpedicular screw. This must not be confused with retrospective, selective reconstruction of a certain region of interest inside a larger scanned volume (Table 6.1). The dose distribution outside the volume of interest is very different in the two scanning modes. Therefore, the user should verify whether volume-of-interest scanning is applicable in a certain situation.

Type of detector

(93) Most currently available CBCT systems use a digital FPD. State-of-the-art digital FPDs are offered at several gains and effective dynamic range settings. In general, the dynamic range of digital FPDs is narrower than for MDCT detectors, resulting in lower soft tissue contrast for CBCT scanners. The afterglow of the caesium iodide (CsI) scintillators used in FPDs limits the maximum image frame rate that can be obtained from these detectors. Typically, 30 frames s^{-1} can be obtained at the full FOV; a narrower FOV can provide a faster frame rate of 100–120 frames s^{-1} (Gupta et al., 2008). Slow frame acquisition rate is the main reason for the relatively high acquisition times of CBCT systems (Orth et al., 2008); the fastest clinically available CBCT had an acquisition time of 5 s compared with 80 ms for a dual-source MDCT system. Parameters such as pixel size and scintillation crystal thickness are usually selected based on target application (e.g. maxillofacial imaging or C-arm angiography), and the end-user has no control over their selection. No detector technologies in current use should be strictly avoided from a radiological protection standpoint.

Table 6.1. Volume-of-interest scanning vs standard scanning. Volume-of-interest scanning is a valuable method to reduce the radiation exposure of in-plane structures, if imaging conditions allow (high-contrast structures). It must not be confused with standard scanning for region-of-interest reconstruction.

	Irradiated volume from all directions (from all angular positions)	Reconstructed volume	Radiation exposure	Applications
Volume-of-interest scanning	Limited to cylindrical volume of interest	Limited to cylindrical volume of interest	Only volume of interest receives full dose	Mostly dental and maxillofacial imaging and most interventional C-arm setups when body trunk is scanned
Standard scanning	Large cross-section	Anywhere within body diameter, whole-body diameter, or parts of full cross-section	Whole-body diameter receives full dose	All other

(94) A minority of CBCT systems still use charge-coupled device cameras coupled with x-ray image intensifiers. The convex input screen and image distortion of image intensifier systems result in non-uniform image quality across the output image. In addition, light and electron scattering within the image intensifier limits the contrast resolution of the reconstructed slices. CBCT systems typically have an 8–10-bit dynamic range and can only support a very coarse level of tissue differentiation.

Detector quantum efficiency

(95) Detector quantum efficiency (DQE) is a widely used metric that describes the dose efficiency of an x-ray detector. Without going into detail, it measures the quality of the image produced by the detector from a given dose or fluence to the detector. Intuitively, it captures how well a detector translates the signal incident on it into an image, relative to an ideal detector. Specifically, it is the square of the ratio of input and output SNRs of a detector. For example, a detector that reduces the SNR by 50% has DQE of 0.25. The ideal detector would have DQE of 1 and would translate all incident x-ray photons into image information. DQE is normally given as a function of spatial frequency, and correlates image quality with incident x-ray dose at a detector level.

(96) Current caesium iodide hydrogenated amorphous silicon (CsI-aSi:H) FPDs have DQEs in the range of 0.6–0.7, which are lower than those of MDCT detector

systems (Gupta et al., 2006). This is a fundamental limitation that is beyond the control of the user, and means that CBCT images will be noisier than MDCT images for the same input radiation.

Filtration

(97) A bowtie filter in the imaging chain hardens and attenuates the x-ray beam, reduces the scatter-to-primary ratio, and reduces the x-ray fluence heterogeneity at the detector. Bowtie filters decrease the scatter contribution from the object periphery in MDCT imaging (Orth et al., 2008). Ning et al. (2000a) showed that the quantity [SNR^2/entrance exposure] decreases when kVp increases for a flat-panel-based CBCT system. This means that there is a trade-off between decreased scatter from the object periphery (when the bowtie filter is on) and improved detector efficiency from the 'softer' beam (without a bowtie filter) (Orth et al., 2008). Use of a bowtie filter is standard in MDCT. In CBCT, a bowtie filter is not used commonly, but its use is increasing. Other configurations such as half-bowtie filters that enable coverage of a large area have also been used (Wen et al., 2007). The presence of the filter can reduce patient dose, especially at the patient periphery, and can improve tomographic image quality by improving uniformity, CT number accuracy, and contrast-to-noise ratio. One potential disadvantage, however, is the decrease in detector efficiency due to beam hardening (Mail et al., 2009). In general, a bowtie filter should be used when imaging a wide FOV where the anatomy under consideration only occupies a small central portion. Assessment of spinal hardware would be one example application. Special care must be taken if the bowtie filter is removable; workers can forget to mount the bowtie filter prior to imaging, resulting in additional dose to the patient.

Anti-scatter grid

(98) An anti-scatter grid is placed between patient and detector, and consists of lead septa that are oriented along lines projecting radially outwards from the focal spot. This geometry allows the primary beam to reach the detector while the off-axis radiation is absorbed. As such, an anti-scatter grid in front of the flat panel can prevent the scatter generated by the patient from reaching the detector. The leaves reduce the effective detector area to a small degree. The geometry of the anti-scatter grid, which determines its selectivity and its rejection efficiency, is optimised for the scanner and application. Anti-scatter grids are highly sensitive to the source-to-detector distance; if the latter can be varied, or if a choice of anti-scatter grids is provided, it is essential to match these two parameters.

(99) The efficiency of anti-scatter grids for scatter suppression and image quality improvement has been assessed for CBCT. Although the presence of a grid did not seem to improve the SNR in relation to applied radiation dose (Schafer et al., 2012), a significant decrease in cupping artefacts was observed (Kyriakou and Kalender,

2007). However, in certain high-scatter conditions, the grid could lead to a reduction in dose of up to 50% (Kyriakou and Kalender, 2007).

(100) The anti-scatter grid, if available, is usually a fixed hardware parameter that is optimised for a certain application and a specific geometry. Typically, the end-user has little influence on the geometry of the anti-scatter grid. However, if a choice of different grids and geometric distances is provided, it is essential that the two are matched for the system to function properly.

Scatter correction algorithm

(101) Scatter intensity has a broad angular distribution around the image of the scattering object. One can think of the projection image obtained by the detector as a 2D-smeared image of the object that includes both the primary and the scatter radiation. At any point that can receive both the primary and scatter photons, these two components may be difficult to separate. However, in areas that are shielded from the primary beam by the collimator, the scattered component is observable because of the broad distribution of the scatter. An assessment of this can be used to estimate the amount of scatter in the rest of the image. By assuming a scattering function, the scatter profile throughout the image can be estimated. This can then be subtracted from the measured signal to compute the contribution from the primary signal. If a particular CBCT scanner provides a set of steps for computing the scatter function, that protocol should be strictly followed. Besides vendor-implemented algorithms, the user has little influence over the scatter correction algorithms.

Data correction algorithms

(102) Multiple correction algorithms are typically applied to the raw projection data, before they can be reconstructed into a 3D stack. The following is a partial list of data conditioning algorithms typically employed to compensate for system imperfections: (1) offset subtraction; (2) afterglow correction; (3) adaptive filter mask; (4) normalisation; (5) theta correction; (6) cross-talk difference correction; (7) air calibration; (8) beam hardening correction; and (9) detector z-gain non-uniformity correction. These corrections tend to be vendor specific, over which the end-user has no control.

6.2.2. Operator-dependent factors

Reduced arc scanning

(103) Many CBCT systems are capable of reconstruction from less than 360° angular acquisitions. In general, a coverage of 180° plus the cone angle is sufficient for tomographic reconstruction. This gives the operator considerable flexibility in selectivity, allowing reduction of patient exposure. For example, an appropriate

choice of starting and stopping angle can be used to limit projection images of a patient's head to posterior angles, reducing the dose to the lens of the eye (Kyriakou et al., 2008a) (Fig. 6.2). Daly et al. (2006) observed a five-fold decrease in dose to the eye when 3D images were generated using a C-arm half-cycle (178°) rotation performed with the x-ray tube posterior to the skull rather than anterior. Another example where this is used is in CBCT imaging of the breast, where the imaging angles can be chosen to limit unnecessary exposure of the heart and lungs. These manoeuvres typically have no appreciable effect on the image quality in the central portions of the scan. Selecting an appropriate angular span for the scan arc, a parameter that has a direct impact on the dose distribution, is a user-selectable parameter. The user should select the scan arc so that radiosensitive organs are on the detector side of the imaging chain.

(104) Dental and maxillofacial CBCT differs regarding the use of a reduced arc. Firstly, the start- and endpoints of a 180° rotation cannot be selected by the user, with the detector typically being on the anterior side of the patient. However, simulations and phantom studies have shown that patient dose may be lower when the tube is on the anterior side, although differences were 10% or lower (Morant et al., 2013; Zhang et al., 2013; Pauwels et al., 2014). This can be explained by the anterior placement of FOVs for dental examinations, which results in several radiosensitive organs being posterior to the centre of rotation (e.g. salivary glands or thyroid). More evidence is needed before a definitive recommendation can be made to manufacturers.

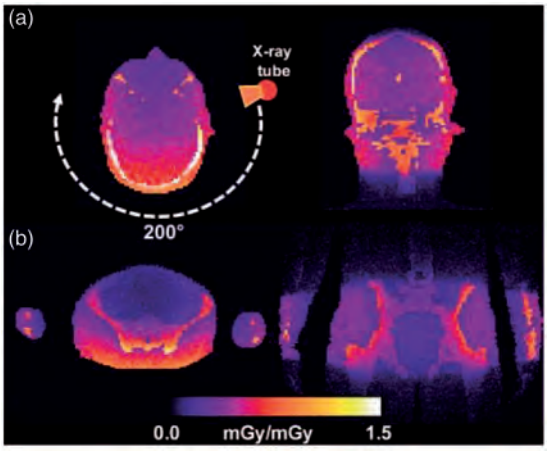

Fig. 6.2. In contrast to multi-detector computed tomography, cone beam computed tomography is mostly performed with a half scan angle (180° plus cone angle). As such, the position of the scan angle has a significant influence on the dose distribution within the patient (Kyriakou et al., 2008a).

Setting of kVp and mAs

(105) The parameters that determine x-ray beam flux and energy spectrum (i.e. mA and kVp settings) should be kept as low as possible without compromising the image quality and clinical utility of the scan. kVp and mA are the main user-selectable variables that determine the overall dose to the patient. If all other parameters are held constant, the radiation dose is directly proportional to the applied mAs (tube current × duration of scan rotation), and this parameter influences the noise in the image significantly. As long as the detector is not saturated, there is a direct relationship between the level of image quality and increasing mAs. The dependence of the radiation dose and image quality on the kVp setting is more complex. Higher-energy photons result in less interaction with tissue; they give poorer contrast between tissues, but a larger number of photons pass through the tissue and reach the detector to form the image. The right kVp and mAs setting depends heavily on the anatomy being scanned, whether or not a contrast medium was used, and several design factors such as filter systems, frame rate, and detector type. Therefore, it is difficult to provide absolute guidelines. All commercial CBCT scanners come with a manufacturer-recommended protocol for each application. The best advice to the user is to start with this protocol and, working in conjunction with a medical physicist or another domain expert, adapt it to the local conditions. One should also monitor publications and guidelines dedicated to the particular scanner setup or type of examination.

Automatic exposure control

(106) AEC systems adapt the radiation exposure to obtain a desired level of image quality and adjust the dose to that needed for the specific body part of the patient. Similar to MDCT, AEC modulates the tube current according to patient attenuation in a given angular direction. Usually, AEC is implemented as a feedback loop that controls the x-ray source based on feedback from the detector. Reductions in dose by 20–40% through the use of AEC systems have been reported in CT (McCollough, 2005). It has been found that absorbed doses vary considerably during a CBCT acquisition, which shows the potential of using tube current modulation (He et al., 2010).

(107) Many CBCT systems do not employ AEC, instead using a fixed tube current setting for the entire scan. AEC is almost not available in head and neck, and dental cone beam scanners (fixed settings protocols), and is more widely implemented in whole-body C-arm systems. The use of tube current modulation is reduced in CBCT due to the wide *z*-axis coverage. Also, the demand for AEC is less stringent when scanning the head compared with other parts of the body. The requirements and demands on AEC are still evolving, and general guidelines are difficult to formulate. More details on the patient-specific factors involved in the potential application of AEC can be found in Section 6.2.3.

Scan modes: number of projections

(108) In contrast to MDCT scanning, where the user is unable to select the number of projections explicitly, this parameter is often directly selectable in CBCT. The most commonly used detectors in CBCT systems have a much slower time to readout, and require a wait time after each projection in order to account for the afterglow of the scintillator. The dose delivered in each scan is also limited because of the number of photons that can be collected by each projection without overexposing the detector. Optimisation of the scan time using a tight control over each exposure is much more critical in CBCT than in MDCT. These considerations limit the range of dwell time and dose in each projection. By controlling the number of projections, for example, or changing the total scan time, one can control the dose for a scan protocol; increasing the number of projections increases the applied radiation dose proportionately. In CBCT, the number of projections, together with the associated changes in the total scan time, provides a trade-off between image quality and the delivered dose that is influenced directly by user-selected parameters.

Scan modes: binning and spatial resolution

(109) The detector elements in angiographic C-arm CBCT systems, in contrast to MDCT detector systems, are much smaller in order to provide the necessary spatial resolution for fluoroscopy and angiography modes. For example, a common FPD for C-arm systems offers a native pixel size of 154 μm in a 1920×2480 matrix. The time to readout such a large matrix, coupled with the afterglow of the CsI scintillators, limits the maximum frame rate achievable on such a detector. The frame rate of a CBCT detector can be as much as one to two orders of magnitude lower than that in MDCT. A low readout frame rate accounts for the relatively high acquisition times of CBCT systems. For example, the fastest available clinical CBCT had an acquisition time of a few seconds compared with 80 ms for a dual-source MDCT system (Orth et al., 2008).

(110) While it may not be possible to control the afterglow or afterlag of the scintillator, the size of the image matrix that needs to be readout can be decreased to make the image transfer faster. A set of binning modes is provided to accomplish this. Each binning mode combines neighbouring detector rows and columns in order to reduce the matrix size and the readout time. Typical binning modes involve a 2×2 and 3×3 area, thereby reducing the data to be streamed out by a factor of four and nine, respectively. Despite this averaging, the spatial resolution of CBCT is higher than that in MDCT and is often above the demands of the clinical application. Since the image noise, spatial resolution, and radiation dose are inter-related, the user must decide on the acceptable image quality and the spatial resolution. This choice, in turn, determines the radiation dose. The user should not be tempted to reduce the image noise (e.g. by increasing the tube current or increasing the number of projections using modes such as the 'high-

quality scan mode' offered on some systems) to reach a noise level that is comparable to that of MDCT. The dose penalty associated with these scans can be much higher than would be warranted by the clinical question at hand (Blaickner and Neuwirth, 2013). Postprocessing techniques, such as slice averaging, thick multi-planar reformation, and use of a softer reconstruction kernel, are preferable when trading off among competing metrics such as image noise, low-contrast resolution, spatial resolution, and radiation dose.

Scan modes: predefined scan protocols

(111) The use of an organ-specific protocol (e.g. 'routine head') or a clinical indication-specific protocol (e.g. 'appendicitis protocol') is established practice in MDCT. In routine clinical care, vast libraries of such scan protocols are available. Similar to MDCT, many CBCT systems also provide predefined scan protocols that encapsulate detector settings, reconstruction kernels, and other scanner parameters. In CBCT, however, the use is less well established, with many protocols named suggestively with prefixes such as 'low-quality' or 'high-quality', the latter unflatteringly implying that the base protocol might not provide appropriate image quality in certain situations (Table 6.2). Generally, the naming of the scan protocols refers to the well-known and, within limits, physically fixed trade-off between image quality parameters and radiation dose. High-quality scan protocols usually provide 'better' image quality at 'higher' radiation dose. These simple prefixes often belie the magnitude of the change that occurs; a high-quality protocol may entail a 6- to 10-fold increase in radiation dose compared with a low-quality or standard-quality protocol. In CBCT, the selection of the scan mode or scan protocol is one of the most significant factors influencing radiation dose (Kyriakou et al., 2008a). A low-dose scan protocol may be sufficient for high-contrast structures, such as bones, teeth, kidney stones, and contrast-enhanced blood vessels. The manufacturers are beginning to provide scan protocols that are named for the diagnostic challenge they are trying to address (e.g. 'bone', 'kidney stone', 'rule out intracranial haemorrhage', or 'skull base' protocol). There should be a dedicated section for paediatric protocols. These have special significance when the imaging system does not have AEC (e.g. in most dental and maxillofacial CBCT scanners) to account for the lower diameter of children's body parts.

(112) The user interface for CBCT scanners also deserves a special mention. The checks and balances that are routine in MDCT scanners may be missing in CBCT scanners. For example, two vastly different but similarly named protocols may be adjacent to each other on the user interface, or a single mouse click may cause a 10-fold change in the delivered dose. This is in sharp contrast to MDCT where such a large increase in radiation requires several purposeful manipulations of scan parameters and concomitant confirmation to affect the change. The user must understand the consequences of scan protocol selection, not only in terms of image quality, but also in terms of applied dose. This is especially important for

Table 6.2. Overview of available scanning protocols, applications, and typical protocol names. Protocols that are only a single click away from each other have vastly different dose consequences. In addition to patient positioning and selection of the scanning arc, appropriate protocol selection is the most significant user-determined factor for radiation dose calculation.

Protocol dose	Protocol spatial resolution	No. of projections	Regions	Clinical indication	Names (examples)
Low	Low	Low	Abdomen, thorax	Rule out kidney stone, assess position of instrument/implants, treatment planning	'−', 'low-quality', 'low-dose'
Medium	High	Low/ medium	Skull/bones	Dental and maxillofacial imaging, assess bone structures, arterial contrast media angiography	'Dental', 'bone', 'high-resolution'
High	High	High	Abdomen, head	Assess soft tissue structures, intracranial haemorrhage, venous contrast media angiography	'+', 'CT angiography', 'high-quality'

CT, computed tomography.

CBCT, where such information may be entirely (and sometimes ambiguously) encoded in the protocol name. There has been considerable variability in terms used in imaging, and this creates difficulty in dose registry. The Commission recommends standardisation of terminology used in imaging protocols.

Scan modes: partial panel

(113) In order to expedite readout of the panel, the detector control electronics generally allow readout of partial panels; an arbitrary number of central rows may be readout as needed. While most systems have built-in hardware features that ensure effective use of the beam, it is essential, from a radiological protection point of view, that the x-ray beam is collimated appropriately to irradiate only that portion of the detector that is being readout.

Keep unnecessary body parts out of the x-ray beam

(114) It is good practice to limit the radiation field to the body parts that must be imaged. Inclusion of unnecessary body parts not only has dose consequences, but may also increase image artefacts significantly. Many CBCT scanners only have a limited scan FOV, with a diameter lower than the body region that is being

examined. Positioning of arms or legs outside the irradiated area can reduce the level of artefacts significantly, and therefore increase the image quality without increasing unnecessary radiation dose.

Making judicious use of CBCT acquisitions during a procedure

(115) CBCT imaging can quickly provide 3D images intra-operatively with minimal effort on the part of the interventionalist or surgeon. These datasets are useful as they relieve the operators from the effort of trying to distinguish overlapping structures in 2D fluoroscopy images. They can also save dose by replacing multiple digitally subtracted angiography runs in different C-arm angulations with a single CBCT run. It has been shown that 3D acquisition provides valuable clinical information and limits the need for 2D imaging: hence, CBCT can also lower the dose in one procedure. Given this facility, and the ease with which 3D images can be acquired, operators may be tempted to overuse the 3D imaging features of their equipment. Although CBCT has the potential to decrease dose in comparison with fluoroscopy and MDCT, this effect could be cancelled by overuse of volumetric acquisition with C-arm and other intra-operative CBCT machines. 3D data must be acquired judiciously for purposeful clinical problem solving when fluoroscopy is insufficient for the task at hand.

Bismuth shielding

(116) Bismuth shielding for the eyes, thyroid, breast, or other organs in CBCT should be used with caution. With CBCT, reduced arc scanning will be more effective (Section 6.2.2), and such shielding must not be used in conjunction with this. Bismuth shielding can be effective in certain situations if placed in a manner that does not interfere with AEC of the CBCT scanner. If the shield is positioned after AEC has adjusted the tube current to be used, this may be beneficial provided that the image is not degraded excessively by the presence of the shield in the FOV (AAPM, 2012a). If the bismuth shield is placed before selection of AEC, its effect may be totally negated by the increased current from AEC. The issues surrounding the use of bismuth shielding are similar in both MDCT and CBCT, and available guidelines for MDCT apply to CBCT.

Reconstruction algorithms

(117) In a standard CBCT reconstruction algorithm such as the modified Feldkamp–Davis–Kress (FDK) algorithm, the noise level is proportional to the applied tube current. However, image filtering, compressed sensing, and iterative reconstruction algorithms, which are becoming increasingly popular in MDCT, have the potential to disrupt this direct relationship between the applied dose and image quality. At the present time, such novel reconstruction algorithms are not

widely available for CBCT scanners, and it is not possible to provide specific guidelines on how they should be used in practice. In many circumstances, the application of these specialised algorithms is not universal. Instead, a user-selectable mixing parameter is provided. This percentage factor determines the level to which the output of the specialised reconstruction algorithm should be incorporated and added to the output of the traditional algorithm. The exact setting for this mixing factor will depend on the algorithm and the acceptable image quality, and will have to evolve with experience.

6.2.3. Patient-specific factors

Thickness of the body part in the beam

(118) In response to the varying thickness of the anatomy, many CBCT machines adjust radiation exposure automatically through AEC. This electronic system has a sensor that detects how much signal is being produced at the image receptor, and adjusts the x-ray generator to increase or decrease exposure factors (typically tube current and, in many cases, tube voltage) so that each projection image is of a consistent quality. When a thicker body part is in the beam, or a thicker patient is being imaged (compared with a thinner patient), the machine will increase the exposure automatically. The result is a similar image quality but an increase in the entrance dose.

(119) In MDCT, AEC is able to vary the tube current both in the angular as well as the longitudinal or *z*-direction. As a result of the angular variation, the dose in the AP direction is lower than that in the lateral direction for any fixed, user-selected image quality parameters. The *z*-axis adaptation of the dose controls the mA value in the superior–inferior direction, resulting in a higher dose to the abdomen and pelvis compared with the chest. In CBCT, as most acquisitions are performed in an axial mode rather than a helical mode, the angular variation of tube current is more important.

(120) Some CBCT systems lack AEC. These systems operate under the assumption that patient size does not vary significantly in the angular direction, although absorbed doses can vary considerably during a CBCT rotation (He et al., 2010). The assumption can be true for dental and maxillofacial, or head and neck applications, but should be investigated further. When AEC is not available, guidance should be provided for the user on how to adjust the exposure parameters for different patient sizes.

Use of CBCT in children

(121) For any given exposure settings (same tube exposure parameter settings, collimation, amount of projections, etc.), a thinner patient will receive a higher dose (which is energy deposited per mass) than a larger patient, although the larger patient will absorb a greater fraction of the radiation (AAPM, 2011b). This is because the lower attenuation in a thinner body results in a smaller range in dose

through the body tissues for the smaller patient (e.g. a child). This may also sometimes be true even when the exposure factors are adjusted for body size or are controlled by AEC. In general, especially for large patients, a greater fraction of the x-ray beam is absorbed in the more superficial portions of the anatomy being imaged. In other words, the skin dose is much higher than the central dose. For thinner patients, this dose gradient is smaller, which implies that the dose is high throughout the entire body. Figs. 6.3 and 6.4 illustrate the absorbed radiation dose as a function of the patient's body habitus and size when AEC compensates for variations in body size. Thus, it is important to pay particular attention to optimising radiological protection for children to ensure that exposure factors are not higher than necessary.

Monitoring of patient dose indices

(122) Unfortunately, the field of patient dose monitoring in CBCT lags behind that in MDCT. There is a lack of standardisation in dosimetry methods for CBCT; different manufacturers have provided different ways of measuring and reporting dose in CBCT, and these are not adopted universally. It is hoped that if the recommendations of Report 87 (ICRU, 2012) are adopted by manufacturers and clinicians, there is a good possibility that dosimetry in CBCT will be standardised and this will provide more coherent patient dose data in the future. Means to estimate and report patient dose will require a collaborative effort between the manufacturers of CBCT equipment and the regulatory bodies. Methods for storing patient dose indices and dose reports in Picture Archiving and Communication Systems (PACS) also have to evolve as the use of CBCT becomes more prevalent.

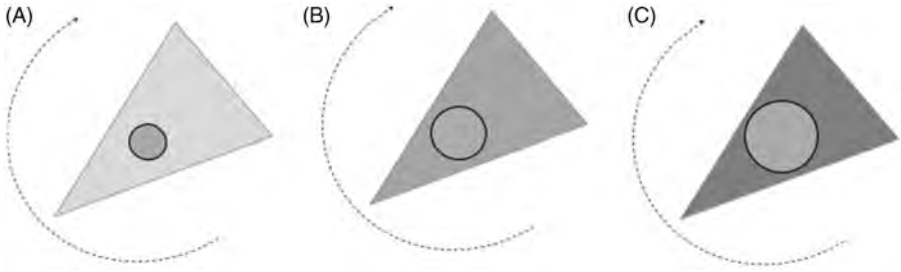

Fig. 6.3. Qualitative illustration of the effects of automatic exposure control (AEC) on patient exposure. AEC keeps the image quality at a given level and adjusts for variations in patient size. The impact of patient size on the radiation dose with AEC is shown. A shows the smallest patient diameter, C shows the largest patient diameter, and B is in between A and C. Radiation exposure is indicated by the darkness of the grey of the radiation fan. The bigger the patient, the higher the applied radiation exposure.

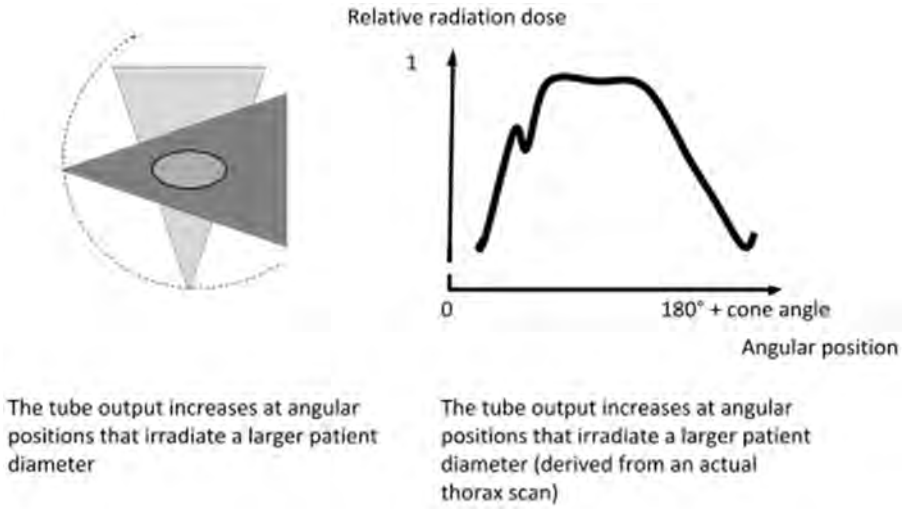

Fig. 6.4. Effect of the variation in patient diameter at different angular positions in-plane on tube output controlled by automatic exposure control (AEC). At angles where the patient diameter is greater, the exposure is increased by AEC. The plot of tube output is an example derived from an actual torso scan (provided by Rolf Kueres).

(123) In view of recent cases of skin injuries to patients in CT examinations, there is a need to provide checks and balances to avoid overexposures through alerts, and control patient dose prospectively in comparison to locally defined reference values (Cadet, 2010; IAEA, 2010; AAPM, 2011c; NEMA, 2013). Manufacturers need to incorporate suitable features to facilitate this.

6.2.4. Factors influencing dose to worker

(124) Occupational radiation exposure is expected to be small in the case of clinic-based CBCT systems. When using a C-arm or other CBCT device in an interventional suite or operating theatre, physicians, technologists, and other workers can protect themselves by using shielding devices. As required under national regulations in most countries, radiation workers must comply with regular individual dose monitoring requirements for managing radiation exposure, and keep a comprehensive dose record. Further, unless necessary, workers should move outside the fluoroscopy room radiation area when CBCT acquisition is taking place.

(125) In one study, the unshielded CBCT exposure at 35-cm distance from the operating table, measured over a 60-s scan, was found to be 0.26 mSv (Daly et al., 2006). Schulz et al. (2012) measured dose to the eye ranging from 28.0 to 79.3 μSv for CBCT hepatic arterial embolisation and biliary tube placement procedures. The primary source of radiation is the x-ray tube, and, ideally, the patient alone

should be exposed to the primary x-ray beam. Radiation scattered from the patient, parts of the equipment, and the patient table (so-called 'secondary radiation' or 'scatter radiation') is the main source of radiation exposure to workers. A useful rule of thumb is that radiation dose rates are higher on the side of the patient closest to the x-ray tube. Distance is also an important factor, and workers should increase their distance from the x-ray source and the patient when permitted in the clinical situation. Automatic injectors should be used, as far as possible, if contrast medium injection is necessary.

Shielding: lead apron

(126) Clinical staff taking part in diagnostic and interventional procedures using C-arm devices for fluoroscopy or CBCT imaging wear protective aprons containing lead (sometimes also lined with additional x-ray-absorbent materials) to shield tissues and organs from scattered x rays (NCRP, 1995). Transmission through these aprons will depend on the energies of the x rays and the lead-equivalent thickness of the aprons. If the attenuation of scattered radiation is assumed to be equal to that of the primary (incident) beam, this provides a margin of safety (NCRP, 2005).

(127) All workers present in the room during a CBCT scan must wear a lead apron, as it is the most essential component of personal shielding in an x-ray room. It should be noted that the level of protection afforded by the lead apron depends on the x-ray energy, which is a function of the voltage applied across the x-ray tube (kV). The thicker the part of the patient's body falling in the x-ray beam, the higher the kV set by the fluoroscopic system. Higher kV x-ray photons have greater penetrative power, implying that a greater lead thickness is needed to provide the necessary attenuation.

(128) For procedures performed on thinner patients, particularly children, an apron of 0.25-mm lead equivalence will suffice. However, for thicker patients and with a heavy workload, a 0.35-mm lead apron may be more suitable. The wrap-around aprons of 0.25-mm lead equivalence are ideal; these have a thickness of 0.25 mm at the back and 0.5 mm at the front. Two-piece skirt-type aprons help to distribute the weight, and due to their overlap in front of the abdomen, they provide a 1-mm shielding (e.g. at the level of the uterus). Heavy aprons can pose a problem for workers who have to wear them for long periods of time. There are reports of back injuries due to the weight of lead aprons among workers who wear them for many years (NCRP, 2010). Some newer aprons are lightweight while maintaining lead equivalence, and have been designed to distribute the weight through straps and shoulder flaps.

Ceiling-suspended shielding

(129) Ceiling-suspended screens that contain lead impregnated in plastic or glass are very common in interventional radiology and cardiology suites. However, they

are not usually used in operating theatres. Shielding screens are very effective as they have lead equivalences of 0.5 mm or more, and can reduce x-ray intensity by more than 90%. Practical problems make the use of radiation shielding screens for occupational protection more difficult but not impossible in operating theatres. Manufacturers should develop shielding screens that can be used for occupational protection without hindering the clinical task. There is a need for more than one screen to provide protection effectively to other workers in the operating theatre in addition to the main operator.

Mounted shielding

(130) Mounted shields include table-mounted lead rubber flaps or lead glass screens mounted on mobile pedestals. Lead rubber flaps are very common in most interventional radiology and cardiology suites, but are rarely seen in operating theatres; nevertheless, their use should be promoted. Manufacturers are encouraged to develop detachable shielding flaps to suit practices in operating theatres. Lead rubber flaps, normally impregnated with the equivalent of 0.5-mm lead, should be used as they provide effective attenuation. In interventional fluoroscopy, table-mounted lead rubber drapes protect the legs of the operator; however, for CBCT scans, these may need to be repositioned so that they do not impede movement of the x-ray tube/detector C-arm mount.

Room shielding

(131) Room shielding requirements for CBCT systems used in dental and maxillofacial imaging range from 0.5- to 1.5-mm lead equivalent, depending on the scanner's specifications for scattered radiation dose and its workload (EC, 2012a). In most cases, the image receptor intercepts the entire primary beam, as in most fluoroscopic units and MDCT scanners. The room shielding is for scattered radiation, as is the case with a conventional CT scanner (Sutton et al., 2012). However, for any type of CBCT machine, the shielding should be designed to keep doses to workers and the public as low as reasonably achievable, and, of course, below the existing dose limits that apply in various settings.

Lead glasses

(132) Various types of leaded glass eyewear are available, although they are heavier than common glass eyewear. These include eyeglasses that can be ordered with corrective lenses for individuals who normally wear spectacles. There are also eye shields that can be clipped on to the spectacles of workers, and full-face shields that also function as splash guards. Leaded eyewear should either have side shields to reduce the radiation coming from the sides, or be of a wraparound design with angled lenses. The use of protective devices for the eyes as well as the body is recommended.

Individual protection and monitoring

(133) The principles of radiological protection of workers from ionising radiation are discussed in *Publication 75* (ICRP, 1997) and reiterated in Paragraph 113 of *Publication 105* (ICRP, 2007c). In this section, practical points pertaining to those who need to be monitored and what protective actions should be taken are discussed.

(134) Individual monitoring of workers exposed to ionising radiation using film dosimeters, thermoluminescent dosimeters, optically stimulated luminescence badges, or other appropriate devices is used to verify the effectiveness of radiological protection practices in the workplace. The advice of a radiological protection expert/medical physicist should be sought to determine which method is most appropriate. An individual monitoring programme for external radiation exposure is intended to provide information about the optimisation of protection, and to demonstrate that the worker's exposure has not exceeded any dose limit or the level anticipated for the given activities (IAEA, 1999). As an effective component of a programme to maintain exposures as low as reasonably achievable, it is also used to detect changes in the workplace and identify working practices that minimise dose (NCRP, 2000; IAEA, 2004). In 1990, the Commission recommended a dose limit for workers of 20 mSv $year^{-1}$ (averaged over a defined 5-year period; 100 mSv in 5 years) and other limits as given in Table 3.1; these limits were retained in the 2007 Recommendations (ICRP, 1991, 2007b). However, all reasonable efforts to reduce doses to the lowest possible levels should be used.

(135) The Commission recommended that interventional radiology departments should develop a policy that staff should wear two dosimeters (ICRP, 2000b). A single dosimeter worn under the lead apron will yield a reasonable estimate of effective dose for most instances. Wearing an additional dosimeter at collar level above the lead apron will provide an indication of the thyroid dose (if unprotected) and other parts such as the head and lens of the eye. In view of increasing reports of radiation-induced cataracts in those involved in interventional procedures, monitoring the dose to the lens of the eye is important (Ciraj-Bjelac et al., 2010; Vañó et al., 2010). Recently, dosimetry for the lens of the eye has become an active research area. Many studies have been performed to determine which personal dose equivalent quantity is appropriate, and how it can be used for monitoring the dose to the lens of the eye, and to develop dosimeters to measure dose to the lens of the eye (Domienik et al., 2011). The Commission recommends that methods which provide reliable estimates of dose to the eye under practical situations should be established and used.

(136) A risk-based approach to occupational radiation monitoring should be adopted to avoid unnecessary monitoring of all workers. There is a need to raise awareness of the requirement to use a dosimeter at all times, as there are many examples of infrequent use in practice.

(137) The lack of use or irregular use of personal dosimeters is still one of the main problems in many hospitals (Miller et al., 2010; Padovani et al., 2011). The protection service should provide specialist advice and arrange any necessary monitoring

provisions (ICRP, 2007b). In cases where individual monitoring is inappropriate, inadequate, or not feasible, occupational exposure of workers should be assessed on the basis of the results of monitoring the workplace, and information about the locations and durations of exposure of workers (IAEA, 1996). In addition to individual monitoring, it is recommended that indirect methods using passive or electronic dosimeters (e.g. dosimeters attached to the C-arm device) should be used in these installations to enable the estimation of occupational doses to professionals who do not use their personal dosimeters regularly. Active dosimeters are an asset in the education and practice of radiological protection.

6.3. Limitations of CBCT

6.3.1. Detector dynamic range and reduced contrast resolution

(138) Compared with the detector system used in MDCT scanners, FPDs have a lower dynamic range and lower DQE. For example, the contrast resolution of FPD-based CBCT is approximately 10 Hounsfield units (HU), which is lower than the 1–3 HU available on MDCT. Therefore, applications that require imaging of low-contrast structures (e.g. grey–white matter differentiation in a head CT) will perform poorly on a CBCT scanner compared with an MDCT scanner.

6.3.2. Scatter

(139) The large FOV of these scanners implies that the entire volume generates the scatter radiation. As an anti-scatter grid, which would further decrease the efficiency of the imaging chain, is not used typically, scatter can degrade image quality significantly.

6.3.3. Temporal resolution

(140) FPDs usually employ CsI as the scintillator. CsI is a slow scintillator and suffers from afterglow (i.e. a ghost of the old image is seen in the new image at fast frame rates). As a result, sufficient time must be allowed to elapse after each projection before the next projection is recorded.

6.3.4. Artefacts

(141) CBCT images, in general, suffer from more or less the same types of artefact that are seen in MDCT, but to different degrees. A summary of MDCT artefacts has been provided by Barrett and Keat (2004). Metal and windmill artefacts are generally reduced in CBCT compared with MDCT, particularly for high-density metals

(Pauwels et al., 2013). Motion artefacts, on the other hand, are more prevalent in CBCT.

(142) In MDCT, a smaller number of slices, typically four to 64 (although up to 320 slices in some scanners), is acquired in each rotation as the patient is translated through the gantry. Therefore, any patient motion affects only those slices that were being acquired during the motion. In CBCT, the entire dataset is constructed from projections acquired in one rotation. Therefore, any motion, even for a very short duration, affects the entire volumetric dataset. The rotation speed of CBCT compared with MDCT is approximately 10–20 times slower: as such, CBCT is much more sensitive to motion artefacts.

6.3.5. Hounsfield unit consistency

(143) The HU system is based on the linear attenuation coefficient of water. All CT scanners present clinical images in this system for consistency across vendors and scanner models. The daily calibration of MDCT scanners incorporates scanning of a water cylinder for HU calibration and beam hardening correction. CBCT scanners typically lack detailed radiometric calibration, and the generated HU values are more variable than those from an MDCT scanner. In contrast to MDCT, truncation of the body outlines and drawbacks of the reconstruction algorithm lead to cupping artefacts. When scanning a homogeneous water phantom, the HU units are not uniform over the entire cross-section, but decline towards the edges (Kyriakou et al., 2011).

6.3.6. Geometric distortion

(144) Depending on the type of gantry used, a CBCT scanner is more prone to geometric distortion than an MDCT scanner. For example, when a C-arm is used as a CBCT scanner, the weight of the gantry may deform the unit, so that the isocentre of the imaging chain is not as well defined. This will degrade the image quality. In addition, flexible alignment of many of the CBCT gantries necessitates a collision-avoidance system that may increase the complexity of a scan.

6.4. Future developments

(145) Several technical developments in the field of CBCT are expected to enable interesting new features that will affect image quality and imparted radiation. As these features are only at an early stage of development, and mature implementations are not available in the scanner systems in current use, only general guidance about their efficacy and application can be given at this point in time.

6.4.1. Novel scan trajectories

(146) For tomographic reconstruction, projective data from a rotation of at least 180° plus the cone angle are necessary. This requirement imposes several constraints on the design and operation of CBCT in practice. For example, C-arm systems need to have large clearance in the operating room to complete the scan trajectory, and lack of space may limit the use of certain scan modes of the C-arm CBCT in practice. Novel scanning trajectories, such as eccentric rotation and/or parallel shifting of the imaging chain, may relieve some of these constraints and be useful in extending the scan FOV. These newer, non-traditional scan trajectories lead to a much more complex distribution of the applied dose in the examined volume. Currently, only one commercial robot CBCT system uses these alternative trajectories. However, the dose estimation systems are not designed to handle such systems. In the future, radiological protection measurements will have to account for these non-traditional trajectories, and factor in the associated non-uniform dose deposition.

6.4.2. Advanced methods for exposure control

(147) As mentioned above, AEC is a means to adapt the scan parameters to an individual patient's anatomy and its variations. Usually, AEC is provided by a feedback loop between the radiation measured at the detector side and the x-ray tube exposure settings. In its simplest form, the tube current is varied so as to keep the total radiation measured at the detector constant. This compensatory mechanism can fail when the patient size increases beyond a certain point. After that point, for a given kV setting, the x-ray tube may not be able to deliver any further increase in mA without overheating or causing damage to the x-ray tube anode. Sometimes, in order to accommodate such large variations in photon flux when current modulation alone is not able to meet the demand, the x-ray tube voltage setting is also changed by AEC in CBCT. In order to make this practice workable for CBCT, manufacturers use experimentally measured correlation curves to map the signal measured at one tube voltage to a corresponding reading at another tube voltage. This is clearly an engineering approximation derived empirically; a practice rare in MDCT. In fact, a change of the tube voltage in the middle of a single-energy scan may interfere with the fidelity of HU calibration.

(148) If tube voltage is changed during a scan, inconsistencies in the measured CT values with respect to the Hounsfield scale definition have to be taken into account and corrected. AEC with tube current as well as voltage variations make actual patient dose estimations from tube parameters and phantom experiments very complex. The difficulty is compounded by the fact that the mapping between signals at different kV settings is proprietary information. As this practice becomes more prevalent, further research will be needed in this area of dose measurement practice in order to account for this non-traditional use of AEC systems.

6.4.3. Novel reconstruction algorithms and compressed sensing

(149) Analytical reconstruction algorithms, such as the filtered back projection, have been the mainstay for MDCT. These algorithms provide a single pass solution that is available on nearly all CT scanners. Although they are generally fast and provide good image quality, they are prone to noise and artefacts. In the past decade, a new class of iterative reconstruction algorithms has been introduced for MDCT by various vendors. Instead of using an analytical approach, these algorithms attempt to minimise the error between the projections and the reconstructed slices. Typically, one to 30 iterations are required for the solution to converge. These algorithms generally provide better image quality, and are more robust in minimising noise and artefacts. Their main drawback, besides their complexity, is their slow computational speed. They are generally associated with increased image resolution, decreased radiation dose, and metal artefact reduction. They can also be used for region-of-interest reconstruction.

(150) Currently, a non-iterative, modified FDK algorithm is the industry standard for image reconstruction in CBCT. Similar to the reconstruction algorithms for the MDCT systems, where the use of iterative reconstruction algorithms is now gaining in popularity, a shift in CBCT reconstruction from a modified FDK to an iterative technique is expected. These reconstruction methods have the ability to incorporate prior knowledge in the form of radiation and scatter distribution, as well as knowledge of the anatomy. They also minimise the error between the projections and the reconstructed image in a global sense. These features would be advantageous for CBCT, as it is often performed in situations where repetitive scanning of the same anatomical region is necessary (e.g. to observe the evolution of a contrast bolus through the vasculature and the tissue). Another example of repetitive scanning would be angiographic interventions to deploy interventional devices (e.g. aneurysm coils) and confirm their position. Often, changes in the successive 3D volumes are relatively minor. Iterative algorithms can accommodate these requirements more readily, and thus minimise the number of projections required for 3D or four-dimensional reconstruction.

(151) In order to reconstruct a volume of interest or a slice, a minimum number of data points is needed, in a strict mathematical sense, for the reconstruction task. If the dose per projection is fixed, this minimum number of projections determines the overall patient dose. If certain assumptions can be made about the object, and the requirement that projection images be equally spaced is relaxed, an image can be reconstructed under conditions that contravene the Nyquist–Shannon limit (i.e. the theoretical minimal sampling rate required for reconstruction). These methods, which are generally called ‘compressed sensing’, can reduce the dose by reducing the number of input projections required for reconstruction. Sparse angular sensing, where projections are only acquired from certain angular directions, is one method for reducing dose using compressed sensing.

(152) Both iterative reconstruction techniques and compressed sensing are in their infancy in CBCT. However, these novel techniques are expected to have a major impact on image quality and the associated radiation dose in CBCT in the future. The user has to be aware that long established relationships between radiation dose and image quality may undergo fundamental changes with the use of novel, iterative reconstruction algorithms.

7. RADIATION DOSE MANAGEMENT IN SPECIFIC APPLICATIONS OF CBCT

- **The user of CBCT in interventions can influence the radiation dose imparted to the patient significantly by judicious use of a 'low-image-quality or low-dose' scan instead of a 'high-image-quality or high-dose' scan.**
- **In radiotherapy, justified use of CBCT has potential at different stages of therapy such as: pretreatment verification of patient position and target volume localisation; evaluation of non-rigid misalignments, such as flexion of the spine or anatomical changes in soft tissue; and during or after treatment to verify that the patient position has remained stable throughout the procedure. Low-dose CBCT protocols should be used for pretreatment alignment of bony structures.**
- **Many machines were only capable of fluoroscopy initially, but can now also perform CBCT. Due to the improved clinical information in CBCT and its ability to remove overlying structures, the user may be tempted to over-use the CBCT mode. The CBCT mode should be used judiciously.**
- **In orthopaedics, justified use of CBCT can help in assessing the position of fractures and implants with respect to the bony anatomy, especially in situations where fluoroscopy alone is insufficient, and thus can help in patient dose management.**
- **In urology, low-dose CBCT protocols should be used when imaging high-contrast structures, such as calcified kidney stones.**
- **Dental and maxillofacial CBCT scans should be justified, considering alternative imaging modalities. Once justified, they should be optimised to obtain images with minimal radiation dose without compromising the diagnostic information.**

7.1. Introduction

(153) It is assumed that readers would have gone through Section 4 of this report which deals with the principles of radiological protection. CBCT is used in a multitude of clinical applications. To maximise the practical utility of this publication, this section is organised according to different clinical application domains that use CBCT rather than design considerations, as they tend to be very similar across different applications. For example, a C-arm system used in interventional radiology (neuro, non-vascular, vascular) differs only marginally, if at all, from that used in orthopaedics or urology. However, application-specific radiation varies considerably across these domains, primarily because of patient-related and use-related factors. At the end of each section, practical tips on the use of CBCT are provided that are germane to that application domain.

(154) This section also cites and summarises various published studies that provide typical ranges of CBCT dose values for each clinical application domain. Absolute dose values are provided and may be used by a practitioner as a reasonable starting point.

(155) It should be stressed that disparate methods have been used in the literature to measure and quantify dose. Many manufacturers provide concise dose values for

their machines under varying scanning conditions and protocols. Such data are often required for the regulatory approval process. It is recommended that the user should consult these documents and dose databases. However, documents that have been submitted to regulatory agencies for licensing suffer from a lack of standardisation in dose measurement techniques and units.

(156) The drawing of conclusions from published studies and vendor documents, especially when absolute dose values are compared, should be done with care, keeping in mind the limitations of such comparisons because of variations in the measurement methodology. It is expected that future literature on CBCT will use dose measurement guidelines similar to those discussed in Section 5 and described in more detail in Annex A. Such standardised and consistent dose figures will enable direct comparisons among different machines, protocols, and imaging practices. In parallel, standardisation of digital imaging and communication in medicine (DICOM) dose reporting for CBCT is needed in order to enable retrospective retrieval and review of patient exposure from stored PACS images.

7.2. CBCT in radiotherapy

(157) The primary role of CBCT in radiation therapy is pretreatment verification of patient position and target volume localisation. In the most common workflow pattern, a patient lies on the treatment couch, is positioned approximately for treatment using wall-mounted lasers, and precise positioning is based on CBCT imaging. In addition to correcting the position of the patient, the images are examined for non-rigid misalignments, such as flexion of the spine or anatomical changes in soft tissue. CBCT imaging is also sometimes acquired during or after treatment to verify that the patient position has remained stable throughout the procedure. CBCT can also be used in treatment simulation, prior to the start of a course of treatment.

(158) Most radiation therapy centres use gantry-mounted kV CBCT, with an x-ray tube as the source and amorphous silicon flat-panel imagers as detectors (Jaffray et al., 1999). Typical energies are between 80 and 125 kVp, with typical absorbed doses between 1 and 40 mGy. A less-common modality is MV CBCT, using the treatment accelerator as an x-ray source and a portal imaging FPD (Pouliot et al., 2005). MV CBCT generally uses energies of up to 6 MV, with typical absorbed doses between 20 and 100 mGy. Compared with kV CBCT, the images produced with MV CBCT generally have lower soft tissue contrast due to the lack of photoelectric absorption at higher photon energies. However, these systems do have some advantages, including better geometric alignment of imaging and treatment isocentres, and better imaging for large patients or patients with metallic prostheses.

(159) The choice of imaging technique is based on the treatment site and therapy goals. For cranial or head and neck targets, the treatment site is well accounted for by alignment of bony anatomy. Therefore, a low-dose CBCT technique is appropriate. Similarly, when the treatment target can be aligned using implanted fiducial markers, a low-dose technique is warranted. In these cases, accurate positioning with CBCT can be performed with absorbed doses within irradiated tissues of less

than 10 mGy. Accurate positioning in the pelvis and abdomen, however, may require differentiation of soft tissue boundaries. In these cases, the number of photons used for imaging should be increased and may require imaging at absorbed doses between 10 and 40 mGy.

(160) The overall absorbed doses to tissues of a patient within the field imaged by CBCT are small compared with the prescribed treatment dose (Table 7.1). However, the treatment dose is localised to the disease site, whereas the CBCT imaging dose is spread across the entire imaging volume. When compared with other pretreatment imaging modalities, CBCT can provide better setup accuracy doses with dose equal to or lower than MV port films (Korreman et al., 2010), but uses more dose than orthogonal planar kV x-ray imaging (Kry et al., 2005) or non-ionising setup methods such as optical imaging or ultrasound. Furthermore, one must keep in mind that the primary radiation fields produce Compton scattered x rays that deposit dose in the area around the treatment site. The magnitude of the scattered dose depends upon the distance from the treatment field, and ranges from approximately 0.05% to 0.5% of the maximum dose at the target (d_{max}). The radiation dose at d_{max} is defined as 100%, and decreases as penetration through tissue increases, with the decrease primarily due to energy absorbed within the tissue.

7.2.1. Accounting for imaging dose in radiotherapy

(161) When x-ray imaging is used in a radiotherapy setting, the patient receives radiation from both imaging and therapy. CBCT imaging, especially when employed daily, causes additional accumulated dose which should be considered in the context of the patient's treatment. For this reason, the use of daily CBCT imaging should be evaluated for each patient for sparing sensitive organs that have low thresholds for tissue reactions (deterministic effects), and for paediatric patients who have a higher sensitivity to radiation.

(162) With first-generation linac-mounted kV CBCT systems, imaging doses can account for 2% or more of the prescribed target dose (Amer et al., 2007; Ding et al., 2008; Ding and Coffey, 2009). However, the current trend is towards dose reduction, and second-generation systems have achieved significant dose savings in kV CBCT (Ding and Munro, 2013). When the imaging dose constitutes a significant fraction of the prescription dose (ICRU, 2010), it should be reflected in the patient's prescription dose. For example, the prescription dose can be adjusted to include the imaging dose. A more advanced accounting procedure is to perform patient-specific CBCT dose calculation in the radiotherapy treatment planning system (Alaei et al., 2010). If this technology is available, the patient organ doses that combine the imaging dose and the radiotherapy dose can be optimised in 3D to create a more precise estimate of the patient's total radiation burden.

(163) In summary, for most radiation oncology applications of CBCT, accurate delineation and alignment of the treatment target and critical organs should be a practitioner's

Table 7.1. Doses in cone beam computed tomography (CBCT) procedures in radiotherapy. Listed values are for a single CBCT acquisition and should be multiplied by the number of CBCT scans performed to compute the total dose.

Procedure	Reported value	Method	Reference
MV CBCT			
Head and neck	50–150 mGy	Absorbed dose at isocentre	Pouliot et al., 2005
MV CBCT			
Head and neck	60–73 mGy	TLDs, film and ion chamber measurements in cylin drical and anthropo-morphic phantoms	Gayou et al., 2007
Pelvis	99–121 mGy		
kV CBCT			
Head and neck	1–17 mGy	$CTDI_w$	Song et al., 2008
Chest	11–18 mGy		
Pelvis	24–54 mGy		
kV CBCT			
Head and neck	36.6 mGy	$CTDI_w$	Cheng et al., 2011
Pelvis	29.4 mGy	Effective dose, TLDs in female phantom, absorbed dose to the lens of the eye	
Head and neck	1.7 mSv		
Pelvis	8.2 mSv		
Head and neck	3.8 mGy (new protocol) 59.4 mGy (old protocol)		
kV CBCT			
Head and neck	2.1–10.3 mSv	Effective dose, TLDs in female phantom Mean skin dose at irradiated site, TLDs in female phantom	Kan et al., 2008
Chest	5.2–23.6 mSv		
Pelvis	4.9–22.7 mSv		
Head and neck	13–67 mGy		
Chest	14–64 mGy		
Pelvis	12–54 mGy		
kV CBCT			
Head and neck	7 ± 0.5 mGy (at simulator)	Average absorbed dose, TLD measurements in anthropomorphic phantom	Stock et al., 2012
Pelvis	1 ± 0.05 mGy (at linac) 12 ± 3 mGy (at linac) 36 ± 12 mGy (at linac)		
kV CBCT			
Chest	Spinal cord: 8–22 mGy Left lung: 12–29 mGy Right lung: 16–40 mGy Heart: 17–30 mGy Body: 12–31 mGy	Absorbed doses from Monte Carlo simulation	Spezi et al., 2012
kV CBCT			
Head and neck	Spinal cord: 1.3–1.7 mGy Mandible: 4.5–8.3 mGy Right parotid: 0.3–2.7 mGy Left parotid: 0.5–2.7 mGy Left eye: 0.1–1.8 mGy Right eye: 0.1–1.8 mGy Oral cavity: 1.7–3.8 mGy	Absorbed doses from Monte Carlo simulation	Spezi et al., 2012

(continued on next page)

Table 7.1. *(continued)*

Procedure	Reported value	Method	Reference
	Body: 1.0–2.3 mGy Brainstem: 0.3–1.5 mGy Larynx: 2.6–2.8 mGy		
kV CBCT Pelvis	Rectum: 11–21 mGy Left femoral head: 20–47 mGy Right femoral head: 25–62 mGy Body: 11–33 mGy	Absorbed doses from Monte Carlo simulation	Spezi et al., 2012
kV CBCT Thorax MVCT Thorax (non-CBCT)	0.9–21 mGy 0.3–9 mGy	Absorbed dose, TLD measurements in thorax phantom	Shah et al., 2012
kV CBCT Pelvis MV CBCT Pelvis	18–51 mGy 0.9–8.0 mGy	Absorbed dose, TLD measurements in pelvis phantom	Shah et al., 2012
kV CBCT Pelvis MV CBCT Pelvis kV CBCT Head MV CBCT Head TomoTherapy Pelvis	25–40 mGy 40–80 mGy 1–7 mGy 30–50 mGy 13 mGy	Absorbed dose, IMRT phantom measurements with radio-photoluminescent glass dosimeter	Kouno et al., 2013
kV CBCT Head and neck Chest Pelvis	19 mGy 51 mGy 167 mGy	Primary absorbed doses at the centre of custom-made phantom using a glass dosimeter	Kim et al., 2013
kV CBCT Pelvis Head and neck	0.2–7 mGy 0.03–0.7 mGy	Secondary absorbed doses (20–50 cm from isocentre) measured on custom-made phantom using a glass dosimeter	Kim et al., 2013
kV CBCT Thorax Standard low-dose Reduced mAs Reduced rotation	 5.0 ± 0.3 mSv 2.4 ± 0.2 mSv 1.2 ± 0.3 mSv 1.2 ± 0.3 mSv	Effective dose, radiochromic film in female phantom and Monte Carlo simulation	Alvarado et al., 2013

$CTDI_w$, weighted computed tomography dose index; IMRT, intensity-modulated radiation therapy; TLD, thermoluminescent dosimeter). MVCT, megavoltage CT; TLD, thermoluminescent dosimeter; IMRT, intensity-modulated radiation therapy; CTDIw, weighted computed tomography dose index.

primary concern. Radiation dose arising from CBCT must be weighed within the context of therapy doses that are one to two orders of magnitude higher than the imaging doses. Imaging technique should be chosen to match treatment goals, such as the use of low-dose techniques for alignment of bony structures. In situations where the cumulative CBCT dose adds up to be a non-negligible fraction, it may be reflected in the overall dose schedule and subtracted from the therapeutic dose.

(164) Imaging technique should be chosen to match treatment goals, such as the use of low-dose techniques for alignment of bony structures.

7.3. Neurointerventions

(165) Intraprocedural CT capability in a C-arm, a form of CBCT, has been found to be useful in both diagnostic and therapeutic interventions. In C-arm CT, the same imaging chain that is used for fluoroscopic as well as angiographic imaging is also used for collecting the projection data needed for tomographic reconstruction.

(166) CBCT is used in neurointerventions to acquire 3D angiographic images to assess potential intracranial haemorrhage, and during vertebral augmentation procedures (Psychogios et al., 2010). CBCT may also be used to guide complex, 3D positioning of coils within an aneurysm (Levitt et al., 2011). Some systems also allow over-laying of 3D images on fluoroscopic images (Racadio et al., 2007). It is even possible to create a blood-volume map with data from CT perfusion using CBCT (Fiorella et al., 2014).

(167) Manufacturers may provide high- and low-quality protocols for these applications. Low-quality scan protocols, which typically use fewer projections, are usually sufficient for high-contrast structures such as contrast-enhanced vessels or bony anatomy. Furthermore, the position of intervention instruments can be assessed by low-dose scans. A high-quality imaging protocol is recommended for soft tissue evaluation, such as assessment of intracranial parenchymal or subarachnoid haemorrhage.

(168) The image quality of neurointerventional CT with respect to radiation dose using phantoms was described by Fahrig et al. (2006).

(169) In many neurointerventional scans, the radiosensitive thyroid and lenses of the eyes lie within the scan FOV. To minimise the dose to these organs, the user can take advantage of a feature of CBCT that is only available in some MDCT scanners as an add-on feature. CBCT projections acquired over an angular span of $(180^\circ + \varphi)$, where φ is the cone angle of the x-ray tube, are sufficient for image reconstruction. Depending on the starting position of the $(180^\circ + \varphi)$ rotation arc, a significant reduction in the exposure of the eyes and thyroid can be realised with 'tube under' scan arcs. Shielding of the thyroid (when not in the scan FOV) provides moderate dose reduction (Daly et al., 2006).

(170) A neurointerventionalist can influence the radiation dose from CBCT significantly by:

- Deciding whether or not a 'high-dose' soft tissue scan is needed. This would be required to rule out intracranial haemorrhage or assess a soft tissue structure in a diagnostic scan. For angiographic scans, for which contrast media have been

Table 7.2. Doses in cone beam computed tomography procedures in neurointerventions.

Procedure	Reported value	Method	Reference
Head	2–37 mGy	Absorbed organ doses	Koyama et al., 2010
	1.2 mSv	Effective dose, photodiodes in anthropomorphic phantom	
Neurointerventions (soft tissue/'rule out haemorrhage')	40–48 mGy	Modified CTDI (small-volume ion chamber)	Fahrig et al., 2006
Neurointerventions (soft tissue/'rule out haemorrhage')	75 mGy	Modified CTDI (250-mm-long ion chamber)	Kyriakou et al., 2008a
Interventional head and neck surgery			
Soft tissue of head and neck	10 mGy	Modified CTDI (using customised 16-cm cylindrical head phantom)	Daly et al., 2006
Neurointerventions (angiograms, interarterial contrast media injections)	9 mGy	Modified CTDI (250-mm-long ion chamber)	Kyriakou et al., 2008a
Spine			
Thoracic bone visualisation	1.8 mGy	Modified CTDI using CTDI (head/body) and other (abdomen/thorax) phantoms, small-volume ionisation chamber	Schafer et al., 2011
Lumbar bone visualisation	3.2 mGy		
Thoracic soft tissue visualisation	4.3 mGy		
Thoracolumbar spine			
Small patient setting	3.2 mSv	Effective dose from thoracolumbar spine model, using conversion factors based on dose length product	Lange et al., 2013
Large patient setting	8.1 mSv		
Neurointerventions			
High-dose setting	32 mGy (brain dose)	Mathematical model of an adult standard anthropomorphic phantom	Sanchez et al., 2014

CTDI, computed tomography dose index.

injected, a 'low-dose' scan that displays high-contrast structures is sufficient to image vessels. A low-dose scan is also sufficient for defining the position of high-contrast interventional materials, such as coils, clips, and Onyx^{TM}. The choice of low dose vs high dose may alter the applied dose considerably (Table 7.2).

- Using 'tube under' scans, meaning scans in which the x-ray tube is positioned on the opposite side of the body from radiosensitive organs such as the thyroid and the eyes for the majority of the time, whenever possible in practical situations. This decreases the dose to the radiosensitive organs without any appreciable consequence for image quality or diagnostic power of the examination.

7.3.1. Dose to workers from CBCT in neuroradiology procedures

(171) Workers can reduce their radiation exposure drastically by maintaining sufficient distance from the x-ray source, and should use shielding whenever possible. For example, the in-room unshielded effective dose from a typical intra-interventional CBCT scan (10 mGy to isocentre) is <0.005 mSv at 2 m from the isocentre (Daly et al., 2006). Nottmeier et al. (2013) reported doses ranging between 0 and 1.8 mGy spin^{-1} in badges located at different places around the O-arm under investigation.

(172) Workers should leave the room whenever permitted by the status of the patient during CBCT.

7.4. Vascular interventions

(173) Vascular interventions include a range of procedures, such as angioplasty in peripheral artery disease, (fenestrated branched) endovascular aneurysm repair, vessel occlusion for controlling acute bleeding, treatment of arterio-venous malformations, and tumour embolisation [either bland (such as in uterine fibroid embolisation), with chemotherapy (such as in chemoembolisation of many liver tumours), or with radioactive particles (selective internal radiotherapy treatment)]. Other examples of such interventions include placement of intravascular devices such as vena caval filters, transjugular intrahepatic portosystemic shunt (TIPSS), and catheter-directed thrombolysis. CBCT may be used in these procedures to acquire tomographic images of the vasculature for 3D roadmapping. CBCT is also helpful in verifying the spatial relationship of instruments and surrounding anatomy in situations where relative position or orientation cannot be resolved sufficiently using projective imaging alone. CBCT is being used increasingly for procedural planning (e.g. in transcatheter aortic valve implantation) or image guidance and navigation [e.g. in atrial catheter ablation or TIPSS (Adamus et al., 2009)]. Some of the newer machines also allow acquisition of 3D vascular roadmaps that can be overlaid on fluoroscopic images. Both intra-arterial and intravenous contrast media injections are used. It can be expected that CBCT will play a growing role in vascular interventions.

Table 7.3. Doses in vascular cone beam computed tomography (CBCT) interventions.

Procedure	Reported value	Method	Reference
Cardiac angiography	Median: 2.4 Gy cm^2 (range: 0.35–42 Gy cm^2)	KAP for sample of 756 paediatric patients (age 0–19 years)	Corredoira et al., 2015
Fenestrated branched endovascular aneurysm repair			
Pre-operative	0.27 Gy	Skin dose	Dijkstra et al., 2011
Postoperative	0.55 Gy		
Catheter ablation (CBCT part)	7.9 ± 0.6 mSv	Effective dose derived from total KAP	Ejima et al., 2010
Catheter ablation (CBCT part)	5.5 ± 1.4 mSv[*] 6.6 ± 1.8 mSv[†]	Effective dose from simulation	Wielandts et al., 2010
Liver (in hepatic arterial embolisation therapy)	8.2 ± 1.4 mSv (male) and 5.6 ± 1.2 mSv (female)	Effective dose from KAP of anthropomorphic male and female phantoms	Tyan et al., 2013
	61 Gy cm^2 (male) and 52 Gy cm^2 (female)	KAP from 125 patients	
	11.5 ± 2.3 mSv (male) and 11.3 ± 3.0 mSv (female)	Effective dose corresponding to patients' KAP, using conversion factors based on anthropomorphic phantoms	
Hepatic arterial embolisation therapy	75–175 mGy 16–52 Gy cm^2	Skin entry dose KAP Retrospective analysis of 126 procedures	Paul et al., 2013a,b

(continued on next page)

Table 7.3. *(continued)*

Procedure	Reported value	Method	Reference
Abdominal CBCT scan	2–37 mGy 4–5 mSv	Absorbed organ doses Effective dose, photodiodes in anthropomorphic phantom	Koyama et al., 2010
Abdominal CBCT	2.1–4.2 mSv	Effective dose using 'small' anthropomorphic phantom and Monte Carlo simulations	Suzuki et al., 2011
Hepatic artery embolisation	238 mGy	Skin entry dose, readout from examination protocol	Schulz et al., 2012

KAP, kerma-area product.
*Using *Publication 60* weighting factors (ICRP, 1991).
†Using *Publication 103* weighting factors (ICRP, 2007b).

Table 7.4. Worker doses in vascular cone beam computed tomography (CBCT) interventions.

Procedure	Reported value to worker	Method	Reference
Abdominal CBCT	Eye level: 8 s per rotation: 28.0 μSv 20 s per rotation: 79.3 μSv 5 s per two rotations: 32.5 μSv	Digital dose rate meter	Schulz et al., 2012
Hepatic angiography	Large field of view: 37.6 μSv Eye level: 28–79 μSv per procedure		

(174) The user of CBCT in vascular interventions can influence the radiation dose imparted to the patient significantly by judicious use of protocols with adequate image quality but lower dose if high-contrast objects are visualised (stents, coils, guide wires, or high intravascular iodine contrast), or higher dose if low-contrast objects are visualised (soft tissue or low parenchymal iodine contrast) (Table 7.3).

7.4.1. Dose to workers in vascular interventions

(175) Paul et al. (2013b) found that the dose to the hands and the left knee of the interventionalist was higher than the dose to the assistant physician when using volume imaging. Mean doses received by the interventionalist ranged from 0.01 mGy (shielded thyroid, chest, and gonads) to 0.37 mGy (left finger). Mean doses received by the assistant physician were 0.01 mGy to the shielded thyroid, chest, and gonads, and 0.08 mGy to the left and right eyes. The mean dose to the eye for the interventionalist was 0.11 mGy. Doses associated with the use of CBCT were higher compared with catheter angiography and digitally subtracted angiography. In guided needle interventions, operator hand doses in free-hand procedures ranged from 20 to 603 μSv. Laser guidance alone or in combination with needle holders resulted in a reduction of the hand dose to <36 μSv (5–82 μSv) per procedure (Kroes et al., 2013). Additional worker doses for abdominal CBCT and hepatic angiography can be found in Table 7.4.

(176) Workers should leave the room whenever permitted by the clinical situation during a CBCT scan. For injecting contrast media, an automatic injector should be used whenever possible. Workers who remain in the procedure room during the CBCT exposure should be protected by fixed or mobile shields.

7.5. Non-vascular interventions

(177) Non-vascular interventions include procedures such as vertebroplasty (treatment of vertebral fractures, osteoporosis, or metastases), drainage of abscesses or

fluid collections, image-guided biopsies, percutaneous transhepatic cholangiography drainage (PTCD), and tumour ablation (e.g. liver tumour microwave ablation) (Wallace et al., 2008). These procedures are currently performed either under fluoroscopic guidance or MDCT guidance, with C-arm CBCT becoming increasingly popular as it combines the advantages of both (Orth et al., 2008). Modern C-arm systems allow the planning of percutaneous instrument insertion via preprocedural CBCT, with fluoroscopy as the main modality for intraprocedural instrument guidance. Repeated CBCT may be used for intraprocedural quality control; however, the user should minimise the number of CBCT scans acquired during a given procedure.

(178) The user of CBCT in non-vascular interventions can influence the radiation dose that is applied to the patient significantly by:

- appropriately choosing between a 'high-dose' scan and a 'low-dose' scan; and
- using the CBCT mode judiciously, relying on the fluoroscopy mode as much as possible.

(179) Table 7.5 provides an overview of patient doses in non-vascular interventions. Doses vary considerably depending on the diagnostic application and corresponding exposure settings. Effective doses measured in phantoms were a few mSv for each study. Various other dose quantities are also included. Reported CTDI values were generally a few mGy, but some values >20 mGy have been measured. At the skin and eye level, doses up to a few hundred mGy were found.

7.5.1. Dose to workers in non-vascular interventions

(180) In certain procedures, some dose to the interventionalist cannot be avoided. For example, PTCD, or other biliary drainage procedures often require that one or both hands/fingers are very close to the radiation field. For a short time, these procedures may even require that these organs be in the radiation field, especially in punctures of the left lobe of the liver. The practitioner should be cognisant of these small but potentially repeated exposures. In a long procedure, the dose to the fingers may exceed a few mSv. Protective gloves reduce the exposure of hands or fingers, but increase the dose to the practitioner and patient if the hands with gloves are placed in the primary beam. Auxiliary instrumentation for handling needles and probes in the radiation field should be used whenever possible. Examples of doses to workers from interventional procedures are given in Section 7.4.1; radiation doses in vascular and non-vascular interventions are similar.

7.6. Orthopaedics/surgery

(181) In orthopaedics or trauma surgery, CBCT is used mainly to assess the position of fractures and implants with respect to the bony anatomy, especially in situations where fluoroscopy alone is insufficient to disambiguate the position of an implant with respect to the bony anatomy (Table 7.6). For example, with fluoroscopy alone, the critical relationship of a screw with respect to an articular surface may sometimes

Table 7.5. Doses in non-vascular cone beam computed tomography (CBCT) interventions.

Procedure	Reported value	Method	Reference
Lumbar spine (bone protocol)	3.7 mGy	Modified CTDI*	Schafer et al., 2011
Thoracic spine (bone protocol)	1.9 mGy		
Lumbar spine, low resolution (soft tissue protocol)	6.0 mGy		
Lumbar spine, high resolution (soft tissue protocol)	12.5 mGy		
Thoracic spine (soft tissue protocol)	4.6 mGy		
CBCT-guided vertebroplasty of the thoracic spine	11.5 mGy (total procedure dose)		
CBCT-guided vertebroplasty of the lumbar spine	23 mGy		
Renal biopsy	44.0 Gy cm^2	Mean KAP	Braak et al., 2012
Biliary tube placement (PTCD)	413 mGy	Skin entrance dose	Schulz et al., 2012
Biliary protocol	4.2–8.4 mSv	Effective dose, female anthropomorphic phantom with MOSFET detectors	Kim et al., 2011
Phantom study	Head: 1.2 mSv Chest: 7.3 mSv Abdomen: 7.5 mSv	TLDs in anthropomorphic phantom	Bai et al., 2011
Head	4.4–5.4 mSv (absorbed dose to lens of the eye: 44–174 mGy)	Effective dose, TLDs in anthropomorphic phantom	Kwok et al., 2013
Abdominal	15–37 mSv		

CTDI, computed tomography dose index; KAP, kerma-area product; TLD, thermoluminescent dosimeter; PTCD, percutaneous transhepatic cholangiography drainage.

*Using CTDI (head/body) and oblate (abdomen/thorax) phantoms, measuring at the centre and at four peripheral points with a small-volume ionisation chamber.

Table 7.6. Doses in orthopaedics/surgery cone beam computed tomography (CBCT) interventions. Certain values in Table 7.5 may also be applicable.

Procedure	Reported value	Method	Reference
Extremity scan	6.4–15 mGy	CTDI phantom, small-volume ion chamber in isocentre	Zbijewski et al., 2011
CBCT wrist arthrography	1.7–2.2 mGy	CTDI	Ramdhian-Wihlm et al., 2012
Evaluation of finger fractures	0.8 mSv	Absorbed dose, derived from prior study using TLDs in anthropomorphic phantom	Faccioli et al., 2010
Volumetric scan of wrist joint and the distal radius	133 mGy cm 0.11 mSv	Dose length product, effective dose derived from dose length product	Reichardt et al., 2008

CTDI, computed tomography dose index; TLD, thermoluminescent dosimeter.

remain unclear. CBCT may help to clarify this relationship. CBCT is also very helpful in spine surgery where interventions are being performed in close proximity to critical structures such as spinal nerves. CBCT datasets are also used to confirm the position of implants interprocedurally or to acquire datasets for intra-operative navigation. Dedicated extremity CBCT systems are based on the same principle as other CBCT systems used in interventional radiology or elsewhere, with the C-arm being the most popular platform. Another system (O-arm) is becoming increasingly popular for extremity and spinal fixation procedures. An O-arm system combines the advantages of a CT-gantry-based design with the flexibility of a C-arm-based design. It is essentially a C-arm system with a telescopic gantry that extends to complete the ring and become an O-arm for CT operation. As such, the gantry can function as a standard C-arm, or one can complete the O-ring and turn the system into a CT-like gantry where the FPD and the x-ray tube rotate freely. Usually, CBCT scanning is performed intra-operatively in a prone or supine position. A standing position for imaging of a weight-bearing knee and a sitting position with the upper or lower extremities extended (Zbijewski et al., 2011) have been described (Tuominen et al., 2013).

7.7. Urology

(182) CBCT on a C-arm also enables cross-sectional imaging to be performed in a urological operating room. Apart from standard pulsed fluoroscopy, 3D reconstruction

can be performed intra-operatively during urological procedures. Different operating modes are available. A low-dose protocol may be appropriate when imaging high-contrast structures. For example, when imaging calcified stones or other calcifications during percutaneous nephrolithotomy, a low-dose protocol should be employed because kidney stones should be visible despite high noise in the images obtained. The same reasoning holds true for CBCT imaging of retrograde flow of contrast in the urinary tract and collecting system (Roy et al., 2012; Michel et al., 2014).

(183) The user should use low-dose protocols that are sufficient to detect kidney stones, pelvic calcifications, metallic instrumentation, and contrast-media-filled efferent urinary tract.

7.8. Ear/nose/throat and head diagnostics or surgery

(184) Similar to other applications in the head and neck area, applications of CBCT in ENT take advantage of the fact that this region includes structures, such as the paranasal sinuses, the temporal bone, and the skull base, that have high intrinsic contrast, being composed primarily of bone, air, and soft tissue. Therefore, relatively high noise in the images can be tolerated without compromising the diagnostic utility of the CBCT scans. The high resolution of CBCT systems is ideally suited for the small structures of the skull base and middle ear. In addition, only a relatively small FOV is required to cover the necessary anatomy. In ENT scans, the position of the scan arc is a significant factor that influences radiation exposure of sensitive organs such as the lens of the eye and thyroid (Daly et al., 2006) (Table 7.7). Other applications of CBCT in ENT are described in Hodez et al. (2011), and Miracle and Mukherji (2009b). For most diagnostic ENT procedures such as imaging of the temporal bone and paranasal sinuses, dedicated scanners with the patient in a sitting position are used. Besides low dose and patient comfort, high spatial resolution is another major advantage of these scanners. As a result, these scanners are being used increasingly for surgical planning of temporal bone interventions such as cochlear implantation. There has been a rapid adoption of this technology in routine clinical practice; a trend that is likely to accelerate in future.

7.9. Dental and maxillofacial

(185) CBCT has been used in dental and maxillofacial imaging for several years, and its use is increasing. It is primarily used to acquire images of the teeth and periodontium, their placement within the alveolus of the mandible and maxilla, and their relationship with the adjacent nerves and other structures. The high spatial resolution of CBCT is ideally suited for these high-contrast structures, and generally provides excellent image quality in this field. The images are used for diagnostic purposes, pre-operative planning, postoperative evaluation, and image guidance during navigated surgery in this region. Pathological changes such as fractures,

Table 7.7. Cone beam computed tomography doses in ear/nose/throat and head surgery. Certain values in Table 7.5 may also be applicable.

Procedure	Reported value	Method	Reference
'Head scan mode' – soft tissue mode	10 mGy	Modified CTDI (custom 16-cm cylindrical head phantom)	Daly et al., 2006
Sinus imaging (bone mode)	≥3 mGy		
Endoscopic sinus surgery			Manarey and Anand, 2006
Continuous fluoroscopy	0.9 mGy	Centre	
	1.9 mGy	Maximum surface dose	
	1.5 mGy	Centre	
High-level fluoroscopy	3.4 mGy	Maximum surface dose	
	4.1 mGy	Centre	
	11 mGy	Maximum surface dose,	
Digital ciné		CTDI head phantom, ion chamber	

CTDI, computed tomography dose index.

periapical lesions, or periodontal disease affect high-contrast structures and can therefore be imaged precisely using CBCT. The FOV is usually large enough to cover the maxillofacial region with one orbit around the patient. In addition, dedicated small volumes (e.g. 4×4 cm) allow for high-resolution imaging of a small region of interest, such as a single tooth root. Earlier scanners employed image intensifiers, but in the current systems, FPDs are used almost exclusively. Most systems are seated or standing scanners consisting of a small C-arm that rotates in a horizontal plane along a vertical axis with the patient sitting upright. Applications of dental and maxillofacial CBCT are described in De Vos et al. (2009).

(186) Due to the wide dose range found in dental and maxillofacial CBCT, and the variety of diagnostic needs in dental radiology, proper application of this technique among alternative 2D and 3D dental imaging modalities has been of great concern since its introduction in dentistry in 1998. Due to its relatively low radiation dose and high spatial resolution compared with MDCT, dental and maxillofacial CBCT is considered as a suitable substitute for MDCT for applications requiring 3D imaging of hard tissues. However, its application as a complement or substitute for 2D imaging modalities (e.g. panoramic or cephalometric radiographic) increases the population dose. In many cases, the 3D nature of CBCT results in superior diagnostic efficacy compared with 2D radiographs, but for certain applications, 2D radiographs often suffice. Detailed evidence-based guidelines have been determined during the SEDENTEXCT project (EC, 2012a). The guidelines encompass a variety of topics, covering justification, referral criteria, optimisation, training, QA, and staff protection aspects. Twenty 'basic principles' were defined based on a thorough

Table 7.8. Effective dose ranges in dental and maxillofacial cone beam computed tomography (CBCT).

CBCT type (volume coverage)	Effective dose (μSv)*
Dento-alveolar	11–674 (median: 61)
Craniofacial	30–1073 (median: 87)

*Full list of studies can be found in EC (2012a).
Source: EC (2012a).

literature review in combination with the experimental work performed in SEDENTEXCT on radiation dose, diagnostic use, and other CBCT-related topics.

(187) Several of these basic principles relate to justification, as the excessive use of CBCT in dentistry would increase the population dose. The use of CBCT in dentistry can only be considered as justified, if a patient history and clinical information are available, if it is expected to add new information, and if 2D radiographs do not (or are not expected to) answer the diagnostic question. Repeated CBCT examinations should be avoided unless each examination can be justified individually. In addition, dental and maxillofacial CBCT should not be used in diagnostic soft tissue imaging.

(188) An important optimisation principle in dental and maxillofacial CBCT relates to the choice of the appropriate volume size for each examination. In many cases, the region of interest is known exactly before scanning; in other cases, the required volume is revealed after acquisition of a frontal and lateral scout image. The smallest available volume size should always be chosen, as this could reduce patient dose considerably. The choice between high- and low-dose settings should be made according to the optimisation principle, ensuring adequate image quality for diagnosis at the lowest achievable dose.

(189) As CBCT images often contain structures that are not part of the diagnostic region of interest (although this should be limited as much as possible through FOV reduction), the EC guidelines also state that the entire image should be examined and reported, not just the region of interest. Depending on the scanning region, the involvement of an oral or medical radiologist can be warranted.

(190) Table 7.8 provides an overview of the effective dose range in dental and maxillofacial CBCT, measured using anthropomorphic phantoms (EC, 2012a). An updated overview of effective doses measured in dental and maxillofacial CBCT can be found in the systematic reviews by Bornstein et al. (2014) and Al-Okshi et al. (2015). However, effective dose is not a good quantity to use for describing doses to tissues in the head, as the tissue-weighting factors are only indicative of risk, and use of equivalent doses to specific tissues or absorbed doses within them are generally recommended. Although accuracy and intercomparability of several dosimetric studies are limited due to the varying measurement methodology (e.g. placement of thermoluminescent dosimeter), Table 7.8 shows that patient doses vary considerably, which reflects the wide variation of exposure parameters being applied. Volume sizes range between a few cm^3, sufficient for scanning of a single tooth area, and a few

thousand cm^3, covering most of the head. In addition, there is no standardisation regarding the kVp used in dental and maxillofacial CBCT, with values ranging between 70 and 120 kV. Clinically applied mAs values range more than 20-fold but are generally found between 25 and 150 mAs. The Commission recommends standardisation of exposure parameters in dental and maxillofacial CBCT for each imaging task.

(191) The application of dental and maxillofacial CBCT for paediatric patients is of particular concern due to their higher radiosensitivity and smaller size. Similar to its adult applications, paediatric use of CBCT could lead to considerable dose reduction when used as a replacement for MDCT (e.g. cleft palate), providing that FOV limitation is applied and that exposure factors are optimised. However, its use as a complement to, or replacement for, 2D radiography could lead to patient doses that are disproportionate to the diagnostic benefit, especially when large-volume coverage is required (e.g. orthodontic planning). For most paediatric applications, more evidence regarding diagnostic efficacy of CBCT is needed before widespread application can be considered. Table 7.9 contains effective dose measurements for 10-year-old and adolescent anthropomorphic phantoms. Due to the larger relative coverage of the child's head, effective doses are higher compared with adults if exposure factors are not adapted. For some CBCT models, preset 'child dose' exposure parameters are available, typically corresponding to a reduction in mAs. For other models, exposure factors can be modified by the operator. AEC is largely absent in dental and maxillofacial CBCT, with one manufacturer having applied it for several years.

(192) Corresponding with the wide range in effective dose, absorbed doses of 0.03–10.0 mGy have been reported for the thyroid gland, 0.02–9.3 mGy for the brain, and 0.03–16.7 mGy for the lens of the eye (Ludlow et al., 2006; Hirsch et al., 2008; Ludlow and Ivanovic, 2008; Pauwels et al., 2012b). Various dose indices have also been measured in dental and maxillofacial CBCT. A 2009 report by the UK Health Protection Agency (HPA) measured KAP for 41 dental and maxillofacial CBCT units, and normalised the results to a 4×4 cm field size with values ranging between <100 and >2300 mGy cm^2 (HPA, 2010a).

(193) Exposure of workers is reported to be in the range of 2 to 40 μGy $scan^{-1}$ at 1 m. For comparison, intra-oral and panoramic radiography scatter doses are less

Table 7.9. Overview of radiation doses in dental and maxillofacial cone beam computed tomography (CBCT) for phantoms representing different ages.

Age	CBCT type (volume coverage)	Effective dose (μSv)
10-year-old phantom	Dento-alveolar	16–214 (median: 43)
10-year-old phantom	Craniofacial	114–282 (median: 186)
Adolescent phantom	Dento-alveolar	18–70 (median: 32)
Adolescent phantom	Craniofacial	81–216 (median: 135)

Source: Theodorakou et al. (2012).

than 1 μGy exposure^{-1} at 1 m (EC, 2012a). The EC guidelines on dental and maxillofacial CBCT state that 'for worker protection from CBCT equipment, the guidelines detailed in Section 6 of the EC publication 'Radiation Protection 136. European Guidelines on Radiation Protection in Dental Radiology' should be followed'.

7.10. Breast

(194) Mammography has been the standard imaging method for breast cancer screening for several decades. While digital mammography has replaced screen-film mammography in many locations, the projection-imaging nature of mammography did not change with the introduction of digital mammography; digital mammography still requires compression of the breast in order to acquire a 2D projection image of the 3D breast. Digital mammography was proven to be slightly more effective in detection of small lesions in women under 50 years of age with radiographically dense breasts (Pisano et al., 2005). Digital mammography has also been shown to reduce breast dose in comparison to screen-film radiography. In a 2010 study, mean glandular dose per view averaged 2.37 mGy for screen-film mammography, while it was 22% lower (1.86 mGy per view) for digital mammography (Hendrick et al., 2010). With digital mammography, contrast can be restored (within limits) using digital enhancement techniques. Therefore, a harder x-ray spectrum can be used with digital mammography compared with screen-film mammography, and this is the primary reason that some dose reduction is possible. The harder x-ray spectrum is achieved through the use of different anode/filter combinations (e.g. tungsten/rhodium instead of molybdenum/molybdenum) and higher average tube potentials.

(195) 2D mammography suffers from the superposition of structures that may falsely appear normal or abnormal, and this anatomical noise created by the normal parenchyma of the breast confounds the cancer detection task. 3D approaches relying on the principles of CT may improve breast cancer detection, especially in the dense breast. Two approaches for '3D' imaging of the breast have been proposed: digital breast tomosynthesis and bCT. Breast tomosynthesis is performed using multiple (e.g. 15–30) low-dose digital 2D projection images, acquired on a modified full-field digital mammographic system that allows limited angular movement of the x-ray tube around the breast during acquisition (Niklason et al., 1997; Poplack et al., 2007). Tomosynthesis is the name given to this acquisition strategy, which is formally considered to be limited-angle tomography.

(196) Patient dose in one breast tomosynthesis acquisition, comprising 11 low-dose projections over 28° angular movement, is approximately 4 mSv for a breast of average thickness. This is approximately twice the dose used for digital mammography (Poplack et al., 2007). More recently, doses from breast tomosynthesis were estimated to be between 1.66 and 1.90 mGy for a standard breast, based on

manufacturers' data in the absence of a standard protocol (Michell et al., 2012). More recent tomosynthesis systems use a number of x-ray projections whose cumulative dose to the breast is comparable to conventional single-view digital mammography.

(197) bCT is currently undergoing evaluation before it can be introduced into clinical practice. This technology has been developed to address the shortcomings of conventional mammography such as contrast resolution, and the problems occurring from overlap of structures in 2D images (O'Connell et al., 2010). Most bCT systems make use of FPDs and are therefore CBCT systems; however, helical CT systems for dedicated breast imaging are also being designed (Kalender et al., 2012).

(198) In the early days of bCT, there was no established method for estimating the mean glandular dose to the breast in the pendant geometry used for this modality. Therefore, methods for computing the dose to the breast needed to be developed. Monte Carlo techniques were used to develop comprehensive tables of so-called DgN_{CT} values, which are appropriate for 360° scanning of the pendant breast (Boone et al., 2004, 2005).

(199) Cone-beam-based bCT systems use FPDs that acquire 2D projections which encircle the breast completely. Typically, a complete scan of a single breast requires 10–17 s, within which time approximately 300–500 projections are acquired (O'Connell et al., 2010; Packard et al., 2012). These systems are designed to be low dose, and the mean glandular dose can be as low as that of two-view mammography for each woman. Obviously, radiation dose depends on breast size and composition. Therefore, smaller doses will occur in smaller breasts, and larger breasts will receive higher doses. Reported mean glandular dose values range between 4 and 12.8 mGy (O'Connell et al., 2010) and 2.5 and 10.3 mGy (Lindfors et al., 2008). Average doses from conventional mammography documented in the abovementioned study by O'Connell et al. (2010) were in the range of 2.2–15 mGy.

(200) Currently, bCT technology has some limitations regarding the detection of microcalcifications, as well as coverage of the axillary region, both of which are performed better with conventional mammography (Lindfors et al., 2008; O'Connell et al., 2010). Higher-resolution detector systems will likely improve spatial resolution of bCT, and consequently improve performance in detection of microcalcification (Kalender et al., 2012).

(201) Worker dose concerns for bCT are minimal as workers do not need to be near the patient during image acquisition, as with most CT settings. Of course, proper shielding of the bCT room is considered to be essential. One issue with regards to shielding will emerge if bCT scanners become more commonplace in the clinical imaging environment. These systems make use of higher energy x-ray spectra than mammography systems; therefore, it is likely that additional room shielding will be required if a bCT system is installed in a mammography room. More details on room shielding are given in Section 6.2.4.

8. TRAINING CONSIDERATIONS FOR CBCT

- **The level of training in radiological protection should be commensurate with the level of expected radiation exposure (ICRP, 2009).**
- **All workers intending to use CBCT for diagnostic purposes should be trained in the same manner as for diagnostic CT, and those intending to perform interventional CBCT should be trained in the same manner as for interventional CT.**

8.1. Introduction

(202) *Publication 113* (ICRP, 2009) provides substantial information and guidance on training of healthcare professionals in radiological protection for diagnostic and interventional procedures. Much of the information provided in this section is derived from that publication.

(203) ICRP states that a training programme in radiological protection for healthcare professionals has to be oriented towards the type of practice in which the target audience is involved (ICRP, 2009, 2010).

(204) The main purpose of training is to make a qualitative change in practice that helps operators use radiological protection principles, tools, and techniques to reduce their own exposure without cutting down on work, and to reduce patient exposure without compromising on image quality or intended clinical purpose. The focus has to remain on achievement of skills. Unfortunately, in many situations, training takes the form of complying with requirements measured in terms of the number of hours. While this provides an important yardstick, it is also essential to require trainees to learn skills to reduce occupational and patient exposure. In large parts of the world, clinical professionals engaged in the use of radiation outside imaging departments have either no training or inadequate training. The Commission has recommended that the levels of education and training should be commensurate with the level of radiation use and expected radiation exposure (ICRP, 2009). As the use of CBCT outside imaging departments increases, the need for education and training of workers also increases. Professionals who are involved directly in the operation of CBCT for diagnosis or intervention, and the interpretation of CBCT studies should receive education and training in radiological protection at the start of their career, and refreshment and professional development training should continue throughout their professional life. Continuing education should include specific training on relevant radiological protection tools and procedures as new equipment or techniques are introduced.

(205) Legislation in most countries requires, or should require (if it does not currently do so), that individuals who take responsibility for medical exposures must be trained properly in radiological protection.

(206) Training activities in radiological protection should be followed by an evaluation of the knowledge acquired from the training programme (a formal examination system).

(207) Workers who have completed training should be able to demonstrate that they possess the knowledge specified by the curriculum by passing an appropriate certifying examination.

(208) Nurses and other healthcare professionals who assist during CBCT procedures should be familiar with radiation risks and radiological protection principles in order to minimise their own exposure and that of others.

(209) Medical physicists should become familiar with the clinical aspects of the specific procedures performed at their local facility.

(210) The issue of delivery of training and assessment of competency was dealt with in *Publication 113* (ICRP, 2009).

(211) For dental and maxillofacial applications of CBCT, dedicated basic training requirements have been developed and published by the European Academy of Dentomaxillofacial Radiology (Brown et al., 2014).

8.2. Curriculum

(212) It is anticipated that a large proportion of professionals involved in CBCT will be those who have prior education in medical radiation physics and radiological protection. Thus, simple orientation training may suffice in such cases. All workers intending to use CBCT for diagnostic purposes should be trained in the same manner as for diagnostic CT, and those intending to perform interventional CBCT should be trained in the same manner as for interventional CT, keeping the level of dose and use in view as specified earlier.

(213) It has been observed that most organisations follow the relatively easy route of requiring a certain number of hours of education and training. The Commission gives some recommendations on the number of hours required, but this should act as a guideline and should not be applied rigidly (ICRP, 2009). Providing guidance in terms of the number of hours has advantages in terms of implementation of training and monitoring the training activity, but is only a guide.

(214) Many programmes fail with regard to assessment of whether the objectives have been achieved. Others have pre- and post-training evaluations to assess the knowledge gained, but few training programmes assess the acquisition of practical skills. It would be more appropriate to encourage development of questionnaires and examination systems that assess knowledge and skills, rather than prescribing the number of hours of training. The extent of training depends upon the level of radiation employed in the work, and the likelihood of overexposure of the patient or workers.

8.3. Who should be the trainer?

(215) In view of the importance of this issue, most of the text from *Publications 113* and/or *117* (ICRP, 2009, 2010) is reproduced here. The foremost point in any successful training is that the trainer should have a clear perception about the practicalities of the work that the training has to cover. The primary trainer should

normally be an expert in radiological protection (normally a medical physicist), and should have knowledge about clinical practice involving the use of radiation. That is, the trainer should know about the nature of radiation, the way in which it is measured, how it interacts with the tissues, what type of effects it can lead to, principles and philosophies of radiological protection, and international and national guidelines. As radiological protection is covered by legislation in almost all countries of the world, awareness of national laws and the responsibilities of individuals and organisations are essential (ICRP, 2009).

(216) Training should deal with what people can practice in their day-to-day work. Instead, many trainers in radiological protection cannot resist the temptation to talk about basic topics such as definition of radiation units, interaction of radiation with matter, and even in-depth information on structure of the atom and atomic radiation in more detail than is appropriate for the clinical audience and for the practical purposes of radiological protection training. Such topics, while being essential in basic educational programmes, should only be dealt with to a level such that they make sense in the context of radiological protection training. A successful trainer should not be too focused on definitions that are purely academic, but should be guided by the utility of the information to the audience. The same applies to regulatory requirements. The trainer should speak the language of users to convey the necessary information without compromising on the science and regulatory requirements. Healthcare professionals who use radiation in day-to-day work in hospitals and deliver the radiation dose to patients know about the practical problems in dealing with patients who may be very sick. They understand the time constraints for dealing with large numbers of patients. They should understand the problems associated with the radiation equipment they deal with, and the lack of radiation measuring and radiological protection tools, when they happen. It is recommended that training should also include lectures from practising clinicians and imaging specialists, who can focus on good and bad radiological protection practices. It may be useful for the radiological protection trainer to be available during such lectures to comment on and discuss any issues raised.

8.4. Training of service engineers

(217) In some cases, service engineers are not familiar with CBCT technology. For example, in dental and maxillofacial CBCT, some manufacturers have no prior experience with CT equipment, and service engineers are not adequately geared towards CBCT technology. Manufacturers are challenged to ensure adequate training of service engineers.

9. QUALITY ASSURANCE PROGRAMMES

9.1. Introduction

(218) The purpose of a QA programme is to maintain the safety and performance of the equipment in conformance with specifications, and to ensure the optimisation of protection (i.e. achieving adequate image quality while minimising the radiation dose to the patient and medical staff). In the context of this report, the QA programme consists of the acceptance and commissioning of CBCT equipment, as well as periodic testing and maintenance of equipment performance, patient imaging protocols, worker and patient dose, worker training, and adherence to policies and procedures.

9.2. Quality control of CBCT equipment

(219) Quality control begins when the equipment is installed, and continues throughout its lifetime. The acceptance test, commissioning, and status testing of equipment should ensure that the system is operational according to the manufacturer's specifications, which are based on national or international standards. At the time of acceptance, baseline measurements of image quality and dosimetry should be taken along with parameters that affect these factors. These measurements will be used as a reference for comparison with later measurements, and can indicate if the system performance has degraded and needs corrective action.

(220) Equipment tests fall into six categories: safety system, x-ray generator performance, image quality, geometry, display, and dosimetry. Safety system tests are used to ensure the proper operation of warning lights, door and collision interlocks, portable shielding, and the emergency-off system. X-ray generator tests can ensure that the x-ray system operates properly, including the accurate production of kV, mA, exposure time, and linearity. Image quality tests, such as those that measure noise, uniformity, contrast, and resolution, can ensure that acquired images are suitable for clinical use. The frequency of these quantitative tests should be established to remediate image quality degradation (IEC, 2006). In addition to quantitative testing, images should be inspected visually to identify image artefacts. Geometry tests are used to ensure proper system alignment and scaling. In radiotherapy applications, a daily test of the CBCT image isocentre geometry ensures that images are aligned with the treatment machine. However, dental and maxillofacial and interventional applications may not require alignment with an external coordinate system, and therefore only need test image scaling. Display testing will ensure that image presentation is consistent and faithful to avoid loss of information during interpretation. Finally, dosimetry tests are used to assess the dose to a phantom, using standard measurement protocols appropriate for CBCT, such as those described earlier in this publication and in Annex A. The equipment and methods needed to perform other tests are described in publications such as Radiation Protection Report No. 162 (EC, 2012b) and Report 91 (IPEM, 2005), although the latter does not cover CBCT equipment specifically.

(221) Standardisation of phantoms and tests is warranted for image quality assessment as well as dosimetry. In addition, manufacturers should provide users with appropriate test objects for routine checking of performance.

(222) The schedule and scope of routine testing of CBCT equipment depend to some degree on the clinical application. Inspection schedules recommended by six different organisations (three for dental applications and three for radiotherapy applications) are shown in Table 9.1. One should be aware of national recommendations on this matter (e.g. DIN, 2013, 2014). The schedules are largely in agreement, but some special considerations are worth noting. For CBCT equipment with an exposed moving gantry that might collide with patients or workers, a daily safety system check is recommended. If the CBCT image coordinates are used to control a

Table 9.1. Proposed quality assurance (QA) tests for cone beam computed tomography equipment and corresponding periodicity as recommended by international, national, and professional societies.

QA test	Daily	Monthly	Periodic	Annual
Safety systems: collision, warning lights, and interlocks	142, 179, IAC			
Image quality: uniformity		EC, 142, 179, HPA	179, IAC	
Image quality: image density	IAC	EC, 142, 179, HPA		
Image quality: noise		EC, 142, 179, HPA	179	
Image quality: low-contrast detail		142, 179	179	EC
Image quality: high-contrast resolution		142, 179	179, IAC	EC, HPA
Image quality: image artefacts	IAC	EC		
Geometry: isocentre coincidence	142, 147, ACR			
Geometry: scaling and slice thickness		142, 179	179	EC, HPA
Data storage and transfer			ACR	
Image registration software			ACR	
Image display		EC	HPA	IAC
X-ray quality, linearity, and field size				EC, 179, HPA, IAC
Dose measurements				EC, 142, 179, HPA, IAC

142, AAPM Report 142 (Klein et al., 2009); 179, AAPM (2012b); ACR, ACR (2009); HPA, HPA (2010b); IAC, IAC (2012); EC, EC (2012a).

radiotherapy accelerator or surgical equipment, a daily check of coordinate system integrity is recommended. If accurate density information (such as HU) is used for diagnosis or planning, these values should be tested at least monthly. Users should therefore consider these general guidelines to inform a risk-based QA programme based on their clinical aims.

9.3. Patient dose reporting

(223) The need for dose reporting in CBCT follows from the principles of optimisation of radiological protection. Radiation dose to the patient cannot be optimised to as low as reasonably achievable without accurate tracking of dose. The most straightforward method for achieving dose tracking is through the electronic display of dose on the imaging console (ICRP, 2004), and recording of delivered dose into the patient record as a DICOM-structured dose report (IEC, 2012). Errors for displayed dose estimates should not exceed 20% (IAEA, 2011b; IEC, 2011; EC, 2012b).

(224) In MDCT systems, it is now standard to display estimates of delivered dose directly on the console numerically as $CTDI_{vol}$ and DLP. These estimates represent the dose to a phantom, not the dose to a patient. Methods should be developed for estimating doses to patients based on patient size and the scanning parameters used for individual patients. A medical physicist, as part of the QA programme, should verify the accuracy of these numbers at least annually, or whenever equipment is repaired in a manner that can affect dose. For CBCT systems, the system for dose reporting is not yet standardised at an international level. HPA (2010b) and EC (2012a) recommend that the dose estimate should be displayed as KAP in dental and maxillofacial CBCT systems. The QA programme should be prepared to verify dose estimates as they are reported by each device, whether it be KAP or CTDI and DLP.

(225) Electronic transfer of patient dose to an electronic medical record greatly facilitates the tracking of annual and lifetime radiation dose to a patient over multiple procedures. MDCT systems implement this idea using the DICOM-structured dose report, which usually expresses dose in terms of $CTDI_{vol}$ and DLP. Electronic transmission of $CTDI_{vol}$ and DLP to PACS is now required by California State law in the USA (California Senate Bill SB1237, 2010), and has been proposed by EC (2011). Electronic reporting further supports initiatives to compare recorded doses with DRLs; a concept recommended by ICRP for optimisation (ICRP, 2007c). Dose registries are another potential tool for facilitating evaluation of patient dose.

9.4. Diagnostic reference levels

(226) DRLs have been established through government and professional organisations to guide users in optimising procedure performance for both image quality and radiation reduction. While these efforts have matured for MDCT imaging, little

progress has been made toward setting DRLs for CBCT. Based on a preliminary audit of KAP values on 41 dental and maxillofacial CBCT units by HPA (2010b), an achievable dose of 250 mGy cm^2 (normalised to an area corresponding to 4×4 cm at the isocentre) was proposed for placement of an upper first molar implant in a standard adult patient. This achievable dose value was adapted by the SEDENTEXCT Consortium (EC, 2012a), with the remark that 'further work involving large scale audits is needed to establish robust DRLs' for various dental and maxillofacial CBCT applications. This remark can be extended towards other CBCT applications.

(227) For centres that use standardised imaging protocols, the protocols should be established within published DRLs. Until international or national DRLs are established, local DRLs (LDRLs) should be established as part of the QA programme to inform local policy for common procedures. LDRLs are established from mean doses delivered to average-sized patients, with separate LDRLs established for children (IPEM, 2004). Audits of standardised protocols should be performed periodically to ensure compliance. Currently, there is a dearth of data on DRLs.

9.5. Audit

(228) Periodic audits of patient imaging studies are recommended to ensure optimal use of the imaging system. The audit should consider image quality, positioning, FOV, patient motion, and radiation dose metrics. In particular, the audit should evaluate high-dose CBCT procedures, and repeat CBCT scans. The SEDENTEXCT Consortium report recommends two audits per year for reject analysis, and a patient dose audit every 3 years (EC, 2012a).

10. RECOMMENDATIONS

(229) Expanded availability and newer applications have put CBCT technology in the hands of medical professionals who do not traditionally use CT. ICRP's radiological protection principles and recommendations provided in earlier publications, particularly *Publications 87* and *102* (ICRP, 2000a, 2007a), apply to these newer applications and should be adhered to.

(230) As many applications of CBCT involve patient doses similar to MDCT, the room layout and shielding requirements in such cases need to be similar to protect workers adequately.

(231) Medical practitioners bear the responsibility for making sure that each CBCT examination is justified and appropriate.

(232) When referring a patient for a diagnostic CBCT examination, the referring practitioner should be aware of the strengths and weaknesses for CBCT vis-à-vis MDCT, magnetic resonance imaging, and other competing imaging modalities. The decision to use CBCT should be made in consultation with an imaging professional.

(233) Manufacturers are challenged to practice standardised methods for dosimetry and dose display in CBCT in conformance with international recommendations such as ICRU Report 87 (ICRU, 2012). Unfortunately, at present, there is wide variation in dose quantities being displayed on CBCT machines. The users are unable to compare doses between scanners or protocols.

(234) Use of CBCT systems for both fluoroscopy and tomography poses new challenges in quantitating radiation dose. There is a need to develop methods that aggregate exposures to individual patients during the entire procedure that may use a combination of fluoroscopy and CBCT during a given examination.

(235) Recording, reporting, and tracking of radiation dose for a single patient should be made possible in a consistent manner across vendors.

(236) There is a need to provide checks and balances (e.g. dose check alerts implemented in CT in recent years) to avoid high patient doses compared with locally defined reference values.

(237) Positioning radiosensitive organs such as the thyroid, lens of the eye, breasts, and gonads on the detector side during the partial rotation scan is a useful feature in CBCT that needs to be used for radiological protection of these organs.

(238) Many machines were only capable of fluoroscopy initially, but can now also perform CBCT. Due to the improved clinical information on CBCT, and its ability to remove overlying structures, a user may be tempted to over-use the CBCT mode. Users must understand that the CBCT function of their system is not a low-dose 'fluoroscopy run', and should use this mode judiciously.

REFERENCES

AAPM, 2010. Comprehensive Methodology for the Evaluation of Radiation Dose in X-ray Computed Tomography. AAPM Report 111. American Association of Physicists in Medicine, New York.

AAPM, 2011a. Scope of Practice of Clinical Medical Physics. Policy Number PP 17-B. American Association of Physicists in Medicine, New York. Available at: http://www.aapm.org/org/policies/details.asp?id=317&type=PP (last accessed 5 May 2015).

AAPM, 2011b. Size-specific Dose Estimates (SSDE) in Pediatric and Adult Body CT Examinations. AAPM Report No. 204. American Association of Physicists in Medicine, New York. Available at: http://www.aapm.org/pubs/reports/rpt_204.pdf (last accessed 5 May 2015).

AAPM, 2011c. AAPM Recommendations Regarding Notification and Alert Values for CT Scanners: Guidelines for Use of the NEMA XR 25 CT Dose-check Standard. AAPM Dose Check Guidelines Version 1.0. American Association of Physicists in Medicine, New York. Available at: http://www.aapm.org/pubs/CTProtocols/documents/NotificationLevels Statement.pdf (last accessed 5 May 2015).

AAPM, 2012a. AAPM Position Statement on the Use of Bismuth Shielding for the Purpose of Dose Reduction in CT Scanning. Statement approved by AAPM Board of Directors, February 2012, Policy date 2 July 2012. American Association of Physicists in Medicine, New York. Available at: http://www.aapm.org/publicgeneral/BismuthShielding.pdf (last accessed 5 May 2015).

AAPM, 2012b. Quality Assurance for Image-guided Radiation Therapy Utilizing CT-based Technologies: a Report of the AAPM TG-179. American Association of Physicists in Medicine, New York. Available at: http://www.aapm.org/pubs/reports/RPT_179.pdf (last accessed 5 May 2015).

AAPM, 2015. Task Group No. 200 – CT Dosimetry Phantoms and the Implementation of AAPM Report Number 111. American Association of Physicists in Medicine, New York. Available at: http://aapm.org/org/structure/default.asp?committee_code=TG200 (last accessed 5 May 2015).

Abuhaimed, A., Martin, C.J., Sankaralingam, M., Gentle, D.J., McJury, M., 2014. An assessment of the efficiency of methods for measurement of the computed tomography dose index (CTDI) for cone beam (CBCT) dosimetry by Monte Carlo simulation. Phys. Med. Biol. 59, 6307–6326.

ACR, 2009. ACR Technical Standard for Medical Physics Performance Monitoring of Image-Guided External Beam Radiation Therapy (IGRT). Reston, VA: American College of Radiology. Available at: http://www.acr.org/~/media/ACR/Documents/PGTS/standards/IGRT.pdf (last accessed 5 May 2015).

Adamus, R., Pfister, M., Loose, R., 2009. Transjugular intrahepatic portosystemic shunt (TIPS) puncture by 3D path planning based on the back-projection of two 2D portographies. Radiology 251, 543–547.

Al-Okshi, A., Lindh, C., Salé, H., Gunnarsson, M., Rohlin, M., 2015. Effective dose of cone beam CT (CBCT) of the facial skeleton: a systematic review. Br. J. Radiol. 88, 20140658.

Alaei, P., Ding, G., Guan, H., 2010. Inclusion of the dose from kilovoltage cone beam CT in the radiation therapy treatment plans. Med. Phys. 37, 244–248.

Alvarado, R., Booth, J.T., Bromley, R.M., et al., 2013. An investigation of image guidance dose for breast radiotherapy. J. Appl. Clin. Med. Phys. 14, 4085.

Amer, A., Marchant, T., Sykes, J., Czajka, J., Moore, C., 2007. Imaging doses from the Elekta synergy x-ray cone beam CT system. Br. J. Radiol. 80, 476–482.

Arai, Y., Tammisalo, E., Iwai, K., et al., 1999. Development of a compact computed tomographic apparatus for dental use. Dentomaxillofac. Radiol. 28, 245–248.

Araki, K., Patil, S., Endo, A., et al., 2013. Dose indices in dental cone beam CT and correlation with dose area product. Dentomaxillofac. Radiol. 42, 20120362.

Bai, M., Liu, B., Mu, H., et al., 2011. The comparison of radiation dose between C-arm flat-detector CT (DynaCT) and multi-slice CT (MSCT): a phantom study. Eur. J. Radiol. 81, 3577–3580.

Balter, S., Hopewell, J.W., Miller, D.L., et al., 2010. Fluoroscopically guided interventional procedures: a review of radiation effects on patients' skin and hair. Radiology 254, 326–341.

Barrett, J.F., Keat, N., 2004. Artifacts in CT: recognition and avoidance. Radiographics 24, 1679–1691.

Berris, T., Perisinakis, K., Papadakis, A.E., et al., 2013. Comparison of methods for assessing geometric efficiency on multi-detector CT scanners. Phys. Med. 29, 312–322.

Blaickner, M., Neuwirth, J., 2013. Measurements of occupational and patient exposure as well as image quality for two C-arms. Radiat. Prot. Dosimetry 155, 451–458.

Bogdanich, W., 2009. Radiation overdoses point up dangers of CT scans. New York Times, 16 October 2009, p. A13.

Bogdanich, W., 2010. Afterstroke scans, patients face serious health risks. New York Times, 1 August 2010, p. A1.

Boone, J.M., Shah, N., Nelson, T.R., 2004. A comprehensive analysis of DgN_{CT} coefficients for pendant-geometry cone-beam breast computed tomography. Med. Phys. 31, 226–235.

Boone, J.M., Kwan, A.L.C., Seibert, J.A., et al., 2005. Technique factors and their relationship to radiation dose in pendant geometry breast CT. Med. Phys. 32, 3767–3776.

Boone, J.M., 2009. Dose spread functions in computed tomography: a Monte Carlo study. Med. Phys. 36, 4547–4554.

Bornstein, M.M., Scarfe, W.C., Vaughn, V.M., et al., 2014. Cone beam computed tomography in implant dentistry: a systematic review focusing on guidelines, indications, and radiation dose risks. Int. J. Oral Maxillofac. Implants 29(Suppl.), 55–77.

Braak, S.J., van Melick, H.H.E., Onaca, M.G., et al., 2012. 3D cone-beam CT guidance, a novel technique in renal biopsy – results in 41 patients with suspected renal masses. Eur. Radiol. 22, 2547–2552.

Brenner, D.J., 2010. Slowing the increase in the population dose resulting from CT scans. Radiat. Res. 174, 809–815.

Brown, J., Jacobs, R., Levring Jäghagen, E., et al., 2014. Basic training requirements for the use of dental CBCT by dentists: a position paper prepared by the European Academy of DentoMaxilloFacial Radiology. Dentomaxillofac. Radiol. 43, 20130291.

Cadet, J.V., 2010. CT Makers get Five FDA Recommendations, due to Overdose Controversy. Clinical Innovation + Technology. Providence, RI. Available at: http://www.clinical-innovation.com/topics/ehr-emr/ct-makers-get-five-fda-recommendations-due-overdose-controversy (last accessed 5 May 2015).

California Senate Bill SB1237, 2010. An act to add Sections 115111, 115112, and 115113 to the Health and Safety Code, relating to public health. Available at: http://www.leginfo.ca.gov/pub/09-10/bill/sen/sb_1201-1250/sb_1237_bill_20100929_chaptered.html (last accessed 5 May 2015).

Cheng, H.C., Wu, V.W., Liu, E.S., et al., 2011. Evaluation of radiation dose and image quality for the Varian cone beam computed tomography system. Int. J. Radiat. Oncol. Biol. Phys. 80, 291–300.

Chodick, G., Bekiroglu, N., Hauptmann, M., et al., 2008. Risk of cataract after exposure to low doses of ionizing radiation: a 20-year prospective cohort study among US radiologic technologists. Am. J. Epidemiol. 168, 620–631.

Ciraj-Bjelac, O., Rehani, M.M., Sim, K.H., et al., 2010. Risk for radiation-induced cataract for staff in interventional cardiology: is there reason for concern? Catheter. Cardiovasc. Interv. 76, 826–834.

Ciraj-Bjelac, O., Rehani, M., Minamoto, A., et al., 2012. Radiation-induced eye lens changes and risk for cataract in interventional cardiology. Cardiology 123, 168–171.

Corredoira, E., Vañó, E., Ubeda, C., Gutiérrez-Larraya, F., 2015. Patient doses in paediatric interventional cardiology: impact of 3D rotational angiography. J. Radiol. Prot. 35, 179–195.

Cucinotta, F.A., Manuel, F.K., Jones, J., et al., 2001. Space radiation and cataracts in astronauts. Radiat. Res. 156, 460–466.

Daly, M.J., Siewerdsen, J.H., Moseley, D.J., et al., 2006. Intraoperative cone-beam CT for guidance of head and neck surgery: assessment of dose and image quality using a C-arm prototype. Med. Phys. 33, 3767–3780.

Day, R., Gorin, M.B., Eller, A.W., 1995. Prevalence of lens changes in Ukrainian children residing around Chernobyl. Health Phys. 68, 632–642.

DIN, 2013. Image Quality Assurance in Diagnostic X-ray Departments – Part 161: RöV Acceptance Testing of Dental Radiographic Equipment for Digital Cone-beam Computed Tomography. Berlin: Deutsches Institut für Normung.

DIN, 2014. Image Quality Assurance in Diagnostic X-ray Departments – Part 15: RöV Constancy Testing of X-ray Installations for Dental Radiographic Equipment for Digital Cone-beam Computed Tomography. Berlin: Deutsches Institut für Normung.

De Vos, W., Casselman, J., Swennen, G.R.J., 2009. Cone-beam computerized tomography (CBCT) imaging of the oral and maxillofacial region: a systematic review of the literature. Int. J. Oral Maxillofac. Surg. 38, 609–625.

Dijkstra, M.L., Eagleton, M.J., Greenberg, R.K., et al., 2011. Intraoperative C-arm cone-beam computed tomography in fenestrated/branched aortic endografting. J. Vasc. Surg. 53, 583–590.

Ding, G., Duggan, D., Coffey, C., 2008. Accurate patient dosimetry of kilovoltage cone-beam CT in radiation therapy. Med. Phys. 35, 1135–1144.

Ding, G., Coffey, C., 2009. Radiation dose from kilovoltage cone beam computed tomography in an image-guided radiotherapy procedure. Int. J. Radiat. Oncol. Biol. Phys. 73, 610–617.

Ding, G., Munro, P., 2013. Radiation exposure to patients from image guidance procedures and techniques to reduce the imaging dose. Radiother. Oncol. 108, 91–98.

Dixon, R.L., Boone, J., 2010a. The CTDI Paradigm: a Practical Explanation for Medical Physicists. Image Wisely. Reston, VA: American College of Radiology, 2010. Available at: http://www.imagewisely.org/~/media/ImageWisely%20Files/Medical%20Physicist%20Articles/IW%20Dixon%20Boone%20CTDI%20Paradigm%202.pdf (last accessed 5 May 2015).

Dixon, R.L., Boone, J., 2010b. Cone beam CT dosimetry: a unified and self-consistent approach including all scan modalities – with or without phantom motion. Med. Phys. 37, 2703–2718.

Domienik, J., Brodecki, M., Carinou, E., et al., 2011. Extremity and eye lens doses in interventional radiology and cardiology procedures: first results of the ORAMED project. Radiat. Prot. Dosimetry 144, 442–447.

EC, 2011. Proposal for a Council Directive Laying Down Basic Safety Standards for Protection Against the Dangers Arising from Exposure to Ionising Radiation. European Commission, Brussels. Available at: http://ec.europa.eu/energy/en/topics/nuclear-energy/radiation-protection (last accessed 5 May 2015).

EC, 2012a. Radiation Protection No. 172: Cone Beam CT for Dental and Maxillofacial Radiology. Evidence Based Guidelines. Directorate-General for Energy. European Commission, Brussels. https://ec.europa.eu/energy/sites/ener/files/documents/172.pdf (last accessed 5 May 2015).

EC, 2012b. Radiation Protection No. 162: Criteria for Acceptability of Medical Radiological Equipment Used in Diagnostic Radiology, Nuclear Medicine and Radiotherapy and Maxillofacial Radiology. Evidence Based Guidelines. Directorate-General for Energy. European Commission, Brussels. https://ec.europa.eu/energy/sites/ener/files/documents/162.pdf (last accessed 5 May 2015).

EC, 2014. Radiation Protection No. 174: European Guidelines on Medical Physics Expert. Directorate-General for Energy. European Commission, Brussels. https://ec.europa.eu/energy/sites/ener/files/documents/174.pdf (last accessed 5 May 2015).

Ejima, K., Shoda, M., Yagishita, D., et al., 2010. Image integration of three-dimensional cone-beam computed tomography angiogram into electroanatomical mapping system to guide catheter ablation of atrial fibrillation. Europace 12, 45–51.

Faccioli, N., Foti, G., Barillari, M., et al., 2010. Finger fractures imaging: accuracy of cone-beam computed tomography and multislice computed tomography. Skeletal Radiol. 39, 1087–1095.

Fahrig, R., Fox, A.J., Lownie, S., et al., 1997. Use of a C-arm system to generate true three-dimensional computed rotational angiograms: preliminary in vitro and in vivo results. Am. J. Neuroradiol. 18, 1507–1514.

Fahrig, R., Holdsworth, D.W., Lownie, S., et al., 1998. Computed rotational angiography: system performance assessment using in-vitro and in-vivo models. Proc. SPIE 3336, Medical Imaging 1998: Physics of Medical Imaging, 305.

Fahrig, R., Dixon, R., Payne, T., et al., 2006. Dose and image quality for a cone beam C-arm CT System. Med. Phys. 33, 4541–4550.

Fiorella, D., Turk, A., Chaudry, I., et al., 2014. A prospective, multicenter pilot study investigating the utility of flat detector derived parenchymal blood volume maps to estimate cerebral blood volume in stroke patients. J. Neurointerv. Surg. 6, 451–456.

Fraser, J., Reed, M., 2013. Appropriateness of imaging in Canada. Can. Assoc. Radiol. J. 64, 82–84.

Gayou, O., Parda, D.S., Johnson, M., et al., 2007. Patient dose and image quality from mega-voltage cone beam computed tomography imaging. Med. Phys. 34, 499–506.

Grasruck, M., Suess, C., Stierstorfer, K., et al., 2005. Evaluation of image quality and dose on a flat-panel CT-scanner. Proc. SPIE 5745, 179–188.

Grimmer, R., Oelhafen, M., Elstrøm, U., et al., 2009. Cone-beam CT image reconstruction with extended z range. Med. Phys. 36, 3363–3370.

Gupta, R., Grasruck, M., Suess, C., et al., 2006. Ultra-high resolution flat-panel volume CT: fundamental principles, design architecture, and system characterization. Eur. Radiol. 16, 1191–1205.

Gupta, R., Cheung, A.C., Bartling, S.H., et al., 2008. Flat-panel volume CT: fundamental principles, technology, and applications. Radiographics 28, 2009–2022.

He, W., Huda, W., Magill, D., et al., 2010. Patient doses and projection angle in cone beam CT. Med. Phys. 37, 2359–2368.

Hendrick, R.E., Pisano, E.D., Averbukh, A., et al., 2010. Comparison of acquisition parameters and breast dose in digital mammography and screen-film mammography in the American College of Radiology Imaging Network Digital Mammographic Imaging Screening Trial. AJR Am. J. Roentgenol. 194, 362–369.

Herrnsdorf, L., Söderberg, M., 2013. A method to characterize the radiation output from a cone beam O-arm using a device for dose and dose profile scanning measurement. Proc. SPIE 8668, Medical Imaging 2013: Physics of Medical Imaging, 86682Q.

Hirsch, E., Wolf, U., Heinicke, F., et al., 2008. Dosimetry of the cone beam computed tomography Veraviewepocs 3D compared with the 3D Accuitomo in different fields of view. Dentomaxillofac. Radiol. 37, 268–273.

Hodez, C., Griffaton-Taillandier, C., Bensimon, I., 2011. Cone-beam imaging: applications in ENT. Eur. Ann. Otorhinolaryngol. Head Neck Dis. 128, 65–78.

HPA, 2010a. Health Protection Agency Recommendations for the Design of X-ray Facilities and Quality Assurance of Dental Cone Beam CT (Computed Tomography) Systems. HPA-RPD-065. Health Protection Agency, Chilton.

HPA, 2010b. Health Protection Agency Guidance on the Safe Use of Dental Cone Beam CT (Computed Tomography) Equipment. HPA-CRCE-010. Health Protection Agency, Chilton.

IAC, 2012. The IAC Dental CT Standards for Dental/Maxillofacial Computed Tomography (CT) Practice Accreditation Using Cone Beam Technology. Ellicott City, MD: Intersocietal Accreditation Commission. Available at: http://www.intersocietal.org/dental/standards/IAC_DentalCT_Standards.pdf (last accessed 5 May 2015).

IAEA, 1996. International Basic Safety Standards for Protection Against Ionizing Radiation and for the Safety of Radiation Sources. IAEA Safety Series No. 115. International Atomic Energy Agency, Vienna.

IAEA, 1999. Assessment of Occupational Exposure Due to External Sources of Radiation. IAEA Safety Guide RS-G-1.3. International Atomic Energy Agency, Vienna.

IAEA, 2004. Individual Monitoring. IAEA-PRTM-2 (Rev.1). International Atomic Energy Agency, Vienna.

IAEA, 2010. New Era in CT Scanning. International Atomic Energy Agency, Vienna. Available at: https://rpop.iaea.org/RPOP/RPoP/Content/News/new-era-ct-scanning.htm (last accessed 5 May 2015).

IAEA, 2011a. Status of Computed Tomography Dosimetry for Wide Cone Beam CT Scanners. IAEA Human Health Reports No. 5. International Atomic Energy Agency, Vienna.

IAEA, 2011b. Quality Assurance Programme for Computed Tomography: Diagnostic and Therapy Applications. IAEA Human Health Series 19. International Atomic Energy Agency, Vienna.

ICRP, 1991. 1990 Recommendations of the International Commission on Radiological Protection. ICRP Publication 60. Ann. ICRP 21(1–3).

ICRP, 1997. General principles for the radiation protection of workers. ICRP Publication 75. Ann. ICRP 27(1).

ICRP, 2000a. Managing patient dose in computed tomography. ICRP Publication 87. Ann. ICRP 30(4).

ICRP, 2000b. Avoidance of radiation injuries from medical interventional procedures. ICRP Publication 85. Ann. ICRP 30(2).
ICRP, 2004. Managing patient dose in digital radiology. ICRP Publication 93. Ann. ICRP 34(1).
ICRP 2007a. Managing patient dose in multi-detector computed tomography (MDCT). ICRP Publication 102. Ann. ICRP 37(1).
ICRP, 2007b. The 2007 Recommendations of the International Commission on Radiological Protection. ICRP Publication 103. Ann. ICRP 37(2–4).
ICRP, 2007c. Radiological protection in medicine. ICRP Publication 105. Ann. ICRP 37(6).
ICRP, 2009. Education and training in radiological protection for diagnostic and interventional procedures. ICRP Publication 113. Ann. ICRP 39(5).
ICRP, 2010. Radiological protection in fluoroscopically guided procedures performed outside the imaging department. ICRP Publication 117. Ann. ICRP 40(6).
ICRP, 2012. ICRP statement on tissue reactions/early and late effects of radiation in normal tissues and organs – threshold doses for tissue reactions in a radiation protection context. ICRP Publication 118. Ann. ICRP 41(1/2).
ICRP, 2013. Radiological protection in cardiology. ICRP Publication 120. Ann. ICRP 42(1).
ICRU, 2010. Prescribing, recording, and reporting intensity-modulated photon-beam therapy (IMRT). ICRU Report 83. J. ICRU 10, 1–106.
ICRU, 2012. Radiation dose and image quality assessment in computed tomography. ICRU Report 87. J. ICRU 12, 1–149.
IEC, 2006. Evaluation and Routine Testing in Medical Imaging Departments – Part 26: Constancy Tests – Imaging Performance of Computed Tomography X-ray Equipment. IEC 61223-2-6 ed. 2.0. International Electrotechnical Commission, Geneva.
IEC, 2010. Medical Electrical Equipment – Part 2-44: Particular Requirements for Basic Safety and Essential Performance of X-ray Equipment for Computed Tomography. IEC-60601-2-44 ed. 3.0, Amendment 1; 62B/804/CD. International Electrotechnical Commission, Geneva.
IEC, 2011. Evaluation and Routine Testing in Medical Imaging Departments – Part 3-5: Acceptance Tests – Imaging Performance of Computed Tomography X-ray Equipment. IEC 61223-3-5 ed. 1.0. International Electrotechnical Commission, Geneva.
IEC, 2012. Electromedical Equipment – Part 2-44: Particular Requirements for the Basic Safety and Essential Performance of X-ray Equipment for Computed Tomography. IEC 60601-2-44 ed. 3.1. International Electrotechnical Commission, Geneva.
IPEM, 2004. Guidance and Use of Diagnostic Reference Levels for Medical X-ray Examinations. Report 88. Institute of Physics and Engineering in Medicine, York.
IPEM, 2005. Recommended Standards for the Routine Performance Testing of Diagnostic X-ray Imaging Systems. Report 91. Institute of Physics and Engineering in Medicine, York.
Jaffray, D.A., Drake, D.G., Moreau, M., et al., 1999. A radiographic and tomographic imaging system integrated into a medical linear accelerator for localization of bone and soft-tissue targets. Int. J. Radiat. Oncol. Biol. Phys. 45, 773–789.
Jaffray, A.D., Siewerdsen, J.H., 2000. Cone-beam computed tomography with a flat-panel imager: initial performance characterization. Med. Phys. 27, 1311–1323.
Kalender, W.A., Beister, M., Boone, J.M., et al., 2012. High-resolution spiral CT of the breast at very low dose: concept and feasibility considerations. Eur. Radiol. 22, 1–8.

Kan, M.W., Leung, L.H., Wong, W., et al., 2008. Radiation dose from cone beam computed tomography for image-guided radiation therapy. Int. J. Radiat. Oncol. Biol. Phys. 70, 272–279.

Kawata, Y., Niki, N., Kumazaki, T., 1996. Measurement of blood vessel characteristics for disease detection based on cone beam CT images. IEEE Trans. Nucl. Sci. 43, 3348–3354.

Kim, S., Sopko, D., Toncheva, G., et al., 2011. Radiation dose from 3D rotational x-ray imaging: organ and effective dose with conversion factors. Radiat. Prot. Dosimetry 150, 50–54.

Kim, D.W., Chung, W.K., Yoon, M., 2013. Imaging doses and secondary cancer risk from kilovoltage cone-beam CT in radiation therapy. Health Phys. 104, 499–503.

Klein, B.E., Klein, R., Linton, K.L., et al., 1993. Diagnostic x-ray exposure and lens opacities: the Beaver Dam Eye Study. Am. J. Public Health 83, 588–590.

Klein, E.E., Hanley, J., Bayouth, J., et al., 2009. Task Group 142 report: quality assurance of medical accelerators. Med. Phys. 36, 4197–4212.

Korreman, S., Rasch, C., McNair, H., et al., 2010. The European Society of Therapeutic Radiology and Oncology–European Institute of Radiotherapy (ESTRO–EIR) report on 3D CT-based in-room image guidance systems: a practical and technical review and guide. Radiother. Oncol. 94, 129–144.

Kouno, T., Araki, F., Nakaguchi, Y., et al., 2013. Dose distribution from kV-cone beam computed tomography in image-guided radiotherapy. Nihon Hoshasen Gijutsu Gakkai Zasshi 69, 753–760.

Koyama, S., Aoyama, T., Oda, N., et al., 2010. Radiation dose evaluation in tomosynthesis and C-arm cone-beam CT examinations with an anthropomorphic phantom. Med. Phys. 37, 4298–4306.

Kroes, M.W., Busser, W.M.H., Futterer, J.J., et al., 2013. Assessment of needle guidance devices for their potential to reduce fluoroscopy time and operator hand dose during C-arm cone-beam computed tomography-guided needle interventions. J. Vasc. Interv. Radiol. 24, 901–906.

Kry, S.F., Salehpour, M., Followill, D.S., et al., 2005. Out-of-field photon and neutron dose equivalents from step-and-shoot intensity-modulated radiation therapy. Int. J. Radiat. Oncol. Biol. Phys. 62, 1204–1216.

Kwok, Y.M., Irani, F.G., Tay, K.H., et al., 2013. Effective dose estimates for cone beam computed tomography in interventional radiology. Eur. Radiol. 23, 3197–3204.

Kyriakou, Y., Kalender, W., 2007. Efficiency of anti-scatter grids for flat-detector CT. Phys. Med. Biol. 52, 6275–6293.

Kyriakou, Y., Richter, G., Dorfler, A., et al., 2008a. Neuroradiologic applications with routine C-arm flat panel detector CT: evaluation of patient dose measurements. AJNR Am. J. Neuroradiol. 29, 1930–1936.

Kyriakou, Y., Deak, P., Langner, O., et al., 2008b. Concepts of dose determination in flat-detector CT. Phys. Med. Biol. 53, 3551–3566.

Kyriakou, Y., Kolditz, D., Langner, O., et al., 2011. Digitale Volumentomografie (DVT) und Mehrschicht-Spiral-CT (MSCT): eine objektive Untersuchung von Dosis und Bildqualität. RöFo – Fortschritte auf dem Gebiet der Röntgenstrahlen und der bildgebenden. Verfahren 183, 144–153.

Lange, J., Karellas, A., Street, J., et al., 2013. Estimating the effective radiation dose imparted to patients by intraoperative cone-beam computed tomography in thoracolumbar spinal surgery. Spine (Phila Pa 1976) 38, E306–E312.

Levitt, M.R., Cooke, D.L., Ghodke, B.V., et al., 2011. 'Stent view' flat-detector CT and stent-assisted treatment strategies for complex intracranial aneurysms. World Neurosurg. 75, 275–278.

Lindfors, K.K., Boone, J.M., Nelson, T.R., et al., 2008. Dedicated breast CT: initial clinical experience. Radiology 246, 725–733.

Ludlow, J.B., Davies-Ludlow, L.E., Brooks, S.L., et al., 2006. Dosimetry of 3 CBCT devices for oral and maxillofacial radiology: CB Mercuray, NewTom 3G and i-CAT. Dentomaxillofac. Radiol. 35, 219–226.

Ludlow, J.B., Ivanovic, M., 2008. Comparative dosimetry of dental CBCT devices and 64-slice CT for oral and maxillofacial radiology. Oral Surg. Oral Med. Oral Pathol. Oral Radiol. Endod. 106, 106–114.

Mail, N., Moseley, D.J., Siewerdsen, J.H., et al., 2009. The influence of bowtie filtration on cone-beam CT image quality. Med. Phys. 36, 22–32.

Manarey, C.R.A., Anand, V.K., 2006. Radiation dosimetry of the FluoroCAT scan for real-time endoscopic sinus surgery. Otolaryngol. Head Neck Surg. 135, 409–412.

McCollough, C.H., 2005. Automatic exposure control in CT: are we done yet? Radiology 237, 755–756.

Michel, M.S., Ritter, M., Wertz, H., et al., 2014. Theurological Dyna-CT: ex vivo feasibility study of interventional cross-sectional imaging in the endourological operation room. World J. Urol. 32, 277–280.

Miller, D.L., Vañó, E., Bartal, B., et al., 2010. Occupational radiation protection in interventional radiology: a joint guideline of the Cardiovascular and Interventional Radiology Society of Europe and the Society of Interventional Radiology. J. Vasc. Interv. Radiol. 21, 607–615.

Michell, M.J., Iqbal, A., Wasan, R.K., et al., 2012. A comparison of the accuracy of film-screen mammography, full-field digital mammography, and digital breast tomosynthesis. Clin. Radiol. 67, 976–981.

Miracle, A.C., Mukherji, S.K., 2009a. Conebeam CT of the head and neck, part 1: physical principles. AJNR Am. J. Neuroradiol. 30, 1088–1095.

Miracle, A.C., Mukherji, S.K., 2009b. Conebeam CT of the head and neck, Part 2: clinical applications. AJNR Am. J. Neuroradiol. 30, 1285–1292.

Morant, J.J., Salvadó, M., Hernández-Girón, I., et al., 2013. Dosimetry of a cone beam CT device for oral and maxillofacial radiology using Monte Carlo techniques and ICRP adult reference computational phantoms. Dentomaxillofac. Radiol. 42, 92555893.

Mori, S., Endo, M., Nishizawa, K., et al., 2005. Enlarged longitudinal dose profiles in cone-beam CT and the need for modified dosimetry. Med. Phys. 32, 1061–1069.

Mozzo, P., Procacci, C., Tacconi, A., et al., 1998. A new volumetric CT machine for dental imaging based on the cone-beam technique: preliminary results. Eur. Radiol. 8, 1558–1564.

Nakashima, E., Neriishi, K., Minamoto, A., et al., 2006. A reanalysis of atomic-bomb cataract data, 2000–2002: a threshold analysis. Health Phys. 90, 154–160.

NCRP, 1995. Use of Personal Monitors to Estimate Effective Dose Equivalent and Effective Dose to Workers for External Exposure to Low-LET Radiation. NCRP Report No. 122. National Council on Radiation Protection and Measurements, Bethesda, MD.

NCRP, 2000. Radiation Protection for Procedures Performed Outside the Radiology Department. NCRP Report No. 133. National Council on Radiation Protection and Measurements, Bethesda, MD.

NCRP, 2005. Structural Shielding Design for Medical X-ray Imaging Facilities. NCRP Report No. 147. National Council on Radiation Protection and Measurements, Bethesda, MD.

NCRP, 2010. Radiation Dose Management for Fluoroscopically Guided Medical Procedures. NCRP Report No. 168. National Council on Radiation Protection and Measurements, Bethesda, MD.

NCRP, 2012. Reference Levels and Achievable Doses in Medical and Dental Imaging: Recommendations for the United States. NCRP Report No. 172. National Council on Radiation Protection and Measurements, Bethesda, MD.

NEMA, 2010. Computed Tomography Dose Check. NEMA Standards Publication XR 25-2010. National Electrical Manufacturers Association, Arlington, VA.

NEMA, 2013. New MITA Smart Dose Standard Enhances Dose Optimization and Management in CT Equipment. National Electrical Manufacturers Association, Arlington, VA. Available at: http://www.nema.org/News/Pages/New-MITA-Smart-Dose-Standard-Enhances-Dose-Optimization-and-Management-in-CT-Equipment.aspx (last accessed 5 May 2015).

Neriishi, K., Nakashima, E., Minamoto, A., et al., 2007. Postoperative cataract cases among atomic bomb survivors: radiation dose response and threshold. Radiat. Res. 168, 404–408.

Niklason, L.T., Christian, B.T., Niklason, L.E., 1997. Digital tomosynthesis in breast imaging. Radiology 205, 399–406.

Ning, R., Chen, B., Yu, R., et al., 2000a. Flat panel detector-based cone beam volume CT angiography imaging: system evaluation. IEEE Trans. Med. Im. 19, 949–963.

Ning, R., Colbeth, R.E., Chen, B., et al., 2000b. Real time flat panel detector-based volume tomographic angiography imaging: detector evaluation. Proc. SPIE 3977, Medical Imaging 2000: Physics of Medical Imaging, 396.

Nottmeier, E.W., Pirris, S.M., Edwards, S., et al., 2013. Operating room radiation exposure in cone beam computed tomography-based, image-guided spinal surgery. J. Neurosurg. Spine 19, 226–231.

O'Connell, A., Conover, D.L., Zhang, Y., et al., 2010. Cone-beam CT for breast imaging: radiation dose, breast coverage, and image quality. AJR Am. J. Roentgenol. 195, 496–509.

Orth, R.C., Wallace, M.J., Kuo, M.D., 2008. C-arm cone-beam CT: general principles and technical considerations for use in interventional radiology. J. Vasc. Interv. Radiol. 19, 814–820.

Packard, N.J., Abbey, C.K., Yang, K., et al., 2012. Effect of slice thickness on detectability in breast CT using a prewhitened matched filter and simulated mass lesions. Med. Phys. 39, 1818–1830.

Padovani, R., Le Heron, J., Cruz-Suarez, R., et al., 2011. International project on individual monitoring and radiation exposure levels in interventional cardiology. Radiat. Prot. Dosimetry 144, 437–441.

Paul, J., Jacobi, V., Farhang, M., et al., 2013a. Radiation dose and image quality of x-ray volume imaging systems: cone-beam computed tomography, digital subtraction angiography and digital fluoroscopy. Eur. Radiol. 23, 1582–1593.

Paul, J., Mbalisike, E.C., Vogl, T.J., 2013b. Radiation dose to procedural personnel and patients from an x-ray volume imaging system. Eur. Radiol. 23, 3262–3270.

Pauwels, R., Theodorakou, C., Walker, A., et al., 2012a. Dose distribution for dental cone beam CT and its implication for defining a dose index. Dentomaxillofac. Radiol. 41, 583–593.

Pauwels, R., Beinsberger, J., Collaert, B., et al., 2012b. Effective dose range for dental cone beam computed tomography scanners. Eur. J. Radiol. 81, 267–271.
Pauwels, R., Stamatakis, H., Bosmans, H., et al., 2013. Quantification of metal artifacts on cone beam computed tomography images. Clin. Oral Impl. Res. 24(Suppl. A100), 94–99.
Pauwels, R., Zhang, G., Theodorakou, C., et al., 2014. Effective radiation dose and eye lens dose in dental cone beam CT: effect of field of view and angle of rotation. Br. J. Radiol. 87, 20130654.
Pisano, E.D., Gatsonis, C., Hendrick, E., 2005. Diagnostic performance of digital versus film mammography for breast-cancer screening. N. Engl. J. Med. 353, 1773–1883.
Podnieks, E.C., Negus, I.S., 2012. Practical patient dosimetry for partial rotation cone beam CT. Br. J. Radiol. 85, 161–167.
Popescu, S., Stierstorfer, K., Flohr, T., et al., 2005. Design and evaluation of a prototype volume CT scanner. Proc. SPIE 5745, 600–608.
Poplack, S.P., Tosteson, T.D., Kogel, C.A., et al., 2007. Digital breast tomosynthesis: initial experience in 98 women with abnormal digital screening mammography. AJR Am. J. Roentgenol. 189, 616–623.
Pouliot, J., Bani-Hashemi, A., Chen, J., et al., 2005. Low-dose megavoltage cone-beam CT for radiation therapy. Int. J. Radiat. Oncol. Biol. Phys. 61, 552–560.
Psychogios, M.N., Buhk, J.H., Schramm, P., et al., 2010. Feasibility of angiographic CT in peri-interventional diagnostic imaging: a comparative study with multidetector CT. AJNR Am. J. Neuroradiol. 31, 1226–1231.
Racadio, J.M., Babic, D., Homan, R., et al., 2007. Live 3D guidance in the interventional radiology suite. AJR Am. J. Roentgenol. 189, W357–W364.
Ramdhian-Wihlm, R., Le Minor, J.M., Schmittbuhl, M., et al., 2012. Cone-beam computed tomography arthrography: an innovative modality for the evaluation of wrist ligament and cartilage injuries. Skeletal Radiol. 41, 963–969.
Rastegar, N., Eckart, P., Mertz, M., 2002. Radiation-induced cataract in astronauts and cosmonauts. Graefes Arch. Clin. Exp. Ophthalmol. 240, 543–547.
Rehani, M.M., 2013. Challenges in radiation protection of patients in the 21st Century. AJR Am. J. Roentgenol. 200, 762–764.
Rehani, M.M., Berry, M., 2000. Radiation doses in computed tomography. BMJ. 320, 593–594.
Rehani, M.M., Ortiz López, P., 2006. Radiation effects in fluoroscopically guided cardiac interventions – keeping them under control. Int. J. Cardiol. 109, 147–151.
Rehani, M., Frush, D., 2010. Tracking radiation exposure of patients. Lancet 4, 376, 754–745.
Rehani, M.M., Frush, D.P., 2011. Patient exposure tracking: the IAEA smart card project. Radiat. Prot. Dosimetry 147, 314–316.
Rehani, M.M., Vañó, E., Ciraj-Bjelac, O., et al., 2011. Radiation and cataract. Radiat. Prot. Dosimetry 147, 300–304.
Rehani, M.M., Srimahachota, S., 2011. Skin injuries in interventional procedures. Radiat. Prot. Dosimetry 147, 8–12.
Reichardt, B., Sarwar, A., Bartling, S.H., et al., 2008. Musculoskeletal applications of flat-panel volume CT. Skeletal Radiol. 37, 1069–1076.
Robb, R.A., 1982. Dynamic spatial reconstructor: an x-ray video fluoroscopic CT scanner for dynamic volume imaging of moving organs. IEEE Trans. Med. Im. MI-1, 22–23.

Ross, W.R., Dawn, C., Fitzgerald, P., et al., 2004. Performance and Pre-clinical Results from a Flat-panel-based Volumetric CT System. Proceedings of 90th Scientific Assembly and Annual Meeting of the Radiological Society of North America, 28 November–3 December 2004, Chicago, IL, USA, SSG18-02.

Roy, O.P., Angle, J.F., Jenkins, A.D., et al., 2012. Cone beam computed tomography for percutaneous nephrolithotomy: initial evaluation of a new technology. J. Endourol. 26, 814–818.

Saint-Félix, D., Trousset, Y., Picard, C., et al., 1994. In vivo evaluation of a new system for 3D computerized angiography. Phys. Med. Biol. 39, 584–595.

Sanchez, R.M., Vañó, E., Fernández, J.M., et al., 2014. Brain radiation doses to patients in an interventional neuroradiology laboratory. AJNR Am. J. Neuroradiol. 35, 1276–1280.

Schafer, S., Nithiananthan, S., Mirota, D.J., et al., 2011. Mobile C-arm cone-beam CT for guidance of spine surgery: image quality, radiation dose, and integration with interventional guidance. Med. Phys. 38, 4563–4574.

Schafer, S., Stayman, J.W., Zbijewski, W., et al., 2012. Antiscatter grids in mobile C-arm cone-beam CT: effect on image quality and dose. Med. Phys. 39, 153–159.

Schueler, B.A., Sen, A., Hsiung, H.H., et al., 1997. Three-dimensional vascular reconstruction with a clinical x-ray angiography system. Acad. Radiol. 4, 693–699.

Schulz, B., Heidenreich, R., Heidenreich, M., et al., 2012. Radiation exposure to operating staff during rotational flat-panel angiography and C-arm cone beam computed tomography (CT) applications. Eur. J. Radiol. 81, 4138–4142.

Seuri, R., Rehani, M.M., Kortesniemi, M., 2013. How tracking radiologic procedures and dose helps: experience from Finland. AJR Am. J. Roentgenol. 200, 771–775.

Shah, A., Aird, E., Shekhdar, J., 2012. Contribution to normal tissue dose from concomitant radiation for two common kV-CBCT systems and one MVCT system used in radiotherapy. Radiother. Oncol. 105, 139–144.

Shope, T.B., Gagne, R.M., Johnson, G.C., 1981. A method for describing the doses delivered by transmission x-ray computed tomography. Med. Phys. 8, 488–495.

Sierzenski, P.R., Linton, O.W., Amis, E.S., Jr, et al., 2014. Applications of justification and optimization in medical imaging: examples of clinical guidance for computed tomography use in emergency medicine. J. Am. Coll. Radiol. 11, 36–44.

Siewerdsen, J.H., Jaffray, D.A, 1999. Cone-beam computed tomography with a flat-panel imager: effects. Med. Phys. 26, 2635–2647.

Siewerdsen, J.H., Jaffray, D.A., 2001. Cone-beam computed tomography with a flat-panel imager: magnitude and effects of x-ray scatter. Med. Phys. 28, 220–231.

Sistrom, C.L., Dang, P.A., Weilburg, J.B., et al., 2009. Effect of computerized order entry with integrated decision support on the growth of outpatient procedure volumes: seven-year time series analysis. Radiology 251, 147–155.

Song, W.Y., Kamath, S., Ozawa, S., et al., 2008. A dose comparison study between XVI and OBI CBCT systems. Med. Phys. 35, 480–486.

Sowards-Emmerd, D., Balakrishnan, K., Wiener, J., Shao, L., Ye, J., 2009. CBCT-subsystem Performance of the Multi-modality Brightview XCT System (M09-26). Nuclear Science Symposium Conference Record (NSS/MIC), 2009 IEEE, p. 3053–3058.

Spezi, E., Downes, P., Jarvis, R., et al., 2012. Patient-specific three-dimensional concomitant dose from cone beam computed tomography exposure in image-guided radiotherapy. Int. J. Radiat. Oncol. Biol. Phys. 83, 419–426.

Stock, M., Palm, A., Altendorfer, A., et al., 2012. IGRT induced dose burden for a variety of imaging protocols at two different anatomical sites. Radiother. Oncol. 102, 355–363.

Sutton, D.G., Martin, C.J., Williams, J.R., et al., 2012. Radiation Shielding for Diagnostic Radiology. British Institute of Radiology, London.

Suzuki, S., Yamaguchi, I., Kidouchi, T., et al., 2011. Evaluation of effective dose during abdominal three-dimensional imaging for three flat-panel-detector angiography systems. Cardiovasc. Intervent. Radiol. 34, 376–382.

Theodorakou, C., Walker, A., Horner, K., et al., 2012. Estimation of paediatric organ and effective doses from dental cone beam CT using anthropomorphic phantoms. Br. J. Radiol. 85, 153–160.

Tuominen, E.K.J., Kankare, J., Koskinen, S.K., et al., 2013. Weight-bearing CT imaging of the lower extremity. AJR Am. J. Roentgenol. 200, 146–148.

Tyan, Y.S., Li, Y.Y., Ku, M.C., et al., 2013. The effective dose assessment of C-arm CT in hepatic arterial embolisation therapy. Br. J. Radiol. 86, 20120551.

Tzedakis, A., Damilakis, J., Perisinakis, K., et al., 2005. The effect of z overscanning on patient effective dose from multidetector helical computed tomography examinations. Med. Phys. 32, 1621–1629.

Vañó, E., González, L., Beneytez, F., et al., 1998. Lens injuries induced by occupational exposure in nonoptimized interventional radiology laboratories. Br. J. Radiol. 71, 728–733.

Vañó, E., Kleiman, N.J., Duran, A., et al., 2010. Radiation cataract risk in interventional cardiology personnel. Radiat. Res. 174, 490–495.

Vañó, E., Kleiman, N.J., Duran, A., et al., 2013. Radiation-associated lens opacities in catheterization personnel: results of a survey and direct assessments. J. Vasc. Interv. Radiol. 24, 197–204.

Wallace, M.J., Kuo, M.D., Glaiberman, C., et al., 2008. Three-dimensional C-arm cone-beam CT: applications in the interventional suite. J. Vasc. Interv. Radiol. 19, 799–813.

Wang, X., 1997. Volume Tomographic Angiography. PhD thesis. University of Rochester, Rochester, NY.

Wen, N., Guan, H., Hammoud, R., et al., 2007. Dose delivered from Varian's CBCT to patients receiving IMRT for prostate cancer. Phys. Med. Biol. 52, 2267–2276.

Wielandts, J.Y., Smans, K., Ector, J., et al., 2010. Effective dose analysis of three-dimensional rotational angiography during catheter ablation procedures. Phys. Med. Biol. 55, 563–579.

Wiesent, K., Barth, K., Navab, N., et al., 2000. Enhanced 3D reconstruction algorithm for C-arm systems suitable for interventional procedures. IEEE Trans. Med. Im. 19, 391–403.

Wintermark, M., Lev, M.H., 2010. FDA investigates the safety of brain perfusion CT. AJNR Am. J. Neuroradiol. 31, 2–3.

Wiper, A., Katira, A., Roberts, D.H., 2005. Interventional cardiology: it's a hairy business. Heart 91, 1432.

Yuan, M.K., Tsai, D.C., Chang, S.C., et al., 2013. The risk of cataract associated with repeated head and neck CT studies: a nationwide population-based study. AJR Am. J. Roentgenol. 201, 626–630.

Zbijewski, W., De Jean, P., Prakash, P., et al., 2011. A dedicated cone-beam CT system for musculoskeletal extremities imaging: design, optimization, and initial performance characterization. Med. Phys. 38, 4700–4713.

Zhang, G., Marshall, N., Bogaerts, R., et al., 2013. Monte Carlo modeling for dose assessment in cone beam CT for oral and maxillofacial applications. Med. Phys. 40, 072103.

ANNEX A. ASSESSING PATIENT DOSES IN CBCT

(A1) This annex provides a more in-depth description of patient dosimetry methods and limitations in CBCT. A summarised version is given in Section 5. A more extensive coverage of dosimetry in CBCT can be found in Report 87 (ICRU, 2012).

A.1. Dosimetry in CBCT

(A2) CBCT uses a wide x-ray beam for 3D imaging of a relatively large volume. Since the mid-1990s, the trend in MDCT has been towards an ever-increasing number of slices with a concomitant increase in x-ray beam width; the *z*-axis coverage of the high-end, wide-area MDCT scanners available today rivals that of CBCT. These developments have created a drive to update CT dosimetry methods so that they are more apropos wide area detectors. As a result, some of the work from MDCT dosimetry, for which established measurement methods and phantoms exist already, can be translated to CBCT dosimetry. This annex discusses the shortcomings of the standard narrow-beam MDCT formalism when it is applied directly to CBCT. In order to construct a comprehensive framework for CBCT dosimetry, methods to overcome these problems are described.

(A3) CT dosimetry has evolved around the concept of CTDI. From its introduction in the 1980s (Shope et al., 1981), CTDI has taken different forms depending on the adopting organisation: the United States Food and Drug Administration, IEC, and other similar agencies. CTDI has mainly been used to compare dose characteristics of different CT machines, to test the stability of equipment performance (quality control), and, in some instances, to estimate patient dose despite the fact that CTDI does not provide a direct assessment of patient dose. An extensive description of the CTDI concept can be found in Report 87 (ICRU, 2012).

(A4) Increasingly, wide beams in modern CT and CBCT scanners complicate CTDI measurements (Abuhaimed et al., 2014). Even for a nominal beam width of 20 mm, it is evident that CTDI measured over a length of 100 mm (i.e. $CTDI_{100}$) does not cover the tails of the dose profile in a poly(methyl methacrylate) (PMMA) phantom. The ratio of $CTDI_{100}/CTDI_{\infty}$ is called 'CTDI measurement efficiency'. Kyriakou et al. (2008b) have shown that for 200-mm collimation, an integration length of >600 mm would be required to approximate $CTDI_{\infty}$ within 1%.

(A5) An alternative method for CTDI estimation in O-arm systems has been proposed, using a point-dose detector that is moved through the CBCT field, preferably in-air (Herrnsdorf and Söderberg, 2013).

(A6) Issues regarding efficiency of CTDI measurements have been the basis of the new approach of wide-beam CT dosimetry. IAEA (2011a) adopted a two-step approach proposed by IEC (2010). More details regarding this modified approach can be found in Report 87 (ICRU, 2012).

(A7) It would be useful to mention that CTDI alone is not a useful indicator of patient dose. In order to connect the CTDI-like measurements with dose, $CTDI_{vol}$

and DLP have been used extensively in clinical practice as relative patient dose indicators. $CTDI_{vol}$ and DLP are connected by the equation:

$$DLP = L.CTDI_{vol}$$

where L is the length of the scan. The $CTDI_{vol}$ paradigm is problematic in cases where there is no helical scan or patient motion (as is the case with many CBCT scanners). In such cases, reported $CTDI_{vol}$ values will overestimate the dose significantly (Dixon and Boone, 2010a).

A.2. Point-of-care scanning and clinic-based CBCT systems

(A8) Clinic-based systems include head and neck CBCT, bCT, and dental and maxillofacial CBCT. A particular property of dental and maxillofacial CBCT scanners is that, depending on the system, varying FOV sizes are offered. This allows for the scanning of localised regions (i.e. a single tooth and its immediate surroundings) as well as maxillofacial scanning. The use of horizontal collimation, as well as other factors, results in complicated dose distributions in the axial plane, providing an additional challenge for dosimetry (Pauwels et al., 2012a). In addition, most dental and maxillofacial CBCT systems are seated or standing, resulting in practical complications regarding phantom and dosimeter placement.

(A9) For dental systems, the SEDENTEXCT Consortium report (EC, 2012a) discussed the use of KAP as well as CTDI-like measurements. It was proposed that CTDI measurements should be performed during commissioning in cases when the machine comes with data on such measurements from the manufacturer. On the grounds that conventional CTDI has drawbacks for use of dental and maxillofacial CBCT (due to wider beams and greater asymmetry of dose distribution in CBCT compared with MDCT), the Consortium tried to define a single CBCT dose index (CBCT DI) (Pauwels et al., 2012a). During this effort, a customised phantom (SEDENTEXCT DI) was developed which is shown in Fig. A.1. It features suitable insets for the placement of measuring equipment. The phantom consists of four ionisation chamber plates (2×22 mm and 2×44 mm), one thermoluminescent dosimeter plate (22 mm thick), and one film plate (22 mm thick). Three adapters with widths of 22, 44, and 66 mm are provided that can reduce the chamber diameter from 26 to 13 mm. Two different measurement setups (Index 1 and Index 2) are depicted in Fig. A.1. Index 1 is defined as the average of seven measurements along the diameter of the phantom, with the measuring line connecting the centre of the FOV and the centre of the phantom; this allows for central or off-axis FOV positioning. Index 2 is an adapted $CTDI_w$, measured using a small-volume ion chamber at the central axial plane and using ½ weighting between the central measurement and the average of four peripheral measurements; the FOV should always be positioned centrally for this index.

(A10) In addition, the German standard DIN 6868-161 describes a dosimetry method for dental and maxillofacial CBCT systems, which is also applicable for any device with an accessible detector surface (DIN, 2013). The proposed method

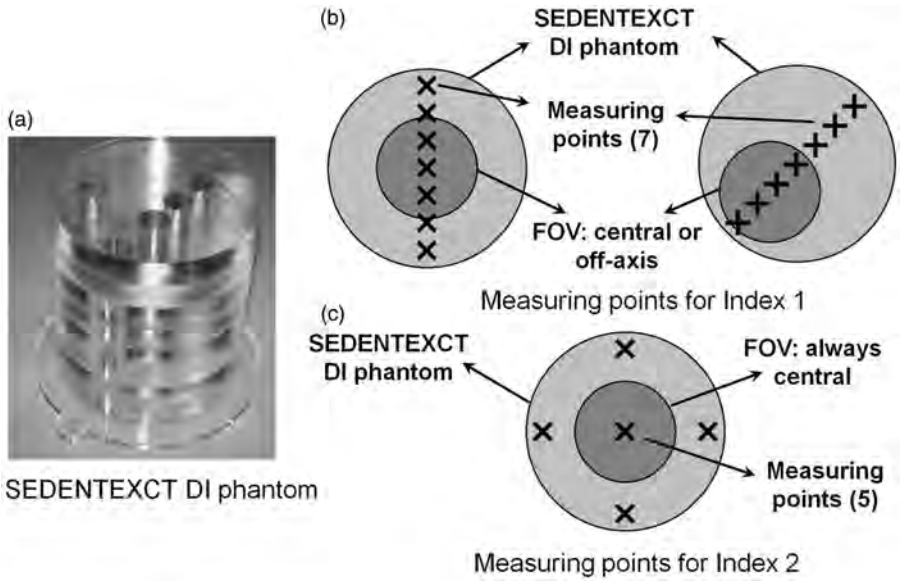

Fig. A.1. (a) The SEDENTEXCT dose index (DI) phantom (Leeds Test Objects, Boroughbridge, UK) for radiation dose measurements in dental and maxillofacial cone beam computed tomography systems. (b, c) Measuring points for the estimation of Index 1 and Index 2. Figure provided by Ruben Pauwels on behalf of the SEDENTEXCT Project Consortium (Pauwels et al., 2012a; EC, 2012a). FOV, field of view.

is based on a phantomless dose measurement at the detector, which is corrected through geometrical factors to estimate the dose at the isocentre.

(A11) Further validation of different possible indices is required, together with a way to translate dose index readings into patient doses. Araki et al. (2013) concluded that CBCT DI and KAP proposed by SEDENTEXCT could be used to establish DRLs for dental and maxillofacial CBCT, and noted that the relationship between these indices and patient dose remains to be determined.

(A12) While a standardised dose metric for clinic-based CBCT systems may differ from that of other CBCT systems, it is important to consider both the practicality of the measurements and their relevance in QA. Until conversion factors for phantomless CBCT dosimetry have been established, phantom measurements hold an important advantage from a QA point of view.

(A13) It has been suggested that if the manufacturer has provided a CTDI dose figure, this quantity should be measured during commissioning. However, not all machines come with such initial measurements. Another dose index used for CBCT dosimetric evaluations is KAP, which is often used in panoramic and cephalometric radiography and, of course, is widely used in radiography and fluoroscopy. Some machines display a KAP value on screen after the exposure. The accuracy of such measurements should be verified by medical physicists. The use of KAP has been

proposed by HPA (2010a). The main advantage of KAP is that it is easy to calculate by measuring dose and beam cross-section at a specific point. It is considered suitable for auditing CBCT dose in dental practices (HPA, 2010b). The SEDENTEXCT Consortium proposes that if such measurements are not provided, the medical physicist should create a log of such readings in all clinically used settings, so that the dentist may compare it with national and international audit levels (EC, 2012a).

(A14) Technically, the methods described above could also be applied to other clinic-based systems including, for example, systems for head and neck imaging, and possibly bCT. However, there is currently no standardisation in the measurements for such units. This highlights the fact that the issue of standardisation in CBCT dosimetry remains largely unresolved.

A.3. C-arm CBCT systems

(A15) C-arm CBCT systems are incapable of performing a full rotation around the patient couch. Some systems can only rotate 180° plus the beam angle (Fahrig et al., 2006), which results in a non-uniform axial dose deposition to the patient/phantom. In a phantom, the maximum dose occurs at the central plane intersecting the z-axis at $z = 0$, on the side of the phantom closest to the x-ray tube. In the ideal case in which the heel effect is absent, the maximum dose would occur on the bisector of the rotation angle. When the heel effect is present, the maximum dose occurs near the bisector.

(A16) For C-arm CBCT systems, Fahrig et al. (2006) proposed a metric representing the average dose to the phantom central plane ($z = 0$):

$$\bar{D}(0) = \frac{1}{3} D_0 + \frac{2}{3} \bar{D}_\mathrm{p}$$

where D_0 is the dose to the central point of the central plane (on the z-axis) and D_p is the average peripheral dose. This equation follows a similar averaging to that used in the calculation of $\mathrm{CTDI_w}$; the metric that is used for dosimetry on any conventional CT scanner performing a rotation smaller than 360°. Fahrig et al. (2006) performed the calculation using a Farmer ionisation chamber, and measured doses at the centre and at eight peripheral positions at 1-cm depth from the head phantom's surface. Podnieks and Negus (2012) showed that effective dose can be estimated from $\mathrm{CTDI_w}$ and irradiated length with acceptable accuracy if the ionisation chamber positions are considered carefully.

A.4. A unified approach to CT dosimetry

(A17) Report 87 (ICRU, 2012) reviewed a considerable body of work in order to propose a method for CT dosimetry that compensates for the shortcomings of

current CTDI-based CT dosimetry methods. In addition, earlier work by Dixon and Boone (2010b) provided a unified formalism for dose measurements on machines capable of helical scanning (e.g. MDCT scanners), as well as on those that only acquire axial images (which is the case with most CBCT scanners). A set of metrics and the use of a new polyethylene 600-mm-long phantom are proposed. This method has been described previously (AAPM, 2010), but in this publication, the notation as presented in Report 87 (ICRU, 2012) was used. The mathematical foundation for the method is beyond the scope of this publication; however, the method is discussed briefly below.

(A18) A dosimetry quantity $CTDI_L$ is proposed, the physical meaning of which is the dose at the centre ($z=0$) of the scanned length for a scan extending from $z=-L/2$ to $z=L/2$. This formalism provides a means to estimate the dose deposited at the central plane of the phantom, at $z=0$. In the case of axial scans, such as those performed with most CBCT machines, the quantity that corresponds intuitively to CTDI is the dose at the central point of the beam on the z-axis. If $f(z)$ is the dose profile function, this dose is $f(0)$. For a number (N) of identical axial scans centred at $z=0$, the dose of interest will be equal to $Nf(0)$.

A.4.1. Formalism

(A19) For a helical CT scan, the accumulated absorbed dose distribution at the centre of the scan length (from $-L/2$ to $+L/2$) is represented by a convolution of the axial dose profile with a rectangular function, $\Pi(z/L)$ of scan length L. This representation is only valid when x-ray tube current modulation is not used. Fig. A.2 shows normalised cumulative absorbed dose distributions for a series of helical CT scans of differing scan lengths, produced by Monte Carlo simulation (Boone, 2009).

(A20) The dose $D_L(0)$ at the central part of the beam ($z=0$) for a beam width L increases as the width of the beam increases. This can be seen in Fig. A.2. $D_L(0)$ approaches a maximum value asymptotically, when the beam width increases. This value is called the 'equilibrium dose' (D_{eq}), and could be understood as $CTDI_\infty$ (i.e. when the entire dose profile has been collected).

A.4.2. Cumulative absorbed dose distribution from a helical scan of length L

(A21) The cumulative absorbed dose distribution $D_L(z)$ for helical scans in which the table moves by a distance b per gantry rotation can be calculated by using the following equation; this is only applicable when tube current modulation is not used.

$$D_L(z) = \frac{1}{b}\int_{-L/2}^{+L/2} f(z-z')dz'$$

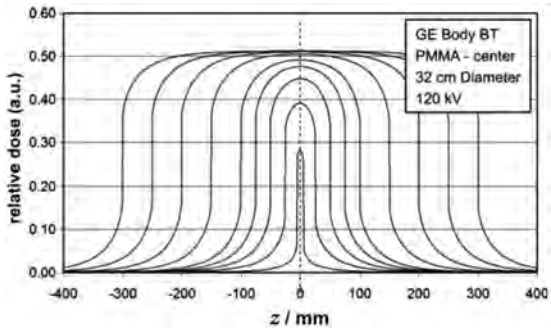

Fig. A.2. Normalised absorbed dose as a function of z-position for a number of different scan lengths: 10 mm, 50 mm, 100 mm, 150 mm, 200 mm, 300 mm, 400 mm, 500 mm, and 600 mm (from centre to edge of graph). These data were derived by convolving the dose spread function computed from the Monte Carlo simulation with rectangular functions characterising the length of the scan, for a 320-mm diameter poly(methyl methacrylate) phantom at 120 kV, using a GE Lightspeed 16-body bowtie filter. Source: ICRU (2012).

(A22) At $z = 0$ and taking into account that pitch (p) is defined as $p = b/nT$, the above equation becomes:

$$D_{\mathrm{L}}(0) = \frac{1}{b}\int_{-L/2}^{+L/2} f(z')dz' = p.\mathrm{CTDI_L}$$

(A23) Note that for $p = 1$, $D_{\mathrm{L}}(0) = \mathrm{CTDI_L}$. Conceptually, $D_{\mathrm{L}}(0)$ as a function of L uses the data points along a vertical line perpendicular to $z = 0$ in Fig. A.2.

(A24) $D_{\mathrm{L}}(0)$ depends on L, until the asymptote D_{eq} is reached at very long scan lengths. A new function capable of representing this dependence needs to be introduced. The mathematical synonym function $h(L) = D_{\mathrm{L}}(0)$ is thus:

$$h(L) = \frac{1}{b}\int_{-L/2}^{+L/2} f(z')dz'$$

(A25) Conceptually, $h(L)$ is the integral of the intercepted dose profile on the z-axis for a scan of length L by keeping the detector at the centre of the phantom.

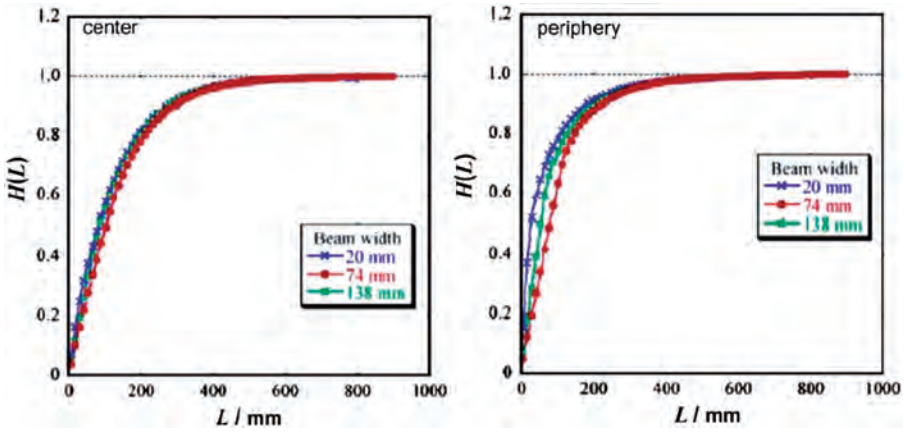

Fig. A.3. Graphs showing measured $H(L)$ curves. These data were measured in a 900-mm-long, 320-mm-diameter poly(methyl methacrylate) phantom, scanned at 120 kV. Three different beam collimation widths are shown in each plot for the centre position (left panel) and the periphery (right panel). Source: Mori et al. (2005).

(A26) If the cumulative absorbed dose at $z = 0$ is normalised to D_{eq}, the above equation becomes:

$$H(L) = \frac{h(L)}{D_{eq}} = \frac{D_L(0)}{D_{eq}}$$

(A27) Fig. A.3 shows $H(L)$ curves measured by Mori et al. (2005). The maximum $H(L)$ value as a function of scan length L approaches unity asymptotically for large scan lengths. This has been referred to as the rise to dose equilibrium curve. As $H(L)$ is normalised to unity at $L \rightarrow \infty$, this function does not contain the tube output information that $h(L)$ does.

(A28) The physical interpretation of the rise to equilibrium curve is that the scan and the phantom need to be long enough so that the asymptote tails of the profiles are reached. The longer the scan, the closer $H(L)$ approaches a value of unity. This representation is therefore good for showing the relatively low efficiency of short scans for collecting the actual dose, and this efficiency increases with longer scans.

A.4.3. Phantoms

(A29) It has been shown that a phantom with a 300-mm diameter would need to be at least 400-mm long to capture approximately 98% of D_{eq} (this is equivalent to

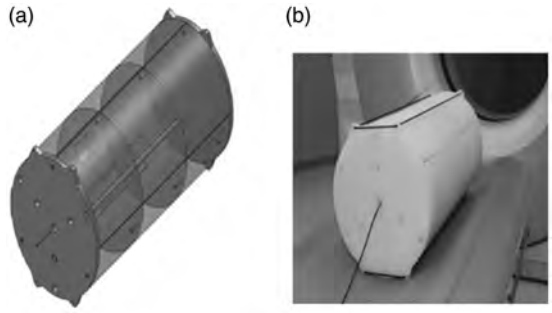

Fig. A.4. The ICRU/AAPM TG 200 phantom. The phantom is made of high-density polyethylene (0.97 g cm^{-3}) with a diameter of 300 mm and a length of 600 mm, which are sufficient for measuring $h(L)$ and $H(L)$. (a) Design of the phantom. (b) Photograph of the phantom. The phantom is large and weighs approximately 41 kg. Therefore, it was designed to be modular with three different sections. Source: ICRU (2012).

saying that the scan profile interception would be 98% efficient). For a phantom with the standard 320-mm diameter, a length of 425 mm would be required for the same measurement efficiency. To tackle this problem, the committee responsible for ICRU Report 87 collaborated with the American Association of Physicists in Medicine (AAPM) task group responsible for Report 200 (AAPM, 2015). As a result of this collaboration, the phantom, ICRU/AAPM TG 200, shown in Fig. A.4, was developed.

A.4.4. Practical measurement of rise-to-equilibrium dose curves

(A30) Methods for measuring the $H(L)$ or $h(L)$ curves have been well described in Report 111 (AAPM, 2010) and Report 87 (ICRU, 2012). Here, a short and intuitive description of the measurement methods is given.

(A31) A long phantom and an integrating thimble ionisation chamber are needed. A series of helical scans of different lengths is performed, and the air kerma integrated by the thimble chamber is recorded. The scans are centred on the position of the chamber. The air kerma readings as measured by the chamber are plotted as a function of the length of the helical scan.

(A32) If a real-time radiation dosimeter is available, the rise-to-equilibrium curve may be plotted using data obtained during a single long scan. In this case, the dosimeter can create a full dose profile along the whole length of the phantom. Different points on the curve may be calculated by integrating the dose profile curve using appropriate integration limits ($-L/2$ to $L/2$), where L is the total

integration length centred on the real-time radiation meter at the centre of the phantom.

A.4.5. Measurements on machines only capable of axial acquisition

(A33) The methods described above are useful for measurements in MDCT machines that provide the option to perform helical scans. However, most CBCT machines do not perform helical scans. When table translation during a scan is not available, it is necessary to modify the method, based on the notion that it is necessary to measure a quantity that corresponds to CTDI of helical scans. As mentioned previously, this quantity is $f(0)$ (Dixon and Boone, 2010b). Practically speaking, $f(0)$ is measured by placing the ionisation chamber at the centre of the phantom and the beam, and varying the beam width starting from the thinnest possible collimation to the widest available. The measurement values can then be plotted against the beam width α. The values may be normalised to A_{eq} which is the equilibrium value that would be reached for $f(0)$ if the beam width was $\geq$470 mm. Such beam widths are, of course, not found in clinical practice. Thus, the normalised approach-to-equilibrium curve for the axial scan is only partial, and does not reach a value of 1 asymptotically. For axial CT scans with a cone beam width α, dose $f(0)_{\alpha} = H(\alpha)A_{eq}$, the conventional CT dose $D_L(0)$ can be described as a function of scan length L, including a common equilibrium dose constant A_{eq}, a common scatter equilibrium length $\alpha_{eq} = L_{eq}$, and a common function $H(\lambda)$ which describes the relative approach to dose equilibrium for both modalities, where $\lambda = \alpha$, or $\lambda = L$, such that $f(0)_{\alpha} = H(\alpha)A_{eq}$ and $D_L(0) = H(L)D_{eq} = H(L)(b/\alpha)A_{eq}$. Axial scanners that do not have the facility to collimate the beam may be equipped with a collimation gauge that could be inserted in front of the x-ray tube for dose measurement purposes.

(A34) It is important to note here that the integration which needs to be performed in order to measure CTDI is a result of the existence of table movement. The definition of CTDI implies that dose to the central area of a phantom is affected by scatter from adjacent areas. This phenomenon is completely absent in axial scans: therefore, CTDI consistently overestimates the dose around the central area of the phantom.

A.4.6. ICRU Report 87 recommendations

$CTDI_{vol}$ and $CTDI_{air}$ measurements

(A35) Traditionally, $CTDI_{vol}$ has been related to measurements of CT dose. IEC has also recommended that $CTDI_{vol}$ should be displayed on the control screen of CT scanners. Due to its widespread use and in order to keep continuity with older measurements on CT scanners, ICRU recommends that both $CTDI_{vol}$ and $CTDI_{vol}$ free-in-air should be measured at acceptance testing using both 160-mm-

and 320-mm-diameter PMMA phantoms at clinically relevant mAs settings across the range of tube potentials used clinically. Furthermore, $CTDI_{vol}$ is used to scale size-specific dose estimates (SSDE) as well as for normalisation of rise-to-equilibrium curves. The x-ray output of the CT scanner, which is also characterised by $CTDI_{air}$, is a fundamental measurement that should be performed during acceptance testing and after changing major components of the scanner related to dose.

Dosimetry in phantoms

(A36) If medical physicists follow the recommendations and measure $CTDI_{vol}$ and $CTDI_{air}$ at acceptance testing, measurements of $CTDI_{vol}$ in phantoms are not needed on a routine basis if periodic $CTDI_{air}$ measurements are stable.

(A37) Manufacturers should measure and provide users with a comprehensive set of data for a reasonably wide range of beam settings used in clinical practice regarding the rise-to-equilibrium curves of the scanner and related metrics such as $H(L)$ and $h(L)$. $G(L)$, which is the $H(L)$ curve normalised by $CTDI_{vol}$ and thus related to patient dose, should also be provided.

(A38) A subset of CTDI measurements performed by only using the central 200-mm section of the phantom should also be provided by manufacturers so that $G(L)$ measured for the full 600-mm phantom can be associated with the partial $G(L)$ measurement acquired with the 200-mm phantom section.

Patient dose estimations

(A39) Patient dose can be estimated by using SSDE coupled with $CTDI_{vol}$. The method has been described in Report 87 (ICRU, 2012) and Report 204 (AAPM, 2011b). It must be considered, however, that $CTDI_{vol}$ calculation can be different for partial rotation axial CT scans, such as in the case of a C-arm CBCT scan. Even for full axial scans in which there is no patient translation, $CTDI_{vol}$ will overestimate patient dose (Dixon and Boone, 2010b). This fact underlines the need for new coefficients for patient dose estimation from $f(0)$ measurements.

A.5. Tracking and reporting of radiation dose

(A40) New challenges emerge with systems being used for both fluoroscopy and tomography (CBCT). While fluoroscopy radiation dose figures are normally available as KAP from the machines, CBCT doses are currently provided by different manufacturers in different units. Currently, there is no way to assess the aggregate radiation dose to a patient during a single procedure. Further, there is a need to facilitate comparison of radiation doses to patients between a single run of CT to one or several digitally subtracted angiography series. This situation needs to be addressed, and a system should provide a means of not only comparing but also consolidating doses from both fluoroscopy and CT. Furthermore, tracking and reporting of radiation dose for a single patient should be made possible, as it is

becoming increasingly important to do this for strengthening the processes involved in the justification and optimisation principles of ICRP (Rehani and Frush, 2011; Seuri et al., 2013). Errors for displayed dose estimates should not exceed 20% (IAEA, 2011b; IEC, 2011; EC, 2012b). An RDSR can be used to report the modality output following the existing RDSR in CT and angiography. KAP values for the different orientation of the beam can be reported inside the RDSR when step-and-shoot acquisition techniques are used; in addition, KAP can be considered for CBCT in fluoroscopy and other applications to facilitate a direct comparison with doses from 2D examinations such as fluoroscopy. Effective dose is not a suitable dosimetric quantity for reporting patient doses.

A.6. Epilogue

(A41) Different methods for CBCT dosimetry have been presented. However, in order to evaluate the usefulness of CBCT in regard to its alleged dose reduction in comparison to CT, a metric which could be used for direct comparison is needed. The unified CT dosimetry method proposed by ICRU (2012) has the potential to standardise CBCT dosimetry. This method can be implemented without updating the equipment already in use in the clinical CT arena. Furthermore, the methods discussed could be used to measure dose for many types of different CBCT systems, including radiotherapy CBCT, clinic-based systems, dedicated breast systems, and C-arm systems. The value of CTDI-based measurements presented in this annex should not be underestimated. Although CTDI has limitations, it has been evaluated on many systems over the years, and provides important comparisons in output for CT scanners from different manufacturers and ages. Also, the coefficients for patient dose estimations that are available today are based on $CTDI_{vol}$.

SAGE

ICRP
Annals of the ICRP

Corrigenda

Corrigenda to ICRP *Publication 116*: Conversion Coefficients for Radiological Protection Quantities for External Radiation Exposures [Ann. ICRP 40(2–5) 2010]

The following errors were introduced into some of the data in Tables A.1, A.2, B.7, B.10, and G.2. Asterisks in the tables below highlight changes in the numerical values from the original values. Supplementary data files v2 available at the publisher's website reflect these corrections.

Table A.1. Photons: effective dose per fluence, in units of pSv cm^2, for monoenergetic particles incident in various geometries.

Energy (MeV)	AP	PA	LLAT	RLAT	ROT	ISO
0.01	0.0685	0.0184	0.0189	0.0182	0.0337	0.0288
0.015	0.156	0.0155	0.0416	0.0390	0.0665*	0.0560
0.02	0.225	0.0261*	0.0654*	0.0573	0.0988*	0.0813*
0.03	0.312*	0.0946*	0.109*	0.0886*	0.159*	0.127
0.04	0.350*	0.163*	0.138*	0.113*	0.199	0.158
0.05	0.369*	0.209*	0.158*	0.132*	0.226	0.180
0.06	0.389*	0.243*	0.174*	0.149*	0.248	0.198*
0.07	0.411*	0.273*	0.191*	0.165*	0.273	0.218
0.08	0.443*	0.302*	0.211*	0.183*	0.297	0.238*
0.1	0.518*	0.363*	0.255*	0.224*	0.356*	0.286*
0.15	0.747*	0.543*	0.391*	0.346*	0.529*	0.429
0.2	1.00	0.745*	0.546*	0.489*	0.722*	0.589
0.3	1.51	1.16	0.880*	0.797*	1.12	0.932

(continued)

Table A.1. (continued)

Energy (MeV)	AP	PA	LLAT	RLAT	ROT	ISO
0.4	2.00	1.58*	1.23*	1.12*	1.53*	1.28
0.5	2.47	1.99*	1.57*	1.45	1.92	1.63
0.511	2.52	2.03	1.61*	1.48*	1.97*	1.66*
0.6	2.91	2.39*	1.91*	1.77*	2.31*	1.97
0.662	3.17	2.63*	2.12*	1.97*	2.54	2.17
0.8	3.73	3.14*	2.57*	2.40*	3.04	2.62
1.0	4.49	3.84*	3.21*	3.02*	3.73*	3.25
1.117	4.90	4.23*	3.56*	3.36*	4.10	3.60
1.33	5.60*	4.90*	4.18*	3.97*	4.75	4.21*
1.5	6.12	5.41*	4.66*	4.43*	5.24	4.67*
2.0	7.48	6.77*	5.94*	5.68*	6.56*	5.91*
3.0	9.75	9.13*	8.18*	7.88*	8.85*	8.08
4.0	11.7	11.2	10.2	9.84*	10.9*	10.0
5.0	13.4	13.2*	12.0	11.6*	12.7	11.8
6.0	15.0	15.0	13.7	13.3*	14.4	13.5
6.129	15.1	15.2	13.9	13.5*	14.6	13.7
8.0	17.8	18.6	16.9*	16.6	17.6	16.6
10.0	20.5	22.1*	20.0*	19.7	20.7*	19.7*
15.0	26.1	30.4*	27.3*	27.1	27.7	26.8
20.0	30.8	38.2	34.4	34.3*	34.4	33.8
30.0	37.9	51.3*	47.4	48.0*	46.0*	46.1
40.0	43.2*	61.8*	59.3*	60.9	56.0	56.9
50.0	47.1	70.1*	69.7*	72.3*	64.3*	66.1*
60.0	50.1	76.5*	78.6*	82.1*	71.1*	74.1
80.0	54.5	86.2*	92.9*	98.1*	81.8*	87.1*
100	57.8	92.7*	103	110	89.5*	97.5
150	63.2*	103*	122*	130	102	116
200	67.2*	110*	134*	144*	110*	129*
300	72.3	118*	149*	161	121	147
400	75.4*	123*	159*	173*	128	159
500	77.4*	127*	166*	181*	132*	167*
600	78.7*	130*	171*	187*	136	174
800	80.4*	134*	179*	195	141*	185
1000	81.6*	137*	184*	202*	145	193
1500	83.7*	141*	194*	213*	151*	208
2000	85.0*	144*	200*	220	156	218
3000	86.6*	147*	208*	230*	161	232

(continued)

Table A.1. (continued)

Energy (MeV)	AP	PA	LLAT	RLAT	ROT	ISO
4000	87.8*	149*	213*	236*	164*	242*
5000	88.6*	151*	217*	241*	167*	251
6000	89.1*	152*	221*	245*	169*	258
8000	89.9*	153*	226*	251	172	268
10,000	90.4*	154*	230*	256*	174*	276

AP, antero-posterior; PA, postero-anterior; LLAT, left lateral; RLAT, right lateral; ROT, rotational; ISO, isotropic.

Table A.2. Photons: effective dose per air kerma free-in-air, in units of Sv Gy^{-1}, for mono-energetic particles incident in various geometries.

Energy (MeV)	AP	PA	LLAT	RLAT	ROT	ISO
0.01	0.0090	0.0024	0.0025	0.0024	0.0044	0.0038
0.015	0.0486*	0.0048	0.0130	0.0122	0.0207	0.0175
0.02	0.131*	0.0151	0.0379	0.0332	0.0572*	0.0471*
0.03	0.422*	0.128*	0.148*	0.120*	0.215*	0.171
0.04	0.798*	0.371*	0.315*	0.258*	0.455	0.360*
0.05	1.12*	0.638*	0.480*	0.402*	0.688	0.547*
0.06	1.33	0.832*	0.595*	0.508*	0.850	0.679*
0.07	1.42	0.940*	0.659*	0.569*	0.939	0.751
0.08	1.43*	0.980*	0.684*	0.594*	0.964*	0.773
0.1	1.39	0.975*	0.685*	0.601*	0.954*	0.768*
0.15	1.25	0.906*	0.651*	0.577*	0.882*	0.715
0.2	1.17	0.869*	0.637*	0.570*	0.843*	0.687
0.3	1.09	0.840*	0.637*	0.577*	0.814*	0.674*
0.4	1.06	0.834*	0.648*	0.592*	0.807*	0.678
0.5	1.04	0.836*	0.660*	0.608*	0.808*	0.684
0.511	1.03	0.836*	0.661*	0.610*	0.808*	0.685
0.6	1.02	0.839*	0.673*	0.623*	0.811*	0.692
0.662	1.02	0.841*	0.680*	0.632*	0.814*	0.697
0.8	1.01	0.848*	0.695*	0.649*	0.822*	0.708
1.0	1.00	0.857*	0.716*	0.673*	0.831*	0.725
1.117	0.999	0.863*	0.726*	0.686*	0.837*	0.734
1.33	0.996	0.872*	0.745*	0.706*	0.846	0.749*
1.5	0.996	0.880*	0.758*	0.721*	0.853	0.760*

(continued)

Table A.2. (continued)

Energy (MeV)	AP	PA	LLAT	RLAT	ROT	ISO
2.0	0.990	0.895*	0.785*	0.752*	0.868*	0.782*
3.0	0.977	0.915*	0.820*	0.790*	0.887*	0.810
4.0	0.960	0.924*	0.837*	0.810*	0.894*	0.824
5.0	0.943	0.928*	0.844*	0.821*	0.894*	0.832*
6.0	0.924	0.928*	0.846*	0.824*	0.890*	0.832
6.129	0.922*	0.928*	0.845*	0.824*	0.889*	0.832
8.0	0.886	0.923*	0.841*	0.823*	0.875*	0.826*
10.0	0.848	0.914*	0.830*	0.815*	0.856	0.814
15.0	0.756	0.881*	0.793*	0.785*	0.804	0.779*
20.0	0.679	0.843	0.758*	0.757*	0.759	0.745*

AP, antero-posterior; PA, postero-anterior; LLAT, left lateral; RLAT, right lateral; ROT rotational; ISO, isotropic.

Table B.7. Photons, female: oesophagus absorbed dose per fluence, in units of pGy cm^2, for monoenergetic particles incident in various geometries.

Energy (MeV)	AP	PA	LLAT	RLAT	ROT	ISO
0.01	4.6E-5*	4.7E-8*	1.4E-6*	1.7E-6*	2.7E-6*	4.0E-5*
0.015	0.0141*	4.1E-6*	1.1E-4*	1.2E-4*	0.0025*	0.0013*
0.02	0.0754*	0.0021*	0.0025*	0.0040*	0.0204*	0.0129*
0.03	0.201*	0.0510*	0.0257*	0.0297*	0.0865*	0.0545*
0.04	0.261*	0.140*	0.0602*	0.0570*	0.149*	0.102*
0.05	0.300*	0.211*	0.0890*	0.0827*	0.189*	0.136*
0.06	0.331*	0.260*	0.110*	0.101*	0.222*	0.164*
0.07	0.360*	0.289*	0.130*	0.120*	0.249*	0.199*
0.08	0.393*	0.330*	0.149*	0.139*	0.283*	0.217*
0.1	0.470*	0.410*	0.189*	0.178*	0.347*	0.268*
0.15	0.702*	0.621*	0.302*	0.288*	0.530	0.408*
0.2	0.948*	0.844*	0.437*	0.411*	0.725*	0.565*
0.3	1.44*	1.30*	0.731*	0.690*	1.15*	0.898*
0.4	1.94*	1.75*	1.03*	0.987*	1.57*	1.23*
0.5	2.41*	2.19*	1.35*	1.28*	1.98*	1.58*
0.511	2.44*	2.23*	1.38*	1.32*	2.03*	1.60*
0.6	2.82*	2.61*	1.67*	1.59*	2.41*	1.91*
0.662	3.07*	2.84*	1.89*	1.78*	2.64*	2.12*
0.8	3.66*	3.35*	2.33*	2.21*	3.16*	2.60*

(continued)

Table B.7. (continued)

Energy (MeV)	AP	PA	LLAT	RLAT	ROT	ISO
1.0	4.41*	4.09*	2.95*	2.78*	3.84*	3.27*
1.117	4.84*	4.51*	3.28*	3.11*	4.24*	3.67*
1.33	5.54*	5.23*	3.85*	3.67*	4.90*	4.26*
1.5	6.05*	5.75*	4.28*	4.14*	5.40*	4.72*
2.0	7.46*	7.08*	5.53*	5.40*	6.84*	5.99*
3.0	9.95*	9.34*	7.73*	7.68*	9.35*	8.13*
4.0	12.1*	11.4*	9.79*	9.63*	11.5*	10.2*
5.0	14.2	13.4*	11.6*	11.6*	13.3*	12.1*
6.0	16.1	15.4*	13.5*	13.5*	15.1*	13.9*
6.129	16.4	15.7*	13.6*	13.8*	15.4*	14.1*
8.0	19.9	19.4*	17.3*	17.0*	18.9*	17.5*
10.0	23.3*	23.1*	20.8*	20.3*	22.5*	20.9*
15.0	30.6*	32.3*	28.8*	28.5*	31.0*	29.7*
20.0	36.5*	41.0*	37.1*	37.2*	38.9*	38.1*
30.0	45.5*	53.4*	54.3*	53.5*	52.1*	51.8*
40.0	51.5*	61.7*	69.2*	68.5*	62.2*	63.7*
50.0	55.6*	67.9*	81.2*	81.6*	70.3*	73.1*
60.0	58.6*	72.4*	91.2*	92.6*	76.6*	81.6*
80.0	63.1*	80.4*	107*	110*	86.3*	94.9*
100	66.4*	84.7*	119*	121*	93.3*	105*
150	71.8*	93.2*	139*	141*	105*	123*
200	76.3*	97.6*	151*	155*	112*	135*
300	82.2*	103*	166*	173*	120*	150*
400	85.2*	108*	175*	184*	126*	160*
500	86.9*	111*	183*	192*	129*	167*
600	87.8*	114*	188*	198*	132*	174*
800	89.4*	116*	196*	206*	136*	184*
1000	90.7*	118*	201*	211*	138*	192*
1500	93.1*	120*	211*	220*	143*	204*
2000	94.2*	122*	218*	226*	147*	213*
3000	95.7*	124*	226*	235*	149*	225*
4000	97.5*	126*	229*	241*	152*	234*
5000	98.7*	127*	232*	245*	154*	243*
6000	99.4*	128*	235*	247*	155*	250*
8000	100*	129*	241*	248*	158*	262*
10,000	100*	129*	247*	248*	159*	272*

AP, antero-posterior; PA, postero-anterior; LLAT, left lateral; RLAT, right lateral; ROT rotational; ISO, isotropic.

Table B.10. Photons, female: remainder absorbed dose per fluence, in units of pGy cm^2, for monoenergetic particles incident in various geometries.

Energy (MeV)	AP	PA	LLAT	RLAT	ROT	ISO
0.01	0.0023	8.0E-4	0.0011	0.0012	0.0014	0.0017
0.015	0.0370	0.0114*	0.0130*	0.0119	0.0177	0.0135
0.02	0.0966*	0.0361*	0.0347*	0.0271	0.0469*	0.0346
0.03	0.210*	0.120*	0.0888*	0.0676*	0.122*	0.0883*
0.04	0.273*	0.187*	0.129*	0.105*	0.178*	0.131*
0.05	0.308*	0.231*	0.156*	0.130*	0.215*	0.159*
0.06	0.335*	0.265*	0.176*	0.150*	0.239*	0.182*
0.07	0.368*	0.296*	0.197*	0.171*	0.266*	0.203*
0.08	0.395*	0.328*	0.219*	0.191*	0.292*	0.225*
0.1	0.470*	0.399*	0.267*	0.235*	0.355*	0.273*
0.15	0.687*	0.596*	0.414*	0.370*	0.533*	0.414*
0.2	0.925*	0.813*	0.580*	0.524*	0.733*	0.572*
0.3	1.41*	1.26*	0.939*	0.855*	1.15*	0.910*
0.4	1.88*	1.70*	1.31*	1.20*	1.56*	1.25*
0.5	2.33*	2.12*	1.68*	1.54*	1.96*	1.60*
0.511	2.38*	2.17*	1.72*	1.57*	2.00*	1.63*
0.6	2.76*	2.53*	2.04*	1.87*	2.35*	1.93*
0.662	3.01*	2.78*	2.26*	2.08*	2.59*	2.14*
0.8	3.56*	3.31*	2.73*	2.53*	3.10*	2.59*
1.0	4.30*	4.03*	3.39*	3.17*	3.80*	3.21*
1.117	4.71*	4.42*	3.76*	3.53*	4.19*	3.57*
1.33	5.40*	5.11*	4.40*	4.16*	4.86*	4.19*
1.5	5.93*	5.63*	4.90*	4.63*	5.36*	4.65*
2.0	7.33*	7.02*	6.23*	5.92*	6.72*	5.93*
3.0	9.75*	9.40*	8.56*	8.20*	9.09*	8.22*
4.0	11.9*	11.5	10.6*	10.2	11.2*	10.3
5.0	13.8	13.5*	12.6*	12.1	13.1	12.1*
6.0	15.7*	15.3*	14.4*	13.9	15.0*	13.9*
6.129	15.9*	15.6*	14.6*	14.1	15.2	14.1*
8.0	19.1*	18.9*	17.9*	17.4*	18.5	17.2*
10.0	22.4*	22.4*	21.3*	20.7*	21.9	20.5*
15.0	29.4*	30.6*	29.2*	28.7	29.9*	28.2*
20.0	35.6*	38.6	36.8	36.4	37.2*	35.9*
30.0	44.7*	50.7*	50.2*	50.6	49.2*	49.4*
40.0	51.0	59.8*	62.0*	63.4*	59.0*	60.6

(continued)

Table B.10. (continued)

Energy (MeV)	AP	PA	LLAT	RLAT	ROT	ISO
50.0	55.6*	66.7*	72.0*	74.3	67.0*	70.1*
60.0	59.3*	71.8*	80.3*	83.5*	73.3*	78.2*
80.0	64.6*	79.8*	92.9*	98.2*	83.3*	91.5*
100	68.5*	85.2*	102*	109*	90.3*	102*
150	75.2*	94.1*	117*	128	102*	120*
200	79.8*	100*	128*	140*	109*	133*
300	85.8*	107*	141*	155*	118*	150*
400	89.6*	111*	149*	166*	124*	161*
500	92.0*	114*	154*	173*	128*	169*
600	93.6*	117*	159*	178*	132*	175*
800	95.4*	120*	165*	186*	136*	185*
1000	97.1*	123*	169*	192*	139*	193*
1500	99.6*	126*	177*	201*	144*	206*
2000	101*	129*	182*	208*	148*	216*
3000	103*	131*	188*	216*	152*	230*
4000	105*	133*	192*	222*	155*	240*
5000	106*	134*	195*	226*	157*	247*
6000	106*	135*	197*	230*	159*	254*
8000	107*	136*	201*	235*	161*	263*
10,000	107*	136*	204*	239*	162*	270*

AP, antero-posterior; PA, postero-anterior; LLAT, left lateral; RLAT, right lateral; ROT rotational; ISO, isotropic.

Table G.2. Local skin absorbed dose per fluence (D/Φ), in $\mu Gy\,cm^2$, for monoenergetic alpha particles normally incident on skin.

Energy (MeV)	D/Φ
6.5	0.00111
6.8	0.0256
7.0	0.0420
7.5	0.0752
8.0	0.103
8.5	0.128
9.0	0.150
9.5	0.172*
10.0	0.180

Subscriptions

The *Annals of the ICRP* (ISSN: 0146-6453) is published in print and online by SAGE Publications (London, Thousand Oaks, CA, New Delhi, Singapore, Washington DC and Boston).

Annual subscription (2015) including postage: Institutional Rate (combined print and electronic) £528/US$633. Note VAT might be applicable at the appropriate local rate. Visit http://www.sagepublications.com for more details. To activate your subscription (institutions only) visit http://online.sagepub.com online. Abstracts, tables of contents and contents alerts are available on this site free of charge for all. Student discounts, single issue rates and advertising details are available from SAGE Publications Ltd, 1 Oliver's Yard, 55 City Road, London EC1Y 1SP, UK, tel. +44 (0)20 7324 8500, fax +44 (0)20 7324 8600 and in North America, SAGE Publications Inc, PO Box 5096, Thousand Oaks, CA 91320, USA.

SAGE Publications is a member of CrossRef

Commercial Sales
For information on reprints and supplements please contact reprints@sagepub.co.uk.

Abstracting and Indexing
Please visit http://ani.sagepub.com and click on More about this journal, then Abstracting/Indexing, to view a full list of databases in which this journal is indexed.

ISBN 978-1-4739-4439-8
ISSN 0146-6453

Published quarterly.

Printed by Page Bros, UK

Annals of the ICRP

Annals of the ICRP is an essential publication for all:

☐ Regulatory and advisory agencies at regional, national and international levels

☐ Management bodies with responsibilities for radiological protection

☐ Professional staff employed as advisers and consultants

☐ Individuals, such as radiologists and nuclear medicine specialists, who make decisions about the use of ionising radiation.

Annals of the ICRP provides recommendations and guidance from the International Commission on Radiological Protection on protection against the risks associated with ionising radiation, from artificial sources such as those widely used in medicine, general industry, and nuclear enterprises, and from naturally occurring sources. Each issue of *Annals of the ICRP* provides in-depth coverage of a specific subject area.

Annals of the ICRP is available as a journal subscription or can be purchased as individual books. *Annals of the ICRP* is also available in electronic format at http://ani.sagepub.com/

ISSN

ISBN